Modulated longitudinal gates on encoded spin qubits via curvature couplings to a superconducting cavity

Rusko Ruskov[*] and Charles Tahan[†]

Laboratory for Physical Sciences, 8050 Greenmead Dr., College Park, Maryland 20740, USA

We propose entangling operations based on the energy curvature couplings of encoded spin qubits to a superconducting cavity, exploring the nonlinear qubit response to a gate voltage variation. For a two-qubit (n-qubit) entangling gate we explore acquired geometric phases via a time-modulated longitudinal σ_z coupling, offering gate times of tens of nanoseconds even when the qubits and the cavity are far detuned. No dipole moment is necessary: the qubit transverse σ_x coupling to the resonator is zero at the full sweet spot of the encoded spin qubit of interest (a triple quantum dot three-electron exchange-only qubit or a double quantum dot singlet-triplet qubit). This approach allows always-on, exchange-only qubits, for example, to stay on their "sweet spots" during gate operations, minimizing the charge noise and eliminating an always-on static longitudinal qubit-qubit coupling. We calculate the main gate errors due to the (1) diffusion (Johnson) noise and (2) damping of the resonator, the (3) $1/f$-charge noise qubit gate dephasing and $1/f$ noise on the longitudinal coupling, (4) qubit dephasing and AC-Stark frequency shifts via photon fluctuations in the resonator, and (5) spin-dependent resonator frequency shifts (via a "dispersivelike" static curvature coupling), most of them associated with the nonzero qubit energy curvature (quantum capacitance). Using spin-echo-like error suppression at optimal regimes, gate infidelities of 10^{-2}–10^{-3} can be achieved with experimentally existing parameters. The proposed schemes seem suitable for remote spin-to-spin entanglement of two spin qubits or a cluster of spin qubits: an important resource of quantum computing.

I. INTRODUCTION

Electron spin qubits in semiconductors have made steady progress in coherence times, gate operations, and quantum measurements, towards the goal of a spin-based quantum computer [1–11]. Despite the inherent protection of single QD spin qubits by the nature of the single electron spin [12–14], spin qubits in multielectron multi-QDs provide further advantages such as: (i) encoding the spin qubit in decoherence free subspaces (DFS) [15,16], where qubit states can be partially protected against charge (electric) and spin (magnetic) global noises, e.g., in triple quantum dot (TQD) three-electron qubits [3,11,17–22]; (ii) the potential to choose gate parameter regimes, including the so-called sweet spots [23–27] (partial or full sweet spots) where, e.g., the charge noise can be further minimized, which was recently experimentally confirmed for singlet-triplet (S-T) DQD qubits [28,29]; (iii) fast single-qubit gates, based only on exchange interaction [3,19–22] (TQD qubits with electric field control and no need of magnetic field gradient), or using interdot magnetic field gradients [30,31] (S-T qubits).

Exchange based two-qubit gates [4,26,32,33], however, are locally operated and do not allow remote coupling of qubits, e.g., at millimeter distances that are much larger than the qubit size (of tens of nanometers). A solution would be to couple spins via a superconducting (SC) GHz resonator using a transverse dipole coupling [10,34–40] (already a resource for SC

qubits [41–46]). Recently, studies of the resonant exchange (RX) "always-on" qubit [23], based on a triple quantum dot (TQD) three-electron system, offered strong spin-cavity coupling, and showed that it can maintain a partial sweet spot to gate detuning fluctuations (see also Refs. [24,47]).

The transverse (σ_x) coupling to a spin qubit [10,34–36,38,48–50] requires a nonzero transition electric dipole moment (e.d.m.) $\boldsymbol{d}_\perp \neq 0$, leading to a Jaynes-Cummings (J-C) interaction with the cavity [23,34]: $\mathcal{H}_{\mathrm{tr}} \propto g_\perp \sigma_x (\hat{a} + \hat{a}^\dagger) \simeq g_\perp(\sigma_-\hat{a}^\dagger + \sigma_+\hat{a})$, where $\hat{a}$ is the electric field cavity mode annihilation operator and $\sigma_- \equiv |-\rangle\langle+|$ is the qubit lowering operator. It was predicted [34,48–50] and recently measured [10,11,51] to be at the range from one to tens of MHz. In a dispersive regime (i.e., avoiding direct excitations), where the qubit-resonator detuning is large ($\Delta \gg g_\perp$), the leading dispersive Hamiltonian $\mathcal{H}_{\mathrm{tr}} \propto \frac{g_\perp^2}{\Delta} \hat{a}^\dagger \hat{a} \sigma_z$ cannot couple directly the qubits via photon exchange since it commutes with the qubit Hamiltonian $\mathcal{H}_q$. (It can entangle the qubits, however, via geometric accumulated phases [52,53], without a net exchange, though the expected entangling rate would be relatively slow, $\sim\frac{g_\perp^4}{\Delta^2}$, see below.) Higher order terms in the J-C interaction can couple two qubits ($\sim\sigma_-^{(1)}\sigma_+^{(2)}$) via virtual photon exchange with a rate [34,47] $\sim\frac{g_\perp^{(1)}g_\perp^{(2)}}{\Delta}$, suppressed in the dispersive limit. Reaching faster entangling gates, with a rate $\sim g_\perp$, is possible using sideband transitions via strong resonant driving of the qubit [47,54–56].

These approaches, however, come with several caveats for encoded spin qubits, namely: (i) the necessity of strong transverse coupling $g_\perp$ will also imply much stronger sensitivity to charge noise via gate voltage fluctuations; (ii) a strong

*ruskovr@lps.umd.edu
†charlie@tahan.com

transverse dipole coupling also would imply an increased coupling to spurious TLS charge fluctuators (that is another source of charge noise, see, e.g., Refs. [57–59]); (iii) the effective entangling interaction will be generally worsened by higher-order transitions in the qubit-resonator system [60] since $[\mathcal{H}_{tr}, \mathcal{H}_q] \neq 0$ in higher orders of $g_\perp/\Delta$; and (iv) also turning off this coupling via a larger detuning Δ may be difficult for both spin and superconducting qubits (see, e.g., Ref. [61]).

In this paper we propose and fully analyze (including all loss mechanisms) an alternative approach for remote spin-spin entanglement by establishing longitudinal *curvature* coupling $\sim \tilde{g}_\parallel \sigma_z (\hat{a} + \hat{a}^\dagger)$ of encoded spin qubits to a superconducting (SC) resonator, via simultaneous gate voltage modulation of the qubits involved, even when the modulation frequency ω_m as well as the qubits frequencies $\omega_q^{(j)}$ are off-resonance. The modulated qubits accumulate multispin phases comprising spin-spin unitary gates, allowing entanglement of various spin clusters, depending on the chosen subset of modulated qubits. The qubits reside in their *full sweet spot to gate voltage fluctuations* [Figs. 1(a) and 1(b)], and at the same time ensuring the absence of transverse coupling [62,63] $g_\perp = 0$, thus minimizing qubits charge dephasing. In what follows, we consider both the triple quantum dot (TQD) always-on exchange only (AEON) qubit in the full sweet spot [26], and the double quantum dot (DQD) singlet-triplet (S-T) qubit in its symmetric operating point [28,29] (SOP) [Figs. 1(a) and 1(b)] which are described in the same terms as to their curvature coupling to a SC resonator [62].

The total Hamiltonian of the resonator plus a system of n multi-QD spin qubits (here $j = 1, \ldots, n$ enumerates the qubits) at their full sweet spots with a generic coupling to the environment $\mathcal{H}_{env}$ reads (scf. Ref. [62])

$$
\begin{aligned}
\mathcal{H}_{tot}/\hbar = &\; \omega_r \hat{a}^\dagger \hat{a} + \sum_{j=1}^{n} \frac{\omega_q^{(j)}}{2} \sigma_z^{(j)} + \mathcal{H}_{env} \\
&+ \sum_{j=1}^{n} \delta\omega^{(j)} \sigma_z^{(j)} \left(\hat{a}^\dagger \hat{a} + \frac{1}{2} \right) \\
&+ \sum_{j=1}^{n} \left[\tilde{g}_\parallel^{(j)} \sigma_z^{(j)} + \tilde{g}_0^{(j)} \right] \cos(\omega_m t + \varphi_m)(\hat{a} + \hat{a}^\dagger) \\
&+ 2\varepsilon_d \cos(\omega_d t + \varphi_d)(\hat{a} + \hat{a}^\dagger).
\end{aligned}
\tag{1}
$$

Besides the system Hamiltonians, Eq. (1) at the full sweet spot includes two curvature interactions: the "dispersivelike" static interaction [second row in Eq. (1)] and the longitudinal dynamical interaction (third row); while the former is always on, the latter is on only when the relevant qubits are modulated simultaneously at a frequency $\omega_m \sim \omega_r$ and phase φ_m ($|\omega_m - \omega_r| \gg \kappa$, with κ the resonator damping), see Figs. 1(a) and 2. We also include the driving of the SC resonator with frequency ω_d and phase φ_d. Other possible interactions, such as the static longitudinal [64] $(g_\parallel^{st} \sigma_z + g_0^{st})(\hat{a} + \hat{a}^\dagger)$ and transverse $g_\perp \sigma_x (\hat{a} + \hat{a}^\dagger)$ interaction, were shown to exactly cancel at the full sweet spot [62] for each qubit since, e.g., $g_\parallel^{st,(j)} \propto \frac{\partial E_q^{(j)}}{\partial V_m} = 0$, while the transverse couplings are zeroed due to
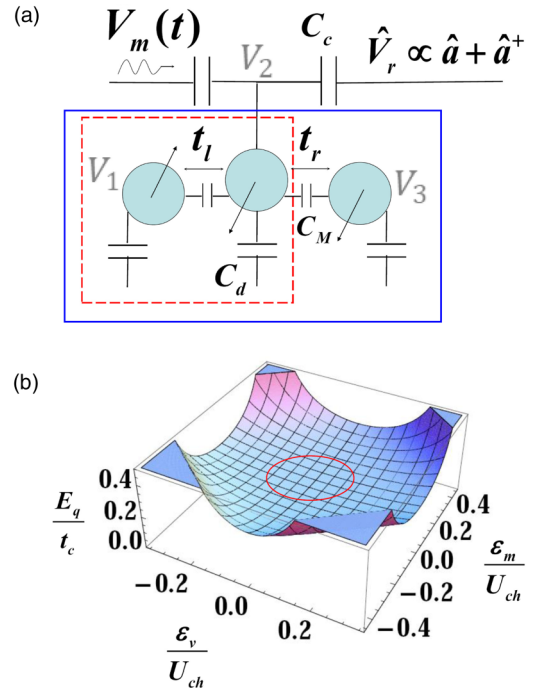

FIG. 1. (a) A TQD exchange only qubit (solid, blue box) or a DQD S-T qubit (dashed, red box) capacitively coupled to a SC resonator (see experimental Refs. [39,40] for a similar layout). The curvature couplings to a SC resonator arise via the resonator quantized voltage drop $\hat{V}_r = V_{vac}(\hat{a} + \hat{a}^\dagger)$ on the coupling (middle) dot, essentially as *quantum capacitance couplings*: these are (i) the dynamical longitudinal coupling, Eq. (4), $\tilde{g}_\parallel \sigma_z (\hat{a} + \hat{a}^\dagger) \sim \hat{V}_r V_m(t)$, that arises via additional qubit gate modulation and (ii) the always-on dispersivelike (quantum capacitance) static coupling $\delta\omega \hat{a}^\dagger \hat{a} \sigma_z \sim \hat{V}_r^2$, Eq. (8). Both couplings can be expressed via the qubit energy curvature $C_q \equiv e^2 \frac{\partial^2 E_q}{\partial \varepsilon_m^2} \propto \frac{t_c^2}{U_{charge}^3}$ that can be significant, $\gtrsim 30$ aF (see Ref. [62] and Table I), for typical dot charging energy $U_{charge} \gtrsim 0.4$ meV and interdot tunnelings $t_c \gtrsim 40$ μeV, reachable experimentally. For a TQD qubit the relevant voltage detuning is $\varepsilon_m \equiv e[(V_3 + V_1)/2 - V_2]$ and for a DQD qubit it is $\varepsilon_v \equiv e(V_1 - V_2)$. (b) Full sweet spot regime of a TQD exchange only qubit (solid, red circle). The energy splitting $E_q(\varepsilon_v, \varepsilon_m)$ as a function of the qubit gate voltage detunings $\varepsilon_v \equiv e(V_3 - V_1)/2$ and ε_m (in units of the dots' charging energy U_{ch}). At the full sweet spot [26] where $\frac{\partial E_q}{\partial \varepsilon_v}, \frac{\partial E_q}{\partial \varepsilon_m} = 0$, while its transverse dipole moment is also zero [62], the TQD qubit is insensitive (in first order) to gate voltage fluctuations, and at the same time qubit dephasing through phonon relaxation and coupling to two-level fluctuators is also minimized as the transition dipole moment is zero [62] as well. A similar sweet spot of the DQD qubit (not shown) with respect to the detuning $\varepsilon_v \equiv e(V_1 - V_2)$ will be referred to as a symmetric operating point (SOP) [28,29].

exact cancellation of contributions to the transition dipole moment of the qubit's higher excited states [62].

The main focus in this paper will be on the two types of curvature interactions that appear through the influence of the resonator quantized voltage $\hat{V}_r = V_{vac}(\hat{a} + \hat{a}^\dagger)$ [Fig. 1(a)] on the QD qubit levels, see Refs. [62,63], where $V_{vac} = \frac{\hbar\omega_r}{e}\sqrt{\frac{Z_r}{\hbar/e^2}}$ reflects the resonator vacuum voltage fluctuations (here $Z_r \simeq \omega_r L_r$ is the resonator impedance, assuming a high quality factor $Q \equiv \frac{\omega_r L_r}{R_r} \gg 1$). In what follows, it is convenient
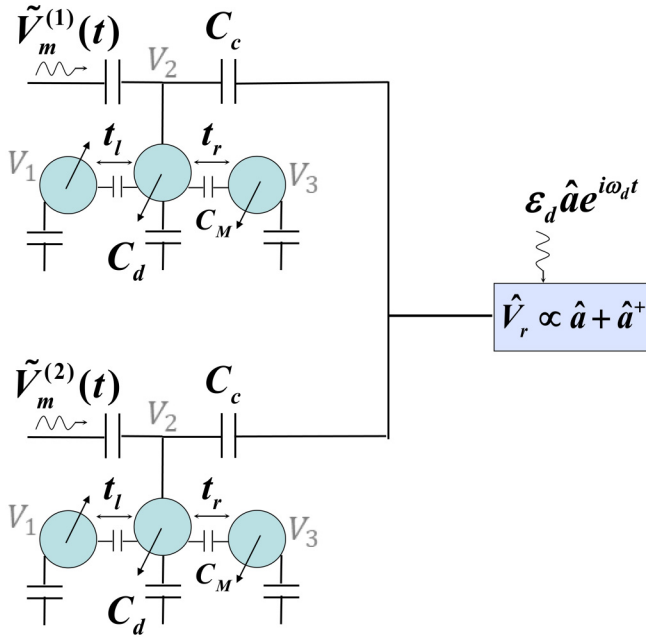
FIG. 2. Two TQD spin qubits [or DQD S-T spin qubits, Fig. 1(a)] can be entangled by modulating their respective dot gate voltages $V_2^{(j)}$ by a modulation $V_m^{(j)}(t) = \tilde{V}_m^{(j)} \cos(\omega_m t + \varphi_m)$, for a finite gate time $t_g = 2\pi/\delta \equiv 2\pi/(\omega_r - \omega_m)$, where $\delta \equiv \omega_r - \omega_m$ is the frequency detuning. For a specially chosen detuning $\delta = \delta_\pi \equiv \pi\sqrt{4N\tilde{g}_\parallel^{(1)}\tilde{g}_\parallel^{(2)}}$, the accumulated geometric phases for each two-qubit spin state amount to a controlled π-phase gate, see Eq. (23) and Appendix A. The defining gate voltages for each qubit as well as the coupling to the (high Q-factor) resonator can be different in general (see text). The qubit frequencies can be different, and they can be strongly detuned from the resonator (beyond the usual dispersive limit).

to introduce the dimensionless ratios related to the qubits-resonator coupling strength:

$$\frac{\eta^{(j)}}{\hbar} \equiv \alpha_c^{(j)} \sqrt{\frac{Z_r}{\hbar/e^2}}, \qquad (2)$$

where $\alpha_c^{(j)} \simeq \frac{C_c^{(j)}}{C_c^{(j)} + C_d^{(j)}}$ are the QDs' lever arms to the SC resonator [Fig. 1(b)]. For a lever arm in the range $\alpha_c \lesssim 0.2$, $\omega_r/2\pi = 10$ GHz, and reachable resonator impedance of $L_r \lesssim 50$ nH one can reach $\frac{\eta}{\hbar} \lesssim 0.2$.

First, one considers the dynamical longitudinal (curvature) Hamiltonian in Eq. (1),

$$\mathcal{H}_\parallel^{(j)} = \hbar\big[\tilde{g}_\parallel^{(j)} \sigma_z^{(j)} + \tilde{g}_0^{(j)}\big] \cos(\omega_m t + \varphi_m)(\hat{a} + \hat{a}^\dagger), \qquad (3)$$

implying the couplings [62,63]

$$\tilde{g}_\parallel^{(j)} = \frac{\omega_r}{2}\left(\frac{\eta^{(j)}}{\hbar}\right)\frac{\partial^2 E_q^{(j)}(V_m^0)}{e\,\partial V_m^2}\tilde{V}_m^{(j)}, \qquad (4)$$

$$\tilde{g}_0^{(j)} = \omega_r\left(\frac{\eta^{(j)}}{\hbar}\right)\frac{\partial^2 G_q^{(j)}(V_m^0)}{e\,\partial V_m^2}\tilde{V}_m^{(j)} \qquad (5)$$

that appears under external voltage modulation of the energy levels of each qubit with a strength $\tilde{V}_m^{(j)}$ [here $E_q^{(j)} \equiv E_+^{(j)} - $

$E_-^{(j)}$ and $G_q^{(j)} \equiv (E_+^{(j)} + E_-^{(j)})/2$ are the (j)-qubit energy combinations].

We note that the spin-independent constants ($\sim\tilde{g}_0^{(j)}$) for the qubits involved in the gate can be canceled at once by synchronous resonator driving; the conditions for this are the equal frequencies of driving and modulation, and special choice of the resonator phase φ_d and driving amplitude ε_d:

$$\omega_d = \omega_m, \quad \varphi_d = \varphi_m + \pi, \quad \varepsilon_d = \varepsilon_d^0 \equiv \frac{1}{2}\sum_{j=1}^n \tilde{g}_0^{(j)}. \quad (6)$$

The always-on dispersivelike (curvature) Hamiltonian in Eq. (1) appears as a second-order effect in $\hat{V}_r$,

$$\mathcal{H}_{\delta\omega}^{(j)} = \hbar\delta\omega^{(j)}\sigma_z^{(j)}\left(\hat{a}^+\hat{a} + \frac{1}{2}\right), \qquad (7)$$

with

$$\delta\omega^{(j)} = \frac{\hbar\omega_r^2}{2}\left(\frac{\eta^{(j)}}{\hbar}\right)^2\frac{\partial^2 E_q^{(j)}}{e^2\partial V_G^2}. \qquad (8)$$

Here the name dispersivelike is convenient since this coupling coincides in its form with the dispersive limit of the J-C transverse coupling, though it has nothing to do with the latter; in fact the transverse coupling is zeroed at the full sweet spot [62], $g_\perp^{\text{sweet spot}} = 0$. The dispersivelike interaction $\mathcal{H}_{\delta\omega}^{(j)}$ causes a resonator frequency shift $\pm\delta\omega^{(j)}$ depending on the (j)th qubit spin state $|\uparrow,\downarrow\rangle_{(j)}$ that can be interpreted as due to the spin-qubit quantum capacitance [62]. In fact, it exactly coincides with an analogous expression for the quantum capacitance of a Cooper pair box see, e.g., Refs. [65–68].

Since the dynamical longitudinal coupling [Eq. (4)] is also proportional to the energy curvature $\tilde{g}_\parallel \propto \frac{\partial^2 E_q}{e^2\partial V_G^2}$, it is a quantum capacitance related coupling as well. We also note that using a quantum capacitance approach here is justified for the resonator/modulation frequency range

$$\omega_r, \omega_m \ll U_{\text{charge}}, \qquad (9)$$

since at the sweet spot the qubit dipole coupling is zero, and one needs to compare with an energy gap to the qubit higher excited states which is of the order of the QD's charging energy [62] U_{charge}. For a typical $U_{\text{charge}} \approx 0.4$ meV ≈ 100 GHz this implies $\omega_r, \omega_m \lesssim 20$ GHz.

With the curvature interactions in Eq. (1), there are two scenarios to perform accumulated geometric phase gates on a system of n qubits. In the first scenario we briefly consider in the next section (Sec. I A), the geometric phase gate is based solely on the always-on $\delta\omega^{(j)}$ couplings (we show the entangling rate to be generally small). The second scenario of a phase gate is realized via the longitudinal dynamical coupling $\tilde{g}_\parallel^{(j)}$, that is the phase gate of interest in this paper, see Secs. I B and II–V.

A. Multispin accumulated phase entangling gates via resonator driving (no qubit gate modulation)

In the first scenario, the qubits are not modulated ($\tilde{g}_\parallel = 0$), and the always-on dispersivelike static curvature interactions $\mathcal{H}_{\delta\omega}^{(j)}$ with the couplings $\delta\omega^{(j)}$ can be used to generate spin-dependent geometric phases via direct driving of the SC

resonator [52] at some detuned frequency $\omega_d \neq \omega_r$, and using a specially modulated spline microwave pulses $\varepsilon_d(t) e^{i\omega_d t}$ to suppress the (remaining) qubit-resonator entanglement as a possible source of gate infidelity [52]. At the TQD full sweet spot [Fig. 1(b)], when the dispersive transverse couplings are off, $\chi^{(j)} \equiv (g_\perp^{(j)})^2/\Delta^{(j)} = 0$, one can use the dispersivelike curvature couplings instead. Following the approach as in the superconducting entangling proposal of Cross and Gambetta [52,53], one is essentially replacing the dispersive couplings $\chi^{(j)}$ by the dispersivelike contributions $\delta\omega^{(j)}$. Then we estimated the entangling rate for two qubits to be

$$\Gamma_{\text{ent},\delta\omega}^{\text{geom}} \simeq \frac{|\varepsilon_d|^2 \delta\omega^{(j_1)} \delta\omega^{(j_2)}}{(\omega_d - \omega_r)^3}. \tag{10}$$

It is worth comparing the result of Eq. (10) to a situation with a transverse coupling [52,53], e.g., in a charge degeneracy point (c.d.p.) [62], where the transition dipole moment is maximal, and correspondingly $g_\perp^{\text{c.d.p.}} \approx \frac{\omega_r}{2}\frac{\eta}{\hbar}$. The entangling gate rate via the dispersivelike coupling at zero dipole moment will be slower than that based on the dispersive coupling at a c.d.p., by a factor of $(\delta\omega/\chi)^2$, where the coupling ratio of the two cases is given by [62]

$$\frac{\delta\omega}{\chi_{\text{c.d.p.}}} = \frac{\hbar\Delta}{e^2/2C_q}. \tag{11}$$

For a typical spin-qubit quantum capacitance of $C_q \approx 20$ aF (see Table I below), and qubit-resonator detuning $\Delta \equiv \omega_r - \omega_q \approx 5$ GHz, this amounts to $\frac{\delta\omega_{\text{sweet spot}}}{\chi_{\text{c.d.p.}}} \approx 1/25$. The suppression factor can be overcome, however, via increasing the TQD quantum capacitance, e.g., by using higher interdot tunneling rates t_c, since $C_q \propto t_c^2$. Also, the dispersive coupling χ is rapidly decreasing (since one is working out of the c.d.p. to avoid large charge noise), and thus the two types of entangling gates can be made comparable in speed.

Overall speed up of the entangling rate [Eq. (10)] can be achieved by increasing the ratio $\frac{\eta}{\hbar}$ in QD qubits, e.g., by using high kinetic inductance ($L_r \gtrsim 200$ nH) resonators [69,70], higher QDs lever arm $\alpha_c \lesssim 0.5$, and higher resonator frequencies $\omega_r \gtrsim 10$ GHz, where ratio of the $\frac{\eta}{\hbar} \sim 1$ may be reached.

In the approach outlined above, contrary to the transverse J-C coupling case in the dispersive limit [52,53], where higher photon numbers in the resonator (higher driving amplitude ε_d) involves infidelities via spurious photon transitions to higher system states (see, e.g. Ref. [60]), here one is allowed to go to higher photon numbers, since the higher-curvature Hamiltonian corrections [62] that arise for $n_{\text{phot}} \gtrsim 1$ still commute with the qubit Hamiltonian. (The role of the higher-curvature Hamiltonians will be investigated elsewhere.)

B. Accumulated phase entangling gates via qubits' longitudinal modulation

In this paper we concentrate on geometric entangling gates obtained when suitable qubits' gate voltages are modulated with the *same modulation frequency and phase* $V_m^{(j)}(t) = \tilde{V}_m^{(j)} \cos(\omega_m t + \varphi_m)$, for each qubit ($j$) participating in the entangling gate, see Fig. 2. The modulation of the qubits' energy levels, in the presence of a capacitive coupling to the resonator, leads to the longitudinal dynamical interactions

$\mathcal{H}_\parallel^{(j)}$ with the (curvature) couplings $\tilde{g}_\parallel^{(j)}$, $\tilde{g}_0^{(j)}$ of Eqs. (4) and (5), where the spin-independent coupling $\tilde{g}_0^{(j)}$ plays the role of another channel of resonator driving [compare with Eq. (6)]. The longitudinal dynamical coupling $\mathcal{H}_\parallel^{(j)}$ corresponds to a periodic in time spin-dependent "force" exerted on the resonator (see Sec. II and Appendix A). A similar approach was explored in ion traps [71–74], and recently it was proposed by Kerman [61] and others [75–78] for superconducting devices. (Similar approaches for encoded spin qubits were also proposed [79,80], see Sec. IV.)

An ideal multiqubit entangling gate arises when simultaneous periodic voltage modulation is applied to each qubit (j) of a chosen subset of n qubits, starting from a product state of the qubits plus resonator:

$$|\psi(0)\rangle = \left(\sum_{s=1}^{2^n} a_s |s\rangle\right) \otimes |0\rangle_{\text{res}}, \tag{12}$$

where

$$|s\rangle \equiv |i_1 \cdots i_j \cdots i_n\rangle, \quad i_j = \pm 1 \tag{13}$$

are the basis n-qubit product states of up (down) qubits.

The corresponding dynamical longitudinal couplings

$$\tilde{g}_\parallel^{(j)}(t) = \tilde{g}_\parallel^{(j)} \cos(\omega_m t + \varphi_m) \tag{14}$$

will be equivalent to a periodic driving of the resonator with a modulation frequency ω_m and with an amplitude dependent on the n-qubit spin state. (To get a nontrivial operation, of course, one needs to prepare the n qubits to a state different from the n-qubit ground state, which can be achieved, e.g., by local qubits' manipulations of their left and right tunnelings t_l, t_r.) Thus, after a time of one full cycle, $T_{\text{cycle}} = 2\pi/(\omega_r - \omega_m)$, when the resonator returns to its initial state (in a rotating frame with ω_r), the qubits and the resonator become again disentangled, leading to *accumulation of nontrivial geometric phases to the multiqubit state* [Eq. (12)]. Various entangling gates can be established by attaching/detaching to the resonator of some subset of qubits, by switching on/off particular qubits' modulations $V_m^{(j)}(t)$.

A substantial longitudinal (curvature) coupling exists [62,63] both at the full sweet spot or far from it, e.g., in the resonant-exchange (RX) qubit regime [3,23] [near the charge degeneracy point, see Fig. 1(b)], where the transverse coupling $g_\perp$ is the largest. In fact, at the charge degeneracy point (c.d.p.) the quantum capacitance C_q increases by a factor of $\frac{U_{\text{charge}}^3}{t_c^3} \approx 10^2$–$10^3$ with respect to the full sweet spot regime (here we have used $U_{\text{charge}} = 0.5$ meV and $t_c = 20$–40 μeV for the dot's charging energy and interdot tunneling, respectively). Since the longitudinal geometric entangling rate is of the order of $\Gamma_{\text{ent},\tilde{g}_\parallel}^{\text{geom}} \sim \tilde{g}_\parallel$ (Sec. II), a comparison with the standard transverse entangling rate $\Gamma_{g_\perp} \sim g_\perp^2/\Delta$ gives at the c.d.p.:

$$\frac{\Gamma_{\text{ent},\tilde{g}_\parallel}^{\text{geom}}}{\Gamma_{g_\perp}} \sim \frac{\tilde{g}_\parallel}{g_\perp^2/\Delta}\bigg|_{\text{c.d.p.}} = 2\left(\frac{\eta}{\hbar}\right)^{-1} \frac{C_q^{\text{c.d.p.}}}{e} \frac{\tilde{V}_m}{\omega_r} \gtrsim 10. \tag{15}$$

This demonstrates that the longitudinal geometric entangling rate can be substantially larger at the c.d.p. (note, however, that this particular estimation implies adiabaticity: $\omega_r \ll$

$\omega_q \sim \frac{t_c}{\hbar}$). The drawback of the c.d.p. regime is obviously the large charge noise, see, e.g., Ref. [9].

At the full spin-qubit sweet spot, referred to as symmetric operating point (SOP) of a DQD-ST qubit, and as the always-on exchange-only (AEON) regime [26] of a TQD qubit, the electric dipole moment goes to zero [62,63], and the longitudinal (curvature) coupling is the only remaining [62,63], while the charge noise to the qubit is suppressed. Despite the much smaller quantum capacitance at the sweet spot, a parameter regime can be provided where fast entangling multispin gates can be performed, *while each of the qubits involved is residing in its full sweet spot*, with a gate time of few tens to a hundred of nanoseconds.

C. Infidelities of the longitudinal entangling geometric phase gate

In this paper we study various kinds of imperfections that can deteriorate the accumulated phase gate performance. One major imperfection may come from the presence of the always-on dispersivelike couplings $\delta\omega^{(j)}$ [Eq. (7)] which leads to a phase-gate infidelity since it leaves small qubit-resonator entanglement at the end of each phase accumulation cycle. This can be partially canceled applying an echolike technique [61,74]. To suppress this infidelity one accumulates the necessary phase in some *even number N of cycles*, where on each next cycle the sign of the dynamical longitudinal coupling is changed by proper change of the phase φ_m of the qubits' gate modulation: $\tilde{g}_{\parallel} \to -\tilde{g}_{\parallel}$. This is, however, not sufficient to reach very small infidelities ($\lesssim 10^{-3}$) and one generally requires the ratio of the two curvature couplings

$$\frac{\delta\omega}{\tilde{g}_{\parallel}} = \frac{\eta}{\hbar} \frac{\hbar\omega_r}{e\bar{V}_m} \qquad (16)$$

to be small (that is reachable experimentally), implying smaller ratio $\frac{\eta}{\hbar}$ and smaller resonator frequencies. The small ratio $\frac{\delta\omega}{\tilde{g}_{\parallel}}$ provides the main restriction on the choice of parameters when one is aiming to approach a high-fidelity phase gate.

Another type of phase-gate infidelity arises from the resonator voltage noise (Johnson noise), which affects the resonator trajectory in the phase space, and thus, the accumulated phases. The gate infidelity shows two distinct contributions: (i) due to the fluctuations of the resonator field that scales with the number of cycles as $\sim\sqrt{N}$, and (ii) due to the fluctuations of the associated accumulated phase with a scaling $\sim 1/\sqrt{N}$. The suppression of the Johnson noise infidelity requires low enough temperatures and weak resonator coupling to environment (i.e., resonator photon leakage κ much smaller than resonator frequency ω_r).

The resonator *photon number fluctuations* also cause qubits' dephasing and AC-Stark frequency shifts, mediated via the qubit-resonator curvature interactions $\mathcal{H}_{\delta\omega}$, $\mathcal{H}_{\parallel}$, leading to small phase gate infidelities that were estimated to be negligible, see Table I.

Finally, we also estimate the phase-gate error due to qubit dephasing via the qubit gate charge noises, which seems to be the main obstacle to obtain a high-fidelity two spin-qubit gate. While charge noise will be minimized at the qubit's full sweet spot due to zeroing of the linear QD voltage fluctuations

(e.g., $\sim \frac{\partial E_q}{\partial V_{\varepsilon,m}} \delta V_{\varepsilon,m} = 0$), there remain two other sources of gate voltage noise: (i) *quadratic effects* $\sim \frac{\partial^2 E_q}{\partial V_{\varepsilon,m}^2} \delta V_{\varepsilon,m}^2$ and (ii) *tunneling gate voltage fluctuations* $\sim \frac{\partial E_q}{\partial t_c} \delta t_c$, both leading to $1/f$ noise [24,25] that cannot be canceled by the simple echolike procedure mentioned above. In the current experiment at the SOP of a DQD qubit [28,29] a dephasing time of $T_2^* \lesssim 1.5\,\mu$s was measured. The estimated $1/f$-noise phase gate-infidelity scales as $\sim (t_{\text{gate}}/T_2^*)^2$ and can reach $\lesssim 10^{-2}$ for moderate parameters; this can be improved by making the geometric phase gate faster, e.g., by increasing the qubit quantum capacitance C_q (respectively, the longitudinal coupling $\tilde{g}_{\parallel}$). While this increases the quadratic noise effects, we show they are still much smaller than the tunneling gate charge noise, which gives a hope to make all the qubit phase gate infidelities to reach the level of 10^{-3}, Table I.

An additional effect of $1/f$-charge noise on the tunnelings $t_{l,r}$ [Fig. 1(a)] leads to fluctuation of the longitudinal couplings $\tilde{g}_{\parallel}^{(j)}$. The corresponding infidelity is shown to be negligible, see Table I.

The remainder of the paper is organized as follows. In Sec. II we consider briefly the ideal case of an n-qubit phase gate, calculating the qubits' phase gate matrix. Then we specialize on the two-qubit case, calculating the gate time for a controlled π-phase gate [73]. In Sec. III the main results for the various kind of phase gate infidelities are obtained for the n-qubit case. Consequences for a two-qubit controlled π-phase gate are considered. Calculated gate times and infidelities for experimentally reachable ranges of parameters are summarized in Table I. In Sec. IV relevance to other works is given. In Sec. V we provide discussion and summary of the obtained results. Figures 1 through 10 sketch the idea of the longitudinal multiqubit phase gates and present numerical plots of the leading infidelities vs chosen range of parameters. In the Appendixes A through E we described important details of the derivations presented in the main text of the paper.

II. SPIN-DEPENDENT FORCE: IDEAL n-QUBIT ENTANGLING GEOMETRIC PHASE GATE

The time modulated longitudinal (curvature) interaction in Eq. (1) for n qubits $\mathcal{H}_{\parallel} \equiv \sum_j \hbar\{\tilde{g}_0^{(j)} \sigma_z + \tilde{g}_0^{(j)}\} \cos(\omega_m t + \varphi_m)(\hat{a} + \hat{a}^+)$ is generating a spin-dependent force: $\hat{F}(t) = -\partial\mathcal{H}_{\parallel}/\partial\hat{x}$, where $\hat{x} \equiv \Delta x_0(\hat{a} + \hat{a}^{\dagger})$ is the "position" operator, with $\Delta x_0 = e\sqrt{\frac{\hbar/e^2}{2\omega_r L_r}}$ being the resonator zero point motion. In a rotating frame with the resonator frequency ω_r and in a rotating wave approximation (RWA), $\hat{F}(t)$ will drive the resonator at the difference frequency $\omega_m - \omega_r$ with an amplitude depending on the n-qubit state $|s\rangle$ [Eq. (13)]. The n-qubit dependent resonator driving amplitude $\Omega_{\parallel,s}$ is given by (see Appendix A)

$$\Omega_{\parallel,s} \equiv \langle s|\hat{\Omega}_{\parallel}|s\rangle = \langle s| \frac{1}{2} \sum_{j=1}^{n} \left[\tilde{g}_0^{(j)} + \tilde{g}_{\parallel}^{(j)}\sigma_z^{(j)}\right] |s\rangle. \qquad (17)$$

Starting with an arbitrary resonator coherent state $|\alpha(0)\rangle$, it evolves for finite time to $|\alpha_s^{\text{id}}(t)\rangle$, with the difference

frequency $\delta \equiv \omega_m - \omega_r$:

$$\alpha_s^{\text{id}}(t) = \alpha(0) - \left(\frac{\Omega_{\parallel,s}}{\delta}\right) e^{-i\varphi_m} \left(1 - e^{-it\delta}\right) \quad (18)$$

(here "id" stands for an ideal evolution). For an initial product state of n qubits plus resonator, at intermediate times they become entangled:

$$|\Psi_i\rangle = \sum_s a_s |s\rangle |\alpha(0)\rangle \rightarrow |\Psi_f(t)\rangle = \sum_s a_s e^{i\Phi_s(t)} |s\rangle |\alpha_s(t)\rangle, \quad (19)$$

via the spin-dependent geometric phases $\Phi_s(t)$; the latter are path dependent in the resonator phase space $\{\text{Re}\,\alpha, \text{Im}\,\alpha\}$ and for harmonic modulation read (independent from the initial modulation phase φ_m)

$$\Phi_s^{\text{id}}(t) = \text{Im}\left[\int^{\alpha_s(t)} \alpha_s^*(t')\, d\alpha_s(t')\right] = \left(\frac{\Omega_{\parallel,s}}{\delta}\right)^2 [\delta t - \sin\delta t]. \quad (20)$$

Using that $\hat{\Omega}_{\parallel,s}$ and $\hat{\Omega}_{\parallel,s}^2$ have the same eigenstates $|s\rangle$, one also derives the general *accumulated phase matrix for n qubits* [dropping the common phase, see Appendix A, Eq. (A11)]:

$$\hat{\Phi}(t) = \frac{(\sin\delta t - \delta t)}{2\delta^2}$$
$$\times \left[\sum_{j<k}^n \tilde{g}_{\parallel}^{(j)} \tilde{g}_{\parallel}^{(k)} \sigma_z^{(j)} \otimes \sigma_z^{(k)} + \sum_{j=1}^n \tilde{g}_0^{(j)} \sum_{k=1}^n \tilde{g}_{\parallel}^{(k)} \sigma_z^{(k)}\right], \quad (21)$$

where the second (double) sum amounts to single qubit operations that can be canceled at once by the synchronous resonator driving [Eq. (6)]. For a gate time of N completed cycles, $t_g = \frac{2\pi N}{\delta}$, the resonator returns to its initial state $|\alpha_s(t_g)\rangle = |\alpha(0)\rangle$, independent of the n-qubit spin configuration. Thus, the qubits-resonator state again becomes disentangled, while the n-qubit state [Eq. (19)] acquires the phases $\Phi_s(t_g) = 2\pi(\Omega_{\parallel,s}/\delta)^2$ that comprises an n-qubit entangling gate.

Specializing for two qubits (and performing N cycles), the spin-dependent accumulated phase matrix is

$$\hat{\Phi}_N = -\frac{2\pi N}{\delta^2}\big[\tilde{g}_{\parallel}^{(1)} \tilde{g}_{\parallel}^{(2)} \sigma_z^{(1)} \otimes \sigma_z^{(2)}$$
$$+ \big(\tilde{g}_0^{(1)} + \tilde{g}_0^{(2)}\big)\big(\tilde{g}_{\parallel}^{(1)} \sigma_z^{(1)} + \tilde{g}_{\parallel}^{(2)} \sigma_z^{(2)}\big)\big], \quad (22)$$

which comprises a two-qubit gate up to single-qubit rotations (Appendix A). For the case of a TQD exchange-only qubit these rotations can be performed for each qubit (j) while residing in their full sweet spot, by simply manipulating the tunneling amplitudes $t_l^{(j)}, t_r^{(j)}$, see Refs. [26,62].

Using Eq. (22) for two particular qubits for the choice of the frequency detuning $\delta_\pi(N)$, such that $\delta_\pi^2 = 4N\tilde{g}_{\parallel}^{(1)} \tilde{g}_{\parallel}^{(2)}$, one obtains an accumulated two-qubit phase matrix $\hat{\Phi}_\pi = -\frac{\pi}{4}\sigma_z^{(1)} \otimes \sigma_z^{(2)}$ corresponding to a controlled π-phase gate [61,73] (Appendix A). For this ideal situation to happen one requires that the frequency detuning to be at least $\delta_\pi(N) \gg \kappa$, with κ being the resonator damping rate, implying a high Q-factor SC resonator ($Q \gtrsim 10^3$–10^6). Other restrictions on the resonator and qubit parameters will follow from minimization
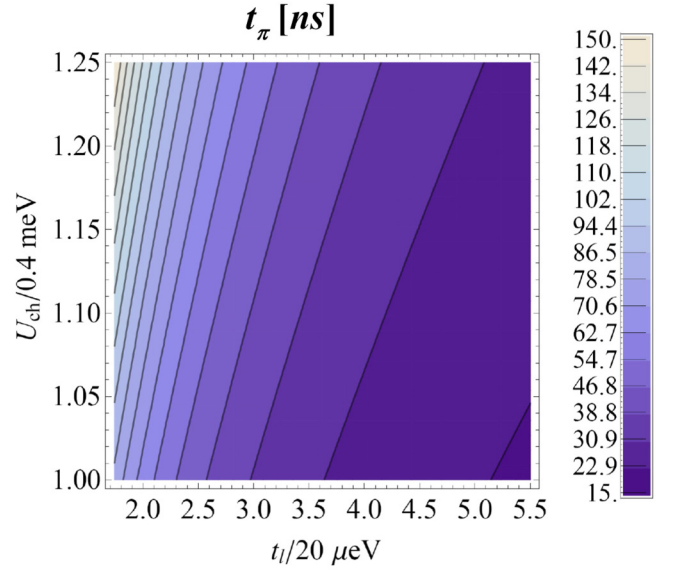

FIG. 3. Gate time t_π of a two-qubit controlled π-phase gate for TQD exchange only qubits [Eq. (23)] is plotted vs interdot tunneling amplitude $t_l = t_r$ and dots' charging energy U_{ch}, for fixed qubits' modulation $\tilde{V}_m = 0.1$ mV, resonator frequency $\omega_r \simeq 6.3$ GHz, resonator inductance $L_r = 50$ nH (impedance $Z_r \simeq \omega_r L_r \simeq 1.85$ kΩ; compare, e.g., with Ref. [81]), and qubits'-resonator lever arm $\alpha_c \simeq 0.14$ that amounts to a reachable coupling ratio of $\eta/\hbar = \alpha_c\sqrt{\frac{Z_r}{\hbar/e^2}} \simeq 0.1$. The gate time t_π ranges from 15 to 150 ns for $t_l \simeq [35, 110]\,\mu$eV and $U_{\text{ch}} \in [0.4, 0.5]$ meV, featuring relatively high tunneling amplitudes and relatively low dots' charging energies. The scaling of the gate time $t_\pi \sim 1/\sqrt{L_r}$ leads to a moderate increase for smaller resonator inductances L_r. By reaching higher experimental values for α_c, ω_r, and $\tilde{V}_m$ one can bring the dots' tunneling and charging energy to experimentally more favorable ranges [9]. Since for a DQD S-T qubit the scaling of the longitudinal coupling [Eq. (4)] with parameters is exactly the same [62], one expects similar ranges for these systems.

of the two-qubit gate infidelities. The entangling gate time reads

$$t_\pi = \frac{2\pi N}{\delta_\pi} = \pi\sqrt{\frac{N}{\tilde{g}_{\parallel}^{(1)} \tilde{g}_{\parallel}^{(2)}}} \quad (23)$$

and reaches 15–150 ns for the parameters of Fig. 3, see also Table I.

III. QUBIT AND RESONATOR WITH DECOHERENCE AND THE PHASE GATE ERRORS

The qubit entangling gate errors arise from several sources (see Fig. 4), including (i) resonator damping κ, (ii) qubit-induced spin-dependent resonator frequency shifts $\delta\omega_s$ via the always-on dispersivelike curvature coupling, Eqs. (7) and (8), (iii) resonator thermal (Johnson) noise, and qubit dephasing due to (iv) photon number fluctuation in the resonator and due to (v) charge $1/f$ noise on the qubit defining gates; (vi) finally, one also considers the effect charge $1/f$ noise on the qubit's tunneling gates, causing additional resonator trajectory deviations via a change of the curvature (longitudinal) coupling $\tilde{g}_{\parallel}$.
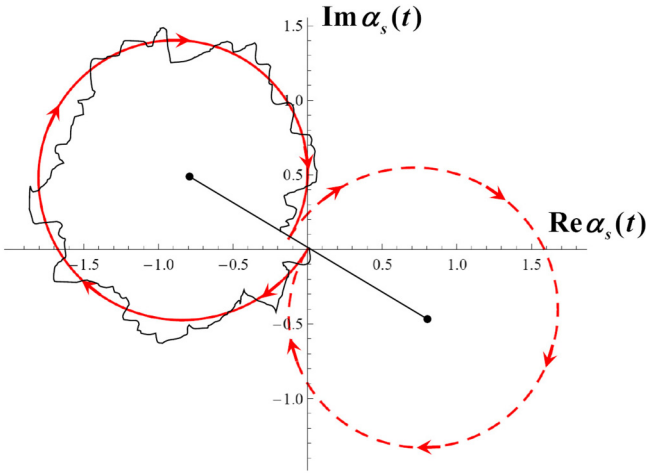
FIG. 4. The nonideal oscillator trajectories in the phase space $\{\text{Re}[\alpha_s(t)], \text{Im}[\alpha_s(t)]\}$ for two subsequent cycles, each of duration $t_g = 2\pi/\delta$. The ideal evolution $\alpha_s^{\text{id}}(t)$ obtains deviations $\delta\alpha_s(t)$ (red solid or dashed decaying circles) due to (i) resonator damping κ [Eqs. (27) and (35)], and (ii) qubit-induced spin-dependent resonator frequency shifts $\delta\omega_s$ [Eqs. (1), (27), and (35)] via the always-on dispersivelike curvature coupling [Eq. (7)]. By changing the modulation phase for every odd cycle: $\varphi_m' = \varphi_m + \pi$, the spin-dependent resonator driving amplitude $\Omega_{\parallel,s}$ flips sign (red, dashed decaying circle; sf. also Fig. 10) that allows partial cancellation of the deviations, for small κ, $\delta\omega_s$. The (iii) resonator thermal (Johnson) noise is shown schematically (black, solid line) as a noisy deviation from the ideal trajectory $\alpha_s^{\text{id}}(t)$. The noisy trajectory is generated by a random force Hamiltonian $\mathcal{H}_f = -\xi_f(t)\hat{x}$ [see Eq. (36) and Appendix D], which is an unraveling of the diffusion term in the ensemble-averaged evolution [Eq. (27)].

The effects (iv), (v), and (vi) of qubits' defining gates charge noise are considered latter on in Secs. III C and III D.

The first three effects, (i)–(iii), as well as (vi), cause (time-dependent) deviations from the ideal *resonator trajectory* in the phase space [Eqs. (18) and (20)], changing both the (spin-dependent) resonator trajectories (Fig. 4)

$$\alpha_s(t) = \alpha_s^{\text{id}}(t) + \delta\alpha_s^{\kappa,\delta\omega} + \delta\alpha_s^{\xi} + \delta\alpha_s^{\tilde{g}_{\parallel},1/f} \quad (24)$$

and the corresponding accumulated phases

$$\Phi_s(t;[\alpha_s(t)]) = \Phi_s^{\text{id}}(t) + \delta\Phi_s^{\kappa,\delta\omega} + \delta\Phi_s^{\xi} + \delta\Phi_s^{\tilde{g}_{\parallel},1/f}, \quad (25)$$

the latter causing path-dependent nonlocal in time errors. Correspondingly, as compared to the ideal values, the change in the final resonator state $|\alpha_s(t_g)\rangle$ leaves some qubit-resonator entanglement at the end of the phase gate accumulation cycle, leading to qubits' phase gate infidelity $\delta\varepsilon_{\text{traject}}$. For small deviations of the trajectory: $\delta\alpha_s^{\kappa,\delta\omega}, \delta\alpha_s^{\xi}, \delta\alpha_s^{\tilde{g}_{\parallel},1/f} \ll 1$ and $\delta\Phi_s^{\kappa,\delta\omega}, \delta\Phi_s^{\xi}, \delta\Phi_s^{\tilde{g}_{\parallel},1/f} \ll 1$, the infidelity splits into separate terms (Appendix C 1):

$$\delta\varepsilon_{\text{traject}} \simeq \delta\varepsilon_{\kappa,\delta\omega} + \delta\varepsilon_{\xi} + \delta\varepsilon_{\tilde{g}_{\parallel},1/f}. \quad (26)$$

The superconducting (SC) resonator-to-environment interaction at finite temperature is described via the Caldeira-Leggett master equation (ME) [82,83] and includes damping

(κ) and diffusion (K_d) contributions. The time evolution of the qubit(s)-resonator density matrix reads

$$\frac{d\rho}{dt} = -i[\tilde{\mathcal{H}}_{\text{tot}}, \rho] - i\frac{\kappa}{2\hbar}[\hat{x}, \{\hat{p}, \rho\}_+] - \frac{K_d}{\hbar^2}[\hat{x}, [\hat{x}, \rho]], \quad (27)$$

$$K_d \equiv \frac{\hbar\omega_r L_r \kappa}{2} \coth\frac{\hbar\omega_r}{2k_B T_r}, \quad (28)$$

where $\hat{x}$ and $\hat{p}$, are the "position" and "momentum" operators [84] [Eq. (B2)], and $\{ , \}_+$ is an anticommutator. The last (double commutator) term in Eq. (27) is governed by a temperature dependent diffusion coefficient K_d, and T_r is the resonator temperature [85]. (An analog of the Caldeira-Leggett ME (27) is the quantum-optics ME [86]; the two master equations coincide in the RWA and especially for Gaussian states considered in this paper. We will use one or another form of the ME for convenience, Appendix B.)

The qubit-resonator density matrix can be expanded in a complete set of qubit operators $|s\rangle\langle s'|$ [87]:

$$\rho = \sum_{s,s'} \hat{\rho}_{s,s'} |s\rangle\langle s'|, \quad (29)$$

where the partial density matrices $\hat{\rho}_{s,s'}$ act only on the resonator subspace. Using Eq. (27), in a general rotating frame with frequency $\omega_{r'}$ and in RWA, one gets the equation for the spin-diagonal resonator density matrices (Appendix B 1):

$$\frac{d\hat{\rho}_{ss}}{dt} = -i\tilde{\omega}_r[a^+a, \hat{\rho}_{ss}] - i\Omega_{\parallel,s}[\hat{X}_{\varphi_m}(t), \hat{\rho}_{ss}]$$
$$- i\varepsilon_d[\hat{X}_{\varphi_d}(t), \hat{\rho}_{ss}] - i\delta\omega_s[a^+a, \hat{\rho}_{ss}]$$
$$- i\frac{\kappa}{2\hbar}[\hat{x}\{\hat{p}, \hat{\rho}_{ss}\}_+] - \frac{K_d}{\hbar^2}[\hat{x}[\hat{x}, \hat{\rho}_{ss}]], \quad (30)$$

where the modulating and driving terms $\hat{X}_{\varphi_m}, \hat{X}_{\varphi_d}$ are given by $\hat{X}_{\varphi}(t) \equiv [\hat{a}e^{i(\tilde{\delta}t+\varphi)} + \hat{a}^+ e^{-i(\tilde{\delta}t+\varphi)}]$, and the detunings are

$$\tilde{\omega}_r = \omega_r - \omega_{r'}, \quad \tilde{\delta} = \omega_m - \omega_{r'}. \quad (31)$$

The resonator frequency shift for n qubits in the $|s\rangle$ state is given by

$$\delta\omega_s = \langle s|\sum_j \delta\omega^{(j)}\sigma_z^{(j)}|s\rangle, \quad (32)$$

with the individual curvature frequency shifts $\delta\omega^{(j)}$ given by Eq. (8). The spin-diagonal Eq. (30) can be reduced to equations for the set of moments, e.g., the averages $\bar{x}_s \equiv \langle\hat{x}\rangle_s = \text{Tr}[\hat{x}\hat{\rho}_{s,s}], \bar{p}_s \equiv \langle\hat{p}\rangle_s = \text{Tr}[\hat{p}\hat{\rho}_{s,s}]$, the variances, $D_x^{(s)} \equiv \langle\hat{x}^2\rangle_s - \langle\hat{x}\rangle_s^2, D_p^{(s)} \equiv \langle\hat{p}^2\rangle_s - \langle\hat{p}\rangle_s^2, D_{xp}^{(s)} \equiv \langle\frac{\hat{x}\hat{p}+\hat{p}\hat{x}}{2}\rangle_s - \langle\hat{x}\rangle_s\langle\hat{p}\rangle_s$, etc., see Appendix B 3. One obtains for the averages:

$$\frac{\dot{\bar{x}}_s}{\Delta x_0} = \frac{\bar{p}_s}{\Delta p_0}(\tilde{\omega}_r - \delta\omega_s) - 2\Omega_{\parallel,s}\sin(\tilde{\delta}t + \varphi_m), \quad (33)$$

$$\frac{\dot{\bar{p}}_s}{\Delta p_0} = -\frac{\bar{x}_s}{\Delta x_0}(\tilde{\omega}_r - \delta\omega_s) - 2\Omega_{\parallel,s}\cos(\tilde{\delta}t + \varphi_m)$$
$$- 2\varepsilon_d e^{-i(\tilde{\delta}t+\varphi_d)} - \kappa\frac{\bar{p}_s}{\Delta p_0}. \quad (34)$$

We notice several important properties of Eqs. (33) and (34) that coincide with the single resonator case [88]. First, for zero temperature a coherent resonator state remains coherent, while it is damped to the ground state $|0\rangle$ at long times

$t \gg 1/\kappa$ (in particular, the state purity is preserved). Second, the equations for the averages $\bar{x}$, $\bar{p}$ are not affected by the diffusion term and decouple from the variances (Appendix B 3). In addition, we show that the variances are not affected by the longitudinal coupling modulation or by the resonator driving (Appendix B 3).

The above statements are correct for any resonator state. In what follows we consider solutions of Eq. (27) with Gaussian density matrices since typical initial states are Gaussian (e.g., a coherent or a thermal state) and Gaussian states are preserved under the evolution of Eq. (27). They are also preserved by continuous measurements (see Ref. [88] and references therein). Thus, Eq. (30) reduces to equations for the set of five Gaussian moments, since the higher moments are expressed by the former.

Using the field variable $\alpha_s \equiv \langle \hat{a} \rangle_s = \frac{1}{2}(\frac{\bar{x}_s}{\Delta x_0} + i\frac{\bar{p}_s}{\Delta p_0})$, Eqs. (33) and (34) are combined to

$$\dot{\alpha}_s = -i(\tilde{\omega}_r - \delta\omega_s)\alpha_s - i\Omega_{\parallel,s}e^{-i(\tilde{\delta}t+\varphi_m)}$$
$$- i\varepsilon_d e^{-i(\tilde{\delta}t+\varphi_d)} - \frac{\kappa}{2}(\alpha_s - \alpha_s^*), \quad (35)$$

where the difference from the quantum optics equation is the last (contrarotating) term that can be neglected in a RWA. Note that disregarding it will be equivalent to neglecting the usual resonator frequency shift due to damping. Equation (35) for α_s does not include the thermal diffusion, the latter is giving a contribution only to the equations for the variances $D_x^{(s)}$, $D_p^{(s)}$, $D_{xp}^{(s)}$, see Appendix B 3, that will contribute to the variances of the field $\langle |\delta\alpha_s(t)|^2 \rangle$ and the accumulated phases $\langle \delta\Phi_s(t)\delta\Phi_{s'}(t) \rangle$, see Sec. III B.

Since the gate error is nonlocal in time [e.g., via the accumulated phases $\Phi_s(t; [\delta\alpha_s(t)]) \propto \int \alpha_s^*(t')d\alpha_s(t')$, Eq. (20)], it is useful to represent the thermal diffusion term as originating from a stochastic time-dependent term (Appendix D)

$$\mathcal{H}_f = -\xi_f(t)\hat{x}, \quad (36)$$

which represents a random force Hamiltonian; here $\xi_f(t)$ is a white noise "random force" with spectral density given by the correlator $\langle \xi_f(t)\xi_f(t') \rangle = \frac{S_f}{2}\delta(t - t')$. Then, the resulting fluctuations of the (spin-dependent) resonator trajectory (Fig. 4) will be integrated into the accumulated variances.

Thus, in Eq. (27) one is replacing the last (double commutator) term by the random force Hamiltonian, Eq. (36). As shown in Appendix D, the two representations are equivalent. Indeed, by adding the random force Hamiltonian to the equation of motion $\frac{d\rho}{dt} \sim -\frac{i}{\hbar}[\mathcal{H}_f, \rho]$, and transforming from Stratonovich form of the equations to its Itô form [88], one reproduces the double commutator term in Eq. (27) if the spectral density is chosen as $S_f = 4K_d$. The "standard" ensemble averaged evolution, Eq. (27), is then obtained by averaging out the noise. In what follows, in Sec. III B, we will use the random force Hamiltonian to calculate the diffusion (Johnson) noise gate error, by averaging out the noise at the end of the procedure. In the next section (Sec. III A) we first consider the situation when the ideal evolution in the phase space is disturbed only by resonator damping and n-qubit spin-dependent detuning.

A. Damping and detuning gate errors for *n* qubits: Two-qubit numerical study

For each n-qubit state $|s\rangle$, damping κ and spin-dependent detuning $\delta\omega_s$ lead to shrinking and deviation of the ideal circle in the phase space {Reα, Imα}, leaving the qubits and the resonator entangled at the time of one cycle, $t_g = 2\pi/\delta$ (see Fig. 4) [since $\alpha_s(\frac{2\pi}{\delta}) \neq 0$], and disturbing the accumulation phases. Starting from an initial product state of n qubits and resonator $|\psi_i\rangle \equiv \sum_s a_s|s\rangle|0\rangle$ [we assume vacuum resonator initial state, for simplicity], one ends up in the state

$$|\psi_f\rangle = \sum_s a_s e^{i\Phi_s(t)}|s\rangle|\alpha_s(t)\rangle|_{t=\frac{2\pi}{\delta}}, \quad (37)$$

where $\alpha_s(t) = \alpha_s^{\text{id}}(t) + \delta\alpha_s^{\kappa,\delta\omega}(t)$ and $\Phi_s(t) = \Phi_s^{\text{id}}(t) + \delta\Phi_s^{\kappa,\delta\omega}(t)$ differ from the ideal values [scf. Eqs. (A3) and (A8)] by the small deviations $\delta\alpha_s^{\kappa,\delta\omega}(t)$, $\delta\Phi_s^{\kappa,\delta\omega}(t)$, due to damping and detuning. Using the matrix element

$$\langle\psi_f|\psi_f^{\text{id}}\rangle = \sum_s |a_s|^2 e^{-i\delta\Phi_s(t)}\langle\alpha_s(t)|0\rangle, \quad (38)$$

one obtains for small deviations $\delta\alpha_s^{\kappa,\delta\omega}$, $\delta\Phi_s^{\kappa,\delta\omega}$, the gate error (infidelity) for n qubits (Appendix C 1):

$$\delta\epsilon_{\kappa,\delta\omega}^{\text{n Qb}} \lesssim \frac{1}{2^n}\sum_s |\delta\alpha_s^{k,\delta\omega}|^2 + \frac{f_{12}^{(n)}}{2}\sum_{s<s'}\left(\delta\Phi_s^{\kappa,\delta\omega} - \delta\Phi_{s'}^{\kappa,\delta\omega}\right)^2, \quad (39)$$

where the averaging over the initial n-qubit state $f_1^{(n)} = f_s^{(n)} \equiv \overline{|a_s|^2}$, $f_{12}^{(n)} = f_{s,s'}^{(n)} \equiv \overline{2|a_s|^2|a_{s'}|^2}$ [using uniformity of the averages, see Eq. (C13) and Appendix C 2] results in

$$f_s^{(n)} = f_{s,s'}^{(n)} = \frac{1}{2^n + \frac{2^{2n}-2^n}{2}}. \quad (40)$$

To lower the average gate infidelity $\delta\epsilon_{\kappa,\delta\omega_s}$, one needs to suppress $\delta\alpha_s$ and $(\delta\Phi_s - \delta\Phi_{s'})$ at the end of the cycle.

The simplest strategy (Appendix C 3) is to change the sign of the driving amplitude $\Omega_{\parallel,s}$ by changing the phase of the qubits gates modulations $\varphi_m \to \varphi_m + \pi$, see Eq. (35). By performing a second cycle, with flipped sign of $\Omega_{\parallel,s}$ an opposite shrinking of the second cycle (Fig. 4) will (partially) compensate the first one (scf. Refs. [61,89]). In the simple case, when detunings are neglected, $\delta\omega_s = 0$, at the end of the second cycle one gets, starting at $\alpha_s(0) = 0$:

$$\delta\alpha_s\left(\frac{4\pi}{\delta}\right) \equiv \tilde{\alpha}_s\left(\frac{4\pi}{\delta}\right) \simeq -\alpha_s\left(\frac{2\pi}{\delta}\right)\left(\frac{\pi\kappa}{\delta}\right), \quad (41)$$

i.e., the α deviation for two cycles is suppressed by extra power of κ/δ, for $\kappa \ll \delta$. Here $\tilde{\alpha}_s(t)$ denotes a time evolution via Eq. (35) with flipping sign of the modulation strength $\Omega_{\parallel,s}$ after each cycle. For the realistic case, when $\delta\omega_s \gg \kappa$, one solves Eq. (35) iteratively, for N cycles ($N = 1, 2, 3, \dots$) with every even cycle with the sign of $\Omega_{\parallel,s}$ flipped, and obtains for the deviation of the resonator variable $\delta\alpha_s$ in Eq. (39):

$$\delta\alpha_s^{\kappa,\delta\omega} \equiv \tilde{\alpha}_s\left(N\frac{2\pi}{\delta}\right) = \alpha_s\left(\frac{2\pi}{\delta}\right)\frac{e^{b_s^* N\frac{2\pi}{\delta}} - (-1)^N}{e^{b_s^*\frac{2\pi}{\delta}} + 1}, \quad (42)$$

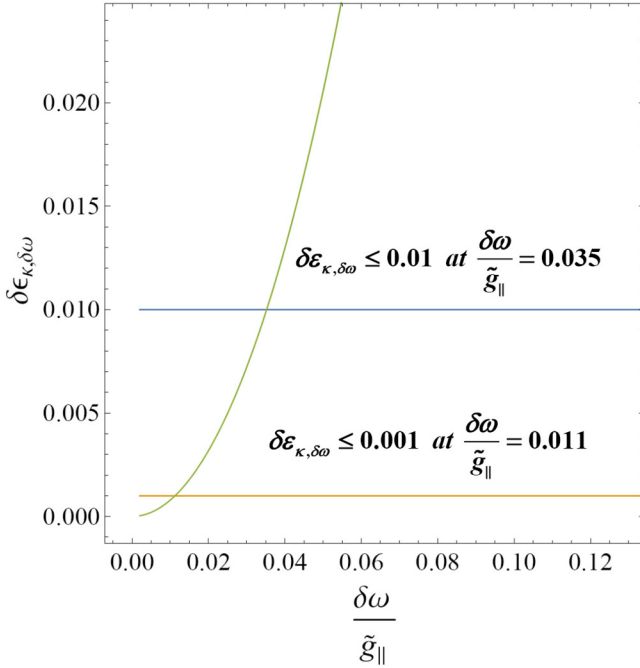where $b_s \equiv -i[\delta - \delta\omega_s] - \frac{\kappa}{2}$.

FIG. 5. The infidelity $\delta\epsilon_{\kappa,\delta\omega}^{2\,\mathrm{Qb}}(\frac{\delta\omega}{\tilde{g}_\parallel},0)$ [Eqs. (39) and (44)] is a growing function of the ratio $\frac{\delta\omega}{\tilde{g}_\parallel} = \frac{\eta}{\hbar}\frac{\hbar\omega_r}{e\tilde{V}_m}$. The values of $\frac{\delta\omega}{\tilde{g}_\parallel} = 0.035$, 0.011 at which $\delta\epsilon_{\kappa,\delta\omega} = 0.01$, 0.001, respectively, are calculated for resonator driving and phase [Eq. (6)] at which the qubits' spin-independent curvature couplings $\tilde{g}_0^{(j)}$ are canceled, see Eq. (43).

FIG. 6. The infidelity $\delta\epsilon_{\kappa,\delta\omega}^{2\,\mathrm{Qb}}(\omega_r,\tilde{V}_m)$ for the range of resonator frequency $\omega_r \in [2, 10]$ GHz and qubits gate modulation voltage (amplitude) $\tilde{V}_m \in [0.05, 0.25]$ mV. Contours where the infidelity reaches the values of 0.1, 0.01, 0.001 are also shown. To keep $\delta\epsilon_{\kappa,\delta\omega}$ constant requires keeping the ratio $\frac{\omega_r^{3/2}}{\tilde{V}_m}$ constant (see text).

The expressions for the calculation of $|\delta\alpha_s^{k,\delta\omega}|^2$ and $(\delta\Phi_s^{k,\delta\omega} - \delta\Phi_{s'}^{k,\delta\omega})^2$ are cumbersome and are presented in Appendix C 3, by Eqs. (C31)–(C41). The n-qubit entangling gate is essentially driven only by the spin-dependent longitudinal couplings $\tilde{g}_\parallel^{(j)}$, see Eq. (21). The modulation of the qubits gates creates, however, *the spin-independent couplings* $\tilde{g}_0^{(j)}$, which affect the infidelity considerably. Aiming to cancel the $\tilde{g}_0^{(j)}$ couplings of the qubits involved into the entangling gate, one is driving the resonator with the same frequency as the modulation $\omega_d = \omega_m$, and with a phase $\varphi_d = \varphi_m + \pi$, see Eq. (6). Then the quantities of interest are shown to depend on a modified spin-dependent driving strength

$$\Omega_{\parallel,s}^\varepsilon \equiv \Omega_{\parallel,s} - \varepsilon_d, \qquad (43)$$

and benefit from the cancellation of the $\tilde{g}_0^{(j)}$, see Eqs. (C38)–(C40). Numerically, for the choice of parameters of Figs. 3 and 5, and Table I, we have shown that the infidelity $\delta\epsilon_{\kappa,\delta\omega}$ improves more than 30 times for the conditions of Eq. (6).

While $\delta\alpha_s$ is effectively suppressed by increasing the number of (pair of) cycles, the accumulated phase deviations $\delta\Phi_s$ may remain large for finite detunings [90] $\delta\omega_s$, and can be suppressed only by suitable choice of the parameters. In what follows, we consider a two-qubit gate infidelity, taking identical curvature couplings $\delta\omega^{(1)} = \delta\omega^{(2)}$ and $\tilde{g}_\parallel^{(1)} = \tilde{g}_\parallel^{(2)}$. From dimensional considerations the infidelity $\delta\epsilon_{\kappa,\delta\omega}^{2\,\mathrm{Qb}}$, see Eq. (39), is a function of two dimensionless ratios:

$$\delta\epsilon_{\kappa,\delta\omega} = \delta\epsilon_{\kappa,\delta\omega}\left(\frac{\delta\omega}{\tilde{g}_\parallel}, \frac{\kappa}{\tilde{g}_\parallel}\right) \simeq \delta\epsilon_{\kappa,\delta\omega}\left(\frac{\delta\omega}{\tilde{g}_\parallel}, 0\right), \qquad (44)$$
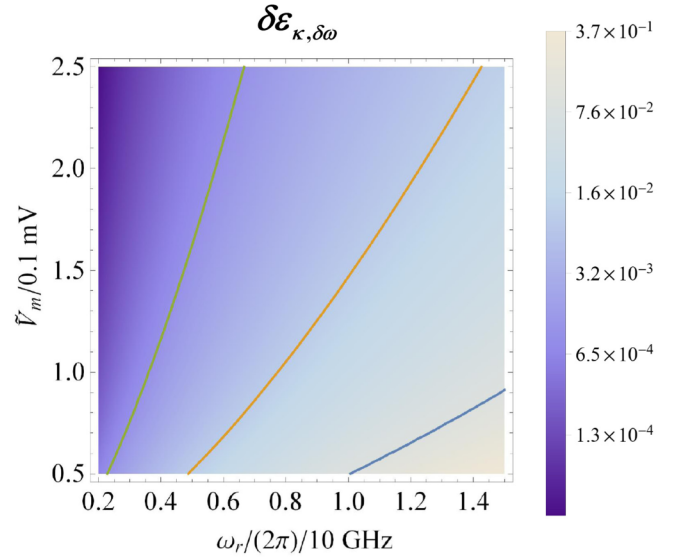
where for high $Q \simeq 10^5$–10^6 the ratio $\frac{\kappa}{\tilde{g}_\parallel}$ can be set to zero. Since $\frac{\delta\omega}{\tilde{g}_\parallel} = \frac{\eta}{\hbar}\frac{\hbar\omega_r}{e\tilde{V}_m}$ [Eq. (16)] the infidelity is independent of the qubits' energy curvature (quantum capacitance). In Fig. 5 is shown numerically the dependence of $\delta\epsilon_{\kappa,\delta\omega}^{2\,\mathrm{Qb}}(\frac{\delta\omega}{\tilde{g}_\parallel},0)$, which grows rapidly with $\frac{\delta\omega}{\tilde{g}_\parallel}$. For the values of $\frac{\delta\omega}{\tilde{g}_\parallel} = 0.035$, 0.011, the infidelity $\delta\epsilon_{\kappa,\delta\omega}$ reaches the levels 0.01 or 0.001, respectively.

In Fig. 6 is shown numerically the dependence of $\delta\epsilon_{\kappa,\delta\omega}^{2\,\mathrm{Qb}}(\omega_r,\tilde{V}_m)$ for the range of resonator frequency $\omega_r \in [2, 10]$ GHz and qubits gate modulation voltage (amplitude) $\tilde{V}_m \in [0.05, 0.25]$ mV. Contours where the infidelity reaches the values of 0.1, 0.01, 0.001 are also shown. To reach a level of 10^{-3}, this infidelity requires higher $\tilde{V}_m \gtrsim 2$ mV, and relatively low $\omega_r \lesssim 6$–10 GHz.

In what follows, for the calculation of the other infidelities (Table I) our strategy is to fix the ratio $\frac{\delta\omega}{\tilde{g}_\parallel} \simeq 0.026$ for which the infidelity $\delta\epsilon_{\kappa,\delta\omega}^{2\,\mathrm{Qb}}$ reaches $\simeq 5 \times 10^{-3}$. For the chosen ratio $\frac{\delta\omega}{\tilde{g}_\parallel}$, an experimentally reachable lever arm of $\alpha_c \simeq 0.14$, resonator inductance, $L_r = 50$ nH, and a voltage modulation amplitude of $\tilde{V}_m = 0.1$ mV, one requires a resonator frequency $\omega_r/2\pi \simeq 6.3$ GHz, see Table I.

It will be beneficial to increase the voltage modulation amplitude $\tilde{V}_m$ in order to increase the longitudinal coupling $\tilde{g}_\parallel$ (e.g., to compensate the smallness of the lever arm α_c, respectively of $\frac{\eta}{\hbar}$), reaching smaller gate times. Then, in order to keep the infidelity $\delta\epsilon_{\kappa,\delta\omega}$ constant (Fig. 6) one will also need a higher resonator frequency, so to keep the ratio $\frac{\omega_r^{3/2}}{\tilde{V}_m}$ constant [Eq. (16)]. Thus, for $\tilde{V}_m = 0.1$, 0.2, 0.3 mV one would obtain $\omega_r/2\pi \simeq 6.3$, 10., 13.1 GHz, which is beneficial for suppressing the charge noise gate error, see Eq. (80) and Table I.

By increasing the modulation amplitude $\tilde{V}_m$, however, one is increasing the relative contribution of the higher-curvature

corrections [62] (for the sweet spot they are proportional to the higher energy curvature $\frac{\partial^4 E_q}{\partial V_m^4}$). Some of these corrections [62] just change $\tilde{g}_\parallel$ and $\delta\omega_s$ (relative corrections are of the order of $\propto [\frac{e\tilde{V}_m}{U_{ch}}]^2$), keeping their ratio nearly the same. In addition, the higher-curvature corrections generate the nonlinear Hamiltonians [62] $\mathcal{H}_{\hat{n}^2} = \hbar(\zeta_0 + \zeta_\parallel \sigma_z)\hat{n}^2$, $\mathcal{H}_{\hat{n}\hat{a}} = \hbar(\xi_0 + \xi_\parallel \sigma_z)(\hat{n}\hat{a} + \hat{a}^\dagger \hat{n})\cos(\omega_m t + \varphi_m)$, with a relative strength suppressed by the factors $\langle \hat{n} \rangle [\frac{\hbar\omega_r}{U_{ch}}]^2 [\frac{\eta}{\hbar}]^2$, which makes them of the order of $\lesssim 10^{-4}$ since the average photon number in the resonator is of order of $\langle \hat{n} \rangle \lesssim 1$, see Table I and Eq. (B51), Appendix B 5.

B. Resonator (Johnson) noise phase gate error for n qubits: Two-qubit numerics

Consider now the situation when one performs ideal evolution in the phase space disturbed only via the random force Hamiltonian $\mathcal{H}_f$, Eq. (36) and Fig. 4 (assuming small noise deviations, Appendix C 1). The random force makes the trajectory in the phase space noisy, by adding a new term in the equation of motion, see Eq. (D13): $\frac{d\alpha_s(t)}{dt} = \cdots + i\frac{\xi_f(t)}{2\Delta p_0}e^{i\omega_r t}$. Correspondingly, as $\alpha_s(t) = \alpha_s^{id}(t) + \delta\alpha_s^\xi(t)$ and $\Phi_s(t) = \Phi_s^{id}(t) + \delta\Phi_s^\xi(t)$, the noise affects the final resonator state (for each n-qubit state $|s\rangle$), as well as the accumulated phase, so that some qubit-resonator entanglement still remains at the time of one cycle $t_g = \frac{2\pi}{\delta}$. Starting from an initial product state of n qubits and resonator, one obtains the fidelity $F \equiv |\langle \Psi_f | \Psi_f^{id} \rangle|^2$, similar to Eq. (38), averaging on the n-qubit initial states and on the noise. The average infidelity $\delta\epsilon_\xi$ reads (Appendix C 1)

$$\delta\epsilon_\xi^{n\,Qb} = 1 - \overline{\langle |\langle \Psi_f | \Psi_f^{id} \rangle|^2 \rangle}_\xi$$
$$= \langle |\delta\alpha_s^\xi|^2 \rangle_\xi + \frac{f_{12}^{(n)}}{2} \sum_{s<s'} \langle (\delta\Phi_s^\xi - \delta\Phi_{s'}^\xi)^2 \rangle_\xi, \quad (45)$$

where we have used that the variance of $\delta\alpha_s^\xi(t)$, and initial state averages $f_s^{(n)} \equiv \overline{|a_s|^2}$, $f_{s,s'}^{(n)} \equiv \overline{2|a_s|^2|a_{s'}|^2}$ are spin independent, see Eqs. (C12) and (C13), Appendix C 2.

To calculate the variances (Appendix D) one uses the noise contribution $\delta\alpha_s(t)$ in rotating frame with ω_r,

$$\delta\alpha_s(t) = i\frac{\Delta x_0}{\hbar} \int_0^t dt' \xi_f(t') e^{i\omega_r t'} \quad (46)$$

and obtains a spin-independent variance of (otherwise spin-dependent evolution of) $\alpha_s(t)$:

$$\langle |\delta\alpha_s(t)|^2 \rangle_\xi = \left(\frac{\Delta x_0}{\hbar}\right)^2 \int_0^t \int_0^t dt' dt'' e^{i\omega_r(t'-t'')} \langle \xi_f(t')\xi_f(t'') \rangle_\xi$$
$$= \frac{K_d}{2(\Delta p_0)^2} t \equiv C_0 t \quad (47)$$

that is linear in time t, as expected for a diffusion process.

To obtain the phase variance $\langle \delta\Phi_s(t)^2 \rangle_\xi = \langle [\text{Im}\,\delta I_{\Phi,s}]^2 \rangle_\xi$ one considers the variation of the accumulated phase integral [scf. Eq. (A8)], assuming small variations:

$$\delta I_{\Phi,s}(t) \simeq \int_0^t dt' \left[\delta\alpha_s^*(t')\frac{d\alpha_s^{id}(t')}{dt'} + \alpha_s^{id\,*}(t')\frac{d\delta\alpha_s(t')}{dt'} \right], \quad (48)$$

and averages over the noise, similar to Eq. (47).

Averaging over the noise, the variance of the accumulated phase differences for N cycles, at $t = \frac{2\pi N}{\delta}$, reads

$$\left\langle [\delta\Phi_s^\xi(t) - \delta\Phi_{s'}^\xi(t)]^2 \right\rangle_\xi = 4C_0 \frac{\left[\Omega_{\parallel,s}^\varepsilon - \Omega_{\parallel,s'}^\varepsilon\right]^2}{\delta^2} \frac{2\pi N}{\delta}. \quad (49)$$

At arbitrary time t the corrections to Eq. (49) are of the order of $\mathcal{O}(\frac{\delta}{\omega_d})$ (some of them are zeroed at completed cycles), and oscillate with frequencies δ, and 2δ, see Appendix D 2. Notice that the variance $\langle [\delta\Phi_s(t) - \delta\Phi_{s'}(t)]^2 \rangle_\xi$ is linear in time units of $\frac{2\pi}{\delta}$ for integer number of cycles N.

The n-qubit infidelity due to resonator (Johnson) noise for N cycles is then obtained from Eq. (45):

$$\delta\epsilon_\xi^{n\,Qb} \lesssim \frac{2\pi N}{\delta}\frac{\kappa}{2}\coth\left(\frac{\hbar\omega_r}{2k_B T_r}\right)$$
$$\times \left[1 + 2f_{12}^{(n)}\sum_{s<s'}\frac{[\Omega_{\parallel,s}^\varepsilon - \Omega_{\parallel,s'}^\varepsilon]^2}{\delta^2}\right], \quad (50)$$

where $f_{12}^{(n)}$ is given by Eq. (40) and in the modulation strength difference the spin-independent terms $\sim \tilde{g}_0^{(j)}$ and the driving ε_d are separately canceled:

$$\Omega_{\parallel,s}^\varepsilon - \Omega_{\parallel,s'}^\varepsilon = \frac{1}{2}\sum_j \tilde{g}_\parallel^{(j)}\left(\langle s|\sigma_z^{(j)}|s\rangle - \langle s'|\sigma_z^{(j)}|s'\rangle\right). \quad (51)$$

For the two-qubit controlled π-phase gate considered in this paper, the modulation-to-resonator detuning is chosen such that $\delta_\pi = 2\sqrt{N\tilde{g}_\parallel^{(1)}\tilde{g}_\parallel^{(2)}}$ so that the variances of interest scale differently with N: $\langle |\delta\alpha_s|^2 \rangle \propto \sqrt{N}$, while $\langle [\delta\Phi_s(t) - \delta\Phi_{s'}(t)]^2 \rangle_\xi \propto \frac{1}{\sqrt{N}}$. The two-qubit gate error due to resonator noise then reads

$$\delta\epsilon_\xi^{2Qb} \lesssim \frac{\pi\sqrt{N}}{\sqrt{\tilde{g}_\parallel^{(1)}\tilde{g}_\parallel^{(2)}}}\frac{\kappa}{2}\coth\left(\frac{\hbar\omega_r}{2k_B T_r}\right)$$
$$\times \left[1 + \frac{4f_{12}^{(2)}}{N}\frac{(\tilde{g}_\parallel^{(1)})^2 + (\tilde{g}_\parallel^{(2)})^2}{\tilde{g}_\parallel^{(1)}\tilde{g}_\parallel^{(2)}}\right]. \quad (52)$$

For two qubits one is using the average over the initial state $f_{12}^{(2)} = \overline{2|a_s|^2|a_{s'}|^2} = 1/10$ [Eq. (40) and Appendix C 2]. We notice that both terms in Eq. (52) are important, especially for small N. For equal couplings $\tilde{g}_\parallel^{(1)} = \tilde{g}_\parallel^{(2)}$ the second term was derived in Ref. [61]. It gives 40% of the first term for $N = 2$. In what follows, higher $N > 2$ are not welcomed since both the gate time and the error scales up as $\sim\sqrt{N}$.

Taking, e.g., a temperature of $T_r = 40$ mK and $\omega_r/2\pi \in [5, 10]$ GHz, notice that the two-qubit gate noise error (infidelity) up to a factor of order 1 is given by $\delta\epsilon_\xi^{2Qb} \approx t_\pi \frac{\omega_r}{2Q}$. In Fig. 7 is shown a density plot of $\delta\epsilon_\xi^{2Qb}(t_\pi, \log Q)$, for the range of parameters that fixes the range of gate times $t_\pi \in [15, 150]$ ns (that implies $N = 2$, $\tilde{V}_m = 0.1$ mV, and $\omega_r/2\pi \simeq 6.3$ GHz, see also Fig. 3). One obtains ranges of the resonator Q factor that provide a corresponding level of the resonator noise two-qubit phase gate error: $\delta\epsilon_\xi^{2Qb} \leqslant 0.1$ for $Q \in [3.4 \times 10^3, 3.4 \times 10^4]$, $\delta\epsilon_\xi^{2Qb} \leqslant 0.01$ for $Q \in [3.4 \times$
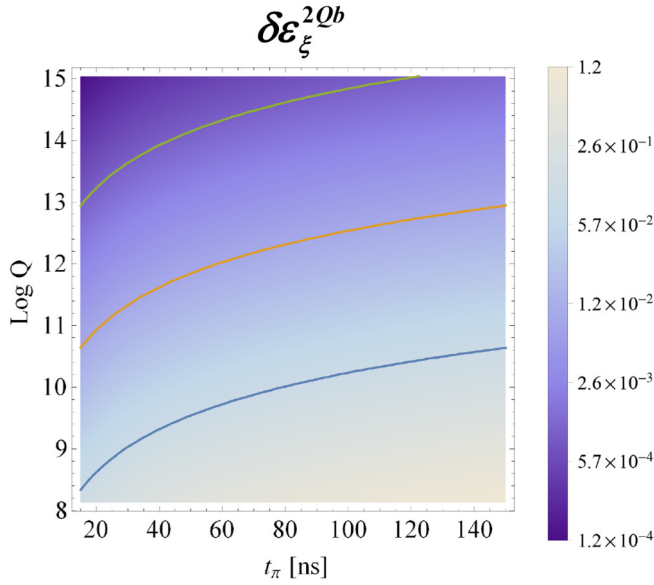
FIG. 7. Density plot of the resonator (Johnson) noise infidelity $\delta\epsilon_\xi(t_\pi, \log Q)$ for a resonator frequency $\omega_r/2\pi \simeq 6.3$ GHz, range of the two-qubit gate time $t_\pi \in [15, 150]$ ns, and resonator Q factor of $Q \in [3.4 \times 10^3, 3.4 \times 10^6]$. Contours where the infidelity reaches the values of 0.1, 0.01, 0.001 are also shown.

$10^4, 3.4 \times 10^5]$, and $\delta\epsilon_\xi^{2Qb} \leqslant 0.001$ for $Q \in [3.4 \times 10^5, 3.4 \times 10^6]$.

C. Qubit charge noise phase gate errors

Due to qubits' gate charge noise, the actual final state of n qubits acquires the random phases $\Delta\phi_s(t)$:

$$|\psi_f\rangle = \sum_s a_s e^{i\Phi_s(t)} e^{-i\omega_s t} e^{-i\Delta\phi_s(t)}|s\rangle|0\rangle, \qquad (53)$$

with the spin-dependent geometric phase $\Phi_s(t)$ and the regular qubits phase $\omega_s t$. The n-qubit random phase $\Delta\phi_s(t)$ is

$$\Delta\phi_s(t) = \sum_j \langle s|\frac{\Delta\phi^{(j)}(t)}{2}\sigma_z^{(j)}|s\rangle,$$

$$\Delta\phi^{(j)}(t) \equiv \int_0^t dt'\, \delta\omega_q^{(j)}(t'), \qquad (54)$$

where the random phase $\Delta\phi^{(j)}(t)$ is accumulated via the (j)th qubit frequency fluctuation $\delta\omega_q^{(j)}(t)$. Averaging over the initial qubits' state and over the random phases $\Delta\phi_s(t)$ [assuming Gaussian distributed $\Delta\phi_s(t)$, see Appendix E] one obtains the n-qubit charge noise infidelity in general form:

$$\delta\epsilon_\phi^{n\,Qb} = f_{12}^{(n)} \sum_{s<s'} \frac{1}{2}\langle [\Delta\phi_s(t) - \Delta\phi_{s'}(t)]^2\rangle_{\xi_q}. \qquad (55)$$

Essentially, the noise average $\langle [\Delta\phi_s(t) - \Delta\phi_{s'}(t)]^2\rangle_{\xi_q}$ will lead to n-qubit dephasing, and below we consider several charge noise dephasing mechanisms.

1. Curvature couplings induced qubit dephasing via the resonator shot noise

One mechanism is via the qubits *curvature coupling* to the resonator. Weak leakage of photons from the resonator (shot noise) will lead to an n-qubit dephasing with rates $\Gamma_{ss'}^{shot}$ and AC-Stark frequency shifts $\delta\omega_{ss'}^{shot}$. These are derived from the Caldeira-Leggett master equation for the n-qubits plus resonator density matrix [Eq. (27)] at zero resonator temperature, via tracing out the resonator. In a long-time limit $t \gg 1/\kappa$, the n-qubit density matrix acquires a dephasing term (Appendix B 6)

$$\rho_{ss'}^q(t) = \rho_{ss'}^q(0)\, e^{-\Gamma_{\phi,ss'}^{shot}\, t}\, e^{i\delta\omega_{ss'}^{shot} t}. \qquad (56)$$

For the dephasing rates one obtains

$$\Gamma_{\phi,ss'}^{shot} \equiv \delta\gamma_{disp,ss'} + \delta\gamma_{long,ss'}, \qquad (57)$$

$$\delta\gamma_{disp,ss'} = \frac{(2A_{-,ss'})^2(\kappa/2)}{(\delta_s^2 + \frac{\kappa^2}{4})(\delta_{s'}^2 + \frac{\kappa^2}{4})}\Omega_{\parallel,s}^\varepsilon\,\Omega_{\parallel,s'}^\varepsilon, \qquad (58)$$

$$\delta\gamma_{long,ss'} = B_{-,ss'}(\kappa/2)\left[\frac{\Omega_{\parallel,s}^\varepsilon}{\delta_s^2 + \frac{\kappa^2}{4}} - \frac{\Omega_{\parallel,s'}^\varepsilon}{\delta_{s'}^2 + \frac{\kappa^2}{4}}\right], \qquad (59)$$

and similarly, for the AC-Stark frequency shifts $\delta\omega_{ss'}^{shot}$,

$$\delta\omega_{ss'}^{shot} \equiv \delta\omega_{disp,ss'} + \delta\omega_{long,ss'}, \qquad (60)$$

$$\delta\omega_{disp,ss'} = -2A_{-,ss'}\left[\delta_s\delta_{s'} + \frac{\kappa^2}{4}\right]\frac{\Omega_{\parallel,s}^\varepsilon\,\Omega_{\parallel,s'}^\varepsilon}{(\delta_s^2 + \frac{\kappa^2}{4})(\delta_{s'}^2 + \frac{\kappa^2}{4})}, \qquad (61)$$

$$\delta\omega_{long,ss'} = B_{-,ss'}\left[\delta_s\frac{\Omega_{\parallel,s}^\varepsilon}{\delta_s^2 + \frac{\kappa^2}{4}} + \delta_{s'}\frac{\Omega_{\parallel,s'}^\varepsilon}{\delta_{s'}^2 + \frac{\kappa^2}{4}}\right], \qquad (62)$$

where we have introduced the shortcomings

$$\delta_s \equiv \delta - \delta\omega_s \equiv \omega_m - \omega_r - \delta\omega_s, \qquad (63)$$

$$A_{-,ss'} \equiv \frac{\delta\omega_s - \delta\omega_{s'}}{2}, \qquad B_{-,ss'} \equiv \Omega_{\parallel,s}^\varepsilon - \Omega_{\parallel,s'}^\varepsilon, \qquad (64)$$

see Appendix B 1. The expressions Eqs. (57)–(62) are derived with the effective spin-dependent driving strength $\Omega_{\parallel,s}^\varepsilon$ [Eq. (43) and Appendix B 6] and a proper choice of the resonator driving [Eq. (6)] can significantly decrease the gate errors.

In the short-time limit of the geometric phase gates one has typical timescales $t^* \sim \frac{1}{\delta} \ll \frac{1}{\delta\omega_s} \ll \frac{1}{\kappa}$, and the dephasing factors differ from that of Eq. (56). In particular, for intermediate times within the cycle, $0 < t < t_g$, the exponents are nonlinear in time and oscillate with a period $\frac{2\pi}{\delta}$ changing considerably (Appendix B 6). At time moments $t_g = \frac{2\pi N}{\delta}$ one is left, however, with linear in time (but modified) exponents of Eq. (56) with dephasing rates and frequency shifts given by

$$\tilde\Gamma_{\phi,ss'}^{shot} \equiv \delta\gamma_{disp,ss'} + 2\,\delta\gamma_{long,ss'}, \qquad (65)$$

$$\delta\tilde\omega_{ss'}^{shot} \equiv \delta\omega_{disp,ss'} + 2\,\delta\omega_{long,ss'}, \qquad (66)$$

instead of Eqs. (57) and (60). In its turn, the frequency shifts $\delta\tilde{\omega}_{ss'}^{\text{shot}}$ can be represented as

$$\delta\tilde{\omega}_{ss'}^{\text{shot}} \equiv \frac{\left(\Omega_{\parallel,s}^{\varepsilon}\right)^2 - \left(\Omega_{\parallel,s'}^{\varepsilon}\right)^2}{\delta} + \delta\tilde{\tilde{\omega}}_{ss'}^{\text{shot}}, \qquad (67)$$

where the first term of the order of $\tilde{g}_{\parallel}$ can be absorbed in the redefinition of the n-qubit energy levels ω_s, see Eqs. (B18) and (B54) (essentially, because $|s\rangle$ are eigenstates of $\hat{\Omega}_{\parallel}^2$). The remaining frequency shifts $\delta\tilde{\tilde{\omega}}_{ss'}^{\text{shot}} \sim \delta\omega_s$ cause a quadratic in time infidelity (Appendix E):

$$\delta\varepsilon_{\delta\omega,\text{shot}}^{n\,\text{Qb}} = \frac{f_{12}^{(n)}}{2} \sum_{s<s'} \left(\delta\tilde{\tilde{\omega}}_{ss'}^{\text{shot}} t_g\right)^2. \qquad (68)$$

The explicit form of the n-qubit shot noise rates $\tilde{\Gamma}_{\phi,ss'}^{\text{shot}}$ cannot be expressed as a sum of individual qubit dephasings. This is equivalent to say that the phase average in Eq. (55) is represented via *correlated qubits white noises*, see Eq. (E8). For small times $t_g \ll 1/\Gamma_{\phi,ss'}$, the n-qubit infidelity is linear in the gate time t_g and reads

$$\delta\varepsilon_{\phi,\text{shot}}^{n\,\text{Qb}} = f_{12}^{(n)} \sum_{s<s'} \tilde{\Gamma}_{\phi,ss'}^{\text{shot}} t_g, \qquad (69)$$

substituting in it the shot noise dephasings $\tilde{\Gamma}_{\phi,ss'}^{\text{shot}}$, Eq. (65). Using the expressions of Eqs. (68) and (69), one can show that these infidelities are negligible for a reasonable set of parameters, see Table I.

2. Uncorrelated white noise gate infidelity

A second charge noise dephasing mechanism is via the voltage fluctuations of the qubit's defining gates. For a TQD qubit these are the gates defining the dots and the gates defining the interdot tunneling, see Fig. 1(a).

It is worth to mention that for a model with *uncorrelated white noises* the n-qubit dephasings can be represented as a sum of appropriate individual qubit dephasings, see Appendix E 2 and Fig. 8. Then, for equal qubits dephasings, $\Gamma_{\phi}^{(1)} = \Gamma_{\phi}^{(2)} \equiv \Gamma_{\phi}^{\text{white}}$, the two-qubit infidelity is obtained from Eq. (69) using $f_{12}^{(2)} = 1/10$ and a gate time t_g given by Eq. (23):

$$\delta\varepsilon_{\phi}^{2\text{Qb}} = \frac{8}{10} \frac{\pi\sqrt{N}\,\Gamma_{\phi}^{\text{white}}}{\tilde{g}_{\parallel}}, \qquad (70)$$

$$\Gamma_{\phi}^{\text{white}} = \sum_{x=\varepsilon_v,\varepsilon_m,t_l,t_r} \frac{S_x}{4\hbar^2}\left(\frac{\partial E_q}{\partial x}\right)^2 \qquad (71)$$

that is minimized at a full sweet spot, where $\frac{\partial E_q}{\partial\varepsilon_v} = \frac{\partial E_q}{\partial\varepsilon_m} = 0$.

3. Uncorrelated $1/f$-noise phase gate infidelity

The dephasing measured in actual experiments, performed for a DQD singlet-triplet qubit in its symmetric operating point [28,29], shows that this model is unrealistic: the experiment is featuring an $1/f$-charge noise spectrum of the qubits' gate noise, leading to a Gaussian (quadratic) dephasing exponent:

$$e^{-\frac{1}{2}\langle[\Delta\phi_{s'}(t)-\Delta\phi_{s'}(t)]^2\rangle_{\xi_q}} = e^{-(\tilde{\Gamma}_{ss'}\,t)^2}, \qquad (72)$$
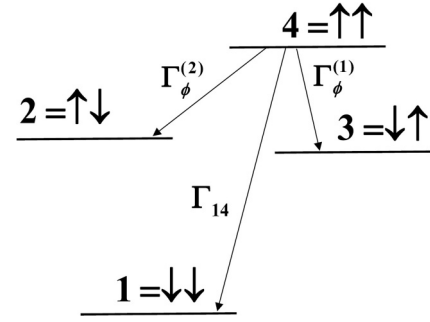

FIG. 8. Schematic of the two-qubit energy levels and the associated charge noise dephasing rates. The individual qubit dephasings are $\tilde{\Gamma}_{\phi}^{(1)} = \tilde{\Gamma}_{34}$ and $\tilde{\Gamma}_{\phi}^{(2)} = \tilde{\Gamma}_{24}$. For uncorrelated white noise $\tilde{\Gamma}_{14} = \tilde{\Gamma}_{\phi}^{(1)} + \tilde{\Gamma}_{\phi}^{(2)}$, see Eq. (70) and Appendix E 2. For correlated white noise and for uncorrelated $1/f$ noise $\tilde{\Gamma}_{14} \neq \tilde{\Gamma}_{\phi}^{(1)} + \tilde{\Gamma}_{\phi}^{(2)}$, see Eqs. (57) and (76), respectively.

compare with Eq. (56). In the case of uncorrelated charge noise to each of the qubits one obtains the relation

$$(\tilde{\Gamma}_{ss'})^2 = \frac{1}{2}\sum_{j=1}^{n}(\tilde{\Gamma}^{(j)})^2\,(1 - i_j\,i'_j), \qquad (73)$$

where $\tilde{\Gamma}^{(j)}$ is the individual jth qubit $1/f$-noise dephasing rate, Appendix E 3. For small fluctuations, $\langle[\Delta\phi_{s'}(t) - \Delta\phi_{s'}(t)]^2\rangle_{\xi_q} \ll 1$, one obtains the n-qubit infidelity:

$$\delta\varepsilon_{\phi,1/f}^{n\,\text{Qb}} = f_{12}^{(n)}\sum_{s<s'}(\tilde{\Gamma}_{ss'}\,t)^2, \qquad (74)$$

that is growing quadratically with time. Since one is assuming $t \ll 1/\tilde{\Gamma}_{ss'}$, the quadratic dependence is beneficial for suppressing the infidelity.

For the two-qubit case one gets from Eq. (73) the relations

$$\tilde{\Gamma}_{12} = \tilde{\Gamma}_{\phi}^{(2)}, \quad \tilde{\Gamma}_{13} = \tilde{\Gamma}_{\phi}^{(1)}, \qquad (75)$$

$$\tilde{\Gamma}_{14} = \sqrt{\left(\tilde{\Gamma}_{\phi}^{(1)}\right)^2 + \left(\tilde{\Gamma}_{\phi}^{(2)}\right)^2}, \text{ etc.} \qquad (76)$$

Note that as compared to the uncorrelated white noise case [Eq. (E23)], here $\tilde{\Gamma}_{14} \neq \tilde{\Gamma}_{24} + \tilde{\Gamma}_{34} \equiv \tilde{\Gamma}_{\phi}^{(1)} + \tilde{\Gamma}_{\phi}^{(2)}$, see Fig. 8. One then obtains the two-qubit gate infidelity for a gate time t_g,

$$\delta\varepsilon_{\phi,1/f}^{2\text{Qb}} = \frac{4}{10}\left[\left(\tilde{\Gamma}_{\phi}^{(1)}\right)^2 + \left(\tilde{\Gamma}_{\phi}^{(2)}\right)^2\right]t_g^2 \qquad (77)$$

$$= \frac{8}{10}(\tilde{\Gamma}_{\phi}\,t_g)^2, \qquad (78)$$

where the second equality is for equal qubits' dephasing $\tilde{\Gamma}_{\phi}^{(1)} = \tilde{\Gamma}_{\phi}^{(2)} \equiv \tilde{\Gamma}_{\phi}$.

In Fig. 9 is shown a density plot of the $1/f$-noise infidelity $\delta\varepsilon_{\phi,1/f}^{2\text{Qb}}(t_{\pi}, T_2^*)$, Eq. (78), for a range of gate times $t_{\pi} \in [15, 150]$ ns, and qubit's dephasing times $T_2^* \in [200, 1500]$ ns. The infidelity levels of $\delta\varepsilon_{\phi,1/f}^{2\text{Qb}} \lesssim 0.1, 0.01, 0.001$ can be reached for gate times $t_{\pi} \lesssim 0.354T_2^*, 0.112T_2^*, 0.0354T_2^*$.
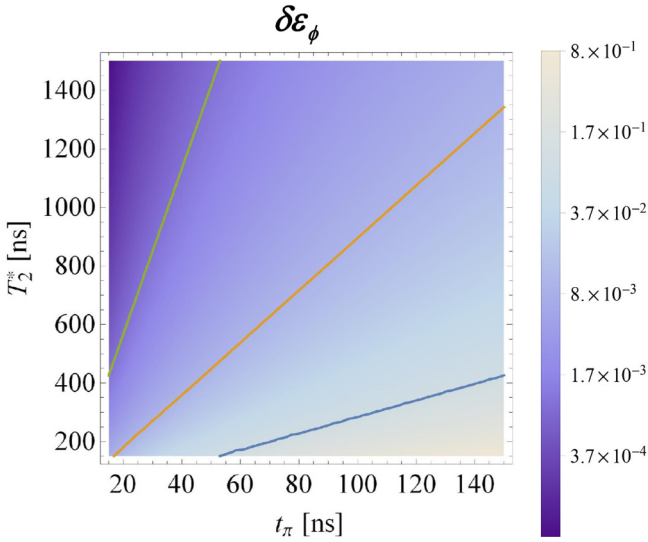
$$\delta\varepsilon_\phi$$

FIG. 9. Density plot of the two-qubit controlled π-phase gate $1/f$ charge noise infidelity $\delta\varepsilon^{2\mathrm{Qb}}_{\phi,1/f}(t_\pi, T_2^*)$, Eq. (78), for a resonator frequency $\omega_r/2\pi \simeq 6.3$ GHz, range of the two-qubit (π-phase) gate time $t_\pi \in [15, 150]$ ns, and qubit's dephasing times $T_2^* \in [200, 1500]$ ns, where $T_2^* \equiv 1/\tilde{\Gamma}_\phi$, Eq. (79). Contours where the infidelity reaches the values of 0.1, 0.01, 0.001 are shown, which corresponds to the relations $t_\pi = 0.354 T_2^*$, $0.112 T_2^*$, $0.0354 T_2^*$, respectively.

In the symmetric case of a TQD (Appendix E 4), one obtains for the single qubit $1/f$-noise dephasing rate

$$\tilde{\Gamma}_\phi \simeq \frac{1}{\hbar}\sqrt{\log r_c \, S_{t_l}} \frac{4 t_l}{U_{\mathrm{ch}}}, \tag{79}$$

where $r_c \equiv \omega_{\mathrm{UV}}/\omega_{\mathrm{IR}}$ is the ratio of the noise ultraviolet-to-infrared frequency cutoffs [25], and S_{t_l} is the spectral density constant of the $1/f$ noise associated with the gates forming the interdot tunnelings t_l, t_r.

The curvature contributions to $\tilde{\Gamma}_\phi$ are shown to give a negligible effect with respect to the noise from the tunneling gates (Appendix E 4) that allows us to increase the quantum capacitance, respectively, to decrease the gate time t_π without additional $1/f$ noise, see Table I and Appendix E 4.

The scaling of the two-qubit gate infidelity for $1/f$ noise with all relevant parameters is obtained as (Appendix E 4)

$$\delta\varepsilon^{2\mathrm{Qb}}_{\phi,1/f} = \frac{4\pi^2 N}{5\hbar^2} \frac{\log(\omega_{\mathrm{UV}}/\omega_{\mathrm{IR}}) \, S_{t_l}}{\omega_r^2 \, (\eta/\hbar)^2 \, (e\tilde{V}_m)^2} \frac{U^4_{\mathrm{ch}}}{t_l^2}. \tag{80}$$

It is worth to comment on the important features of this expression:

(1) The smaller is the spectral density constant S_{t_l} of the interdot tunneling t_l the better. Here the spectral density of the $1/f$ noise is defined as $S(\omega) = \frac{S_{t_l}}{|\omega|}$. One can estimate the spectral density constant from current experiments with DQD singlet-triplet qubit at the symmetric operating point [28,29] as $S_{t_l} \simeq 10^{-5} \, (\mu\mathrm{eV})^2$, see also Appendix E 5.

(2) The dot-to-resonator coupling ratio should be small, $\eta/\hbar \sim 0.1$, in order the make the infidelity $\delta\varepsilon_{\kappa,\delta\omega}$ small, see Appendix C 3. In order to compensate for this smallness one needs to increase the gate voltage modulation amplitude $\tilde{V}_m$, and simultaneously to increase the resonator frequency ω_r, so

that to keep $\delta\varepsilon_{\kappa,\delta\omega}$ fixed. The simultaneous increase of these parameters is beneficial for the suppression of the charge noise infidelity $\delta\varepsilon_{\phi,1/f}$.

(3) The charge noise infidelity is critically sensitive to the dot's charging energy U_{ch} and the tunneling amplitude t_l, featuring relatively small U_{ch} and relatively large t_l, see Table I.

D. Infidelity via the charge fluctuations of the longitudinal (curvature) coupling $\tilde{g}_\parallel$

Charge noise fluctuations of the (TQD) qubit tunnelings $\delta t^{(j)}_{l,r}$ causes fluctuations of the longitudinal (curvature) couplings $\delta\tilde{g}^{(j)}_\parallel$ and, respectively, of the n-qubit spin-dependent resonator driving strength $\delta\Omega^\varepsilon_{\parallel,s}$, scf. Eqs. (17) and (43). Averaging over the charge noise and assuming uncorrelated fluctuations for the different qubits, one obtains for the correlation function

$$\left\langle \delta\Omega^\varepsilon_{\parallel,s}(t')\,\delta\Omega^\varepsilon_{\parallel,s'}(t'') \right\rangle_{\xi_q} \equiv K_{ss'}(t'-t''), \tag{81}$$

$$K_{ss'}(t'-t'') = \sum_{j=1}^{n} \left[\frac{\tilde{g}^{(j)}_\parallel}{t^{(j)}_l}\right]^2 i_j \, i'_j \left\langle \delta t^{(j)}_l(t')\,\delta t^{(j)}_l(t'') \right\rangle_{\xi_q},$$

$$\left\langle \delta t^{(j)}_l(t')\,\delta t^{(j)}_l(t'') \right\rangle_{\xi_q} = \int_{-\infty}^{+\infty} d\omega\, e^{i\omega(t'-t'')} S^{(j)}_{t_l}(\omega), \tag{82}$$

where $|s\rangle \equiv |i_1, \dots, i_j, \dots, i_n\rangle$, and $S^{(j)}_{t_l}(\omega)$ is the spectral density of the tunneling fluctuations. While some of the results below are correct for a general spectral density, for further numerical estimations a $1/f$ noise is assumed: $S^{(j)}_{t_l}(\omega) = \frac{S^{(j)}_{t_l}}{|\omega|}$, with the spectral density constants $S^{(j)}_{t_l}$ extracted from the experiment [28], see Appendix E 5.

The corresponding fluctuation in the resonator trajectory $\delta\alpha^{\xi_q}_s \equiv \delta\alpha^{\tilde{g}_\parallel,1/f}_s$, scf. Eq. (24), then leads to an infidelity similar to the Johnson noise, Eq. (45), but with an averaging over the charge noise ξ_q (see Appendix C 1):

$$\delta\epsilon^{n\,\mathrm{Qb}}_{\tilde{g}_\parallel,1/f} = \frac{1}{2^n}\sum_s \left\langle |\delta\alpha^{\xi_q}_s|^2 \right\rangle_{\xi_q} + \frac{f^{(n)}_{12}}{2}\sum_{s<s'} \left\langle (\delta\Phi^{\xi_q}_s - \delta\Phi^{\xi_q}_{s'})^2 \right\rangle_{\xi_q}. \tag{83}$$

The average of the trajectory fluctuation is spin-independent and is obtained as

$$\left\langle |\delta\alpha^{\xi_q}_s(t)|^2 \right\rangle_{\xi_q} = \int_0^t \int_0^t dt'dt''\, K_{ss}(t'-t'')\, e^{-i\delta(t'-t'')}$$

$$= t^2 \sum_{j=1}^{n} \left[\frac{\tilde{g}^{(j)}_\parallel}{t^{(j)}_l}\right]^2 \int_{-\infty}^{\infty} d\omega\, S^{(j)}_{t_l}(\omega)\, f_\alpha\!\left(\frac{\omega t}{2}, \frac{\delta t}{2}\right), \tag{84}$$

$$f_\alpha(x,y) \equiv \mathrm{sinc}^2(x-y), \tag{85}$$

where $\mathrm{sinc}(x) \equiv \frac{\sin(x)}{x}$.

For the contribution of the accumulated phase fluctuations one proceeds similar to the Johnson noise case (see Appendixes C 1 and D 2). The accumulated phase fluctuation

average is then obtained as

$$\langle \delta \Phi_s(t) \, \delta \Phi_{s'}(t) \rangle_{\xi_q} = \Omega_{\parallel,s}^\varepsilon \, \Omega_{\parallel,s'}^\varepsilon \, \frac{t^4}{4} \sum_{j=1}^n \left[\frac{\tilde{g}_\parallel^{(j)}}{t_l^{(j)}} \right]^2 i_j \, i'_j$$

$$\times \int_{-\infty}^{\infty} d\omega \, S_{t_l}^{(j)}(\omega) \, f_\Phi\left(\frac{\omega t}{2}, \frac{\delta t}{2} \right), \quad (86)$$

$$f_\Phi(x, y) \equiv \frac{[xy \cos x \sin 2y + 2(x^2 \sin^2 y - y^2) \sin x]^2}{x^2 y^2 (x^2 - y^2)^2} \quad (87)$$

[note that $f_\Phi(x, y)$ is smooth at $x = y$]. Integrating over frequencies ω (using infrared and ultraviolet cutoffs $\omega_{IR} < |\omega| < \omega_{UV}$, scf. Appendix E 4), one can show numerically that the resulting functions in Eqs. (84) and (86) are decreasing (and oscillating) functions of $\frac{\delta t}{2}$ and of the order of $\lesssim 1$ (also obtaining additional suppression at complete cycles $t_g = \frac{2\pi N}{\delta}$). Since $\{\Omega_{\parallel,s}, \delta\} \sim \tilde{g}_\parallel$, the order of magnitude of the contributions Eqs. (84) and (86) is given by the ratio $S_{t_l}^{(j)}/t_l^2 \sim 10^{-5} - 10^{-9}$, for $S_{t_l} \simeq 10^{-2} - 10^{-5}$ $(\mu eV)^2$ and $t_l = 40$–80 μeV, that is, the infidelity $\delta\epsilon_{\tilde{g}_\parallel, 1/f}^{2Qb}$ is strongly suppressed, Table I.

E. Switching off the modulation

After completing the n-qubit phase gate, when the (distant) qubits become entangled, the modulation is switched off. Assuming no driving and modulation off, $\varepsilon_d = 0$, $\tilde{g}_\parallel = 0$, $\tilde{g}_0 = 0$, the dephasing is via the dispersivelike coupling $\mathcal{H}_{\delta\omega}$ only, due to leakage of resonator thermal photons. Estimating the single-qubit dephasing rate [91] $\Gamma_{\phi,th} \simeq \kappa \bar{n}_{th}$, for $T = 40$ mK, one obtains $\Gamma_{\phi,th} \simeq 8\pi \times 10^{-2}$ s^{-1}, so pure thermal dephasing is negligible.

At first glance the always-on dispersivelike coupling $\mathcal{H}_{\delta\omega}$ may change the n-qubit entangled state via free evolution with the qubits' frequency shifts $\delta\omega^{(j)}$, see Eqs. (1) and (B18). For the two-qubit system in an arbitrary state (pure or mixed) we show that the state change can be corrected by a local rotation of one of the qubits. Indeed, the two-spin resonator frequency shifts $\delta\omega_s$ are opposite in sign for the relevant $|s\rangle$ states (here $s = 1, 2, 3, 4 \equiv \downarrow\downarrow, \downarrow\uparrow, \uparrow\downarrow, \uparrow\uparrow$), namely $\delta\omega_1 = -(\delta\omega^{(1)} + \delta\omega^{(2)})$, $\delta\omega_2 = (-\delta\omega^{(1)} + \delta\omega^{(2)})$, $\delta\omega_3 = -\delta\omega_2$, $\delta\omega_4 = -\delta\omega_1$. Then the phases acquired by the two-qubit state amplitudes a_s,

$$|\psi\rangle = \sum_1^4 a_s e^{-i\delta\omega_s t} |s\rangle \quad (88)$$

(assuming the qubits are disentangled from the resonator) can be partially compensated via a σ_z rotation of the first qubit:

$$U_{z1} = \begin{pmatrix} e^{-i\Delta\omega_z t} & 0 \\ 0 & e^{i\Delta\omega_z t} \end{pmatrix}, \quad (89)$$

with $\Delta\omega_z \equiv -\frac{\delta\omega_1 + \delta\omega_2}{2}$. After this transformation, the state amplitudes become transformed to

$$a'_s = a_s \, e^{(-1)^s i \frac{(\delta\omega_1 - \delta\omega_2)}{2} t}, \quad s = 1, \dots, 4, \quad (90)$$

which is a pure gauge phase factor, i.e., the two-qubit density matrix elements, see Eqs. (C20)–(C24), remain intact [92].

For the general case of n qubits ($n > 2$), one can preserve the entangled n-qubit state by decreasing the tunnelings

$t_{l,r}^{(j)}$ for each qubit, to decrease couplings to the resonator $[\delta\omega^{(j)} \propto (t_{l,r}^{(j)})^2 \rightarrow 0]$. Another possibility to correct the acquired phases in Eq. (88) is via a spin-echo technique: for the phases acquired after a time interval $\Delta t \ll 1/\kappa$, one performs simultaneous π pulse on all qubits involved into the phase gate (by manipulating the qubits' interdot tunnelings $t_{l,r}^{(j)}$, while still remaining in the sweet spot for each qubit, see Refs. [26,62]). Then one waits for a second time interval Δt, and performs a π pulse again so that the effect of the frequency shifts is canceled out.

IV. RELEVANCE TO OTHER WORK

Similar entangling proposals via a modulated longitudinal coupling, based on a specially designed superconducting qubits [78] or a double quantum dot singlet-triplet qubits [93], have been proposed. While these works utilize essentially the same dynamical longitudinal coupling $\tilde{g}_\parallel$, Eq. (4), as we discussed previously [62,63,94,95], they have ignored the other (curvature) dispersivelike coupling [62,63] $\delta\omega_s$, which is essential in the estimation of accumulated phase gate infidelities, as shown in the present paper. Another missing ingredient in their analysis is the spin-independent modulation coupling $\tilde{g}_0$, Eq. (5). Both these ingredients are important for the associated infidelity $\delta\varepsilon_{\kappa,\delta\omega}$, Eq. (39). As we have shown, taking into account the infidelity $\delta\varepsilon_{\kappa,\delta\omega}$ essentially restricts the field of available parameters.

It is also worthwhile to compare the (Johnson noise) infidelity [Eq. (52)] with an analogous infidelity of Eq. (8) of Ref. [93]. The latter consists of two terms that scale with the number of cycles N as $\sim\sqrt{N}$ and $\sim 1/\sqrt{N}$, respectively. The first term $\sim\sqrt{N}$ exactly corresponds to an uncorrelated white gate noise infidelity [94,95] described by Eq. (70); this term should be zero in a sweet spot. The second term $\sim 1/\sqrt{N}$ exactly corresponds to our term $\sim\langle(\delta\Phi_s^\xi - \delta\Phi_{s'}^\xi)^2\rangle_\xi$, scf. Eq. (45). However, the other (leading) term of Eq. (45), which is proportional to the field variance $\langle|\delta\alpha_s^\xi|^2\rangle_\xi$ and also scales as $\sim\sqrt{N}$, is missing in the analysis of Ref. [93].

As to the $1/f$-charge noise dephasing infidelity, Eq. (80), we have analyzed the situation of an encoded spin qubit residing in its sweet spot, while Ref. [93] deals with a working bias point that is generally not a sweet spot (not an SOP), scf. Eq. (9) of Ref. [93]. While such a working point is eligible to consider, it would imply in addition a nonzero (transverse) dipole coupling that would be essential for the analysis, see, e.g., Ref. [62]. It is also obvious (see Appendix E 4) that it would be beneficial to work in an SOP[28,29], where the charge noise is minimized and the $1/f$ noise will originate only from the fluctuations of the tunneling gate voltages that are generally much weaker [28,29], as is considered in this paper.

V. DISCUSSION AND SUMMARY

In this paper we have presented a careful study of the geometric n-qubit (two-qubit) phase gates based on the modulated longitudinal coupling $\sim\tilde{g}_\parallel\sigma_z(\hat{a} + \hat{a}^\dagger)$, including the phase gate error mechanisms. The results for the various kinds of infidelities presented in Table I imply that infidelities of the order

TABLE I. The leading two-qubit controlled π-phase gate infidelities $\delta\varepsilon_{\kappa,\delta\omega}$, $\delta\varepsilon_\xi$, $\delta\varepsilon_{\phi,1/f}$, $\delta\varepsilon_{\phi,\text{shot}}$, $\delta\varepsilon_{\delta\omega,\text{shot}}$, and $\delta\epsilon_{\tilde{g}_\parallel,1/f}$ are calculated for a range of parameters, see Eqs. (39), (52), (80), (69), (68), and (83), respectively. For an experimentally reachable [9,81] dot-resonator lever arm $\alpha_c \equiv \frac{C_c}{C_c+C_d} \simeq 0.14$, resonator inductance $L_r = 50$ nH, and a Q-factor $Q = 10^6$, one chooses a dot charging energy $U_{\text{ch}} \simeq 0.4$ meV. By setting the error $\delta\varepsilon_{\kappa,\delta\omega} \simeq 5 \times 10^{-3}$, one sets the ratio $\frac{\delta\omega}{\tilde{g}_\parallel} \simeq 2.6 \times 10^{-2}$, that is independent of the QD system quantum capacitance $C_q \propto \frac{t_{l,r}^2}{U_{\text{ch}}^3}$. Since the scaling of $\frac{\delta\omega}{\tilde{g}_\parallel} \propto \omega_r^{3/2}/\tilde{V}_r$, Eq. (16), the increase of $\tilde{V}_r$ requires the moderate increase of ω_r to keep the infidelity $\delta\varepsilon_{\kappa,\delta\omega}$ constant in Table I, see also Fig. 5. The scaling $\eta/\hbar \propto \sqrt{L_r}\omega_r^{3/2}$ leads to the important scalings $\delta\varepsilon_{\kappa,\delta\omega} \propto L_r\omega_r^3$, $\delta\varepsilon_\xi \propto 1/(\sqrt{L_r}\omega_r^{3/2})$, $\delta\varepsilon_{\phi,1/f} \propto 1/(L_r\omega_r^3)$, so that a decrease of L_r can be compensated by a moderate increase of ω_r. The Johnson noise error $\delta\varepsilon_\xi$ easily reaches a level $\lesssim 10^{-3}$ for higher C_q (respectively, higher tunneling t_l) and/or higher modulation voltage $\tilde{V}_m$. The main obstacle is the charge noise error $\delta\varepsilon_{\phi,1/f}$ due to qubit gate $1/f$-charge noise which scales with the gate time as $\propto \bar{\Gamma}_\phi^2 t_\pi^2$, Eq. (78). Generally, to reach an error level of $\delta\varepsilon_{\phi,1/f} \lesssim 10^{-3}$ pushes the dots'-resonator parameters towards relatively low charging energy U_{ch}, relatively high interdot tunnelings $t_{l,r}$, a smaller $1/f$-noise spectral density constant S_{t_l} and higher resonator frequency ω_r, and higher gate voltage modulation amplitude $\tilde{V}_r$, see Eq. (80). (We used $S_{t_l} \simeq 10^{-5}$ (μeV)^2 that is taken from the experiment [28], see Sec. III C 3 and Appendix E 5.) As an illustration, on the fourth group of rows of the Table we take $\omega_r = 5$ GHz while the other parameters are as on the second group of rows. The above scaling of $\delta\varepsilon_{\phi,1/f}$ with ω_r leads to an order of magnitude error increase, which can be compensated by an increase of the lever arm to 0.4 if lower ω_r is needed.

t_l (μeV)	E_q (GHz)	C_q (aF)	$\eta/\hbar$	$\delta\omega$ (MHz)	$\tilde{g}_\parallel$ (MHz)	$\tilde{V}_m$ (mV)	ω_r (GHz)	$\delta\varepsilon_{\kappa,\delta\omega}$	$\delta\varepsilon_\xi$	$\delta\varepsilon_{\phi,1/f}$	$\delta\varepsilon_{\phi,\text{shot}}$	$\delta\varepsilon_{\delta\omega,\text{shot}}$	$\delta\epsilon_{\tilde{g}_\parallel,1/f}$	t_π (ns)
40	3.9	32.		0.16	6.2				3.1×10^{-3}	0.53	2.2×10^{-4}		$<10^{-9}$–10^{-10}	113.6
60	8.7	72.1	0.1	0.36	14.	0.1	6.3	5.3×10^{-3}	1.4×10^{-3}	0.23	1×10^{-4}	1.6×10^{-4}	$<10^{-9}$–10^{-10}	50.5
80	15.5	128.2		0.64	24.9				7.8×10^{-4}	0.13	5.6×10^{-5}		$<10^{-9}$–10^{-10}	28.4
40	3.9	32.		0.64	24.9				1.2×10^{-3}	3.3×10^{-2}	8.9×10^{-5}		$<10^{-9}$–10^{-10}	28.4
60	8.7	72.1	0.125	1.44	56	0.2	10	5.3×10^{-3}	5.5×10^{-4}	1.5×10^{-2}	4×10^{-5}	1.6×10^{-4}	$<10^{-9}$–10^{-10}	12.6
80	15.5	128.2		2.57	99.6				3.1×10^{-4}	8.2×10^{-3}	2.2×10^{-5}		$<10^{-9}$–10^{-10}	7.1
40	3.9	32.		1.44	56				7.2×10^{-4}	6.5×10^{-3}	5.2×10^{-5}		$<10^{-9}$–10^{-10}	12.6
60	8.7	72.1	0.143	3.25	126.1	0.3	13.1	5.3×10^{-3}	3.2×10^{-4}	2.9×10^{-3}	2.3×10^{-5}	1.6×10^{-4}	$<10^{-9}$–10^{-10}	5.6
80	15.5	128.2		5.77	224.2				1.8×10^{-4}	1.6×10^{-3}	1.3×10^{-5}		$<10^{-9}$–10^{-10}	3.2
40	3.9	32.		0.08	8.8				1.8×10^{-3}	0.26	1.3×10^{-4}		$<10^{-9}$–10^{-10}	80.
60	8.7	72.1	0.088	0.18	19.9	0.2	5	6.6×10^{-4}	7.9×10^{-4}	0.12	5.5×10^{-5}	2.1×10^{-5}	$<10^{-9}$–10^{-10}	35.6
80	15.5	128.2		0.32	35.4				4.4×10^{-4}	6.5×10^{-2}	3.1×10^{-5}		$<10^{-9}$–10^{-10}	20.

of $\sim 10^{-3}$ are reachable for a range of parameters, including relatively small charging energy $U_{\text{charge}} \lesssim 0.4$ meV (see, e.g., Ref. [96]) and relatively high qubit interdot tunnelings $t_{l,r} \sim 40\text{–}80$ μeV, e.g., giving a larger quantum capacitance $C_q \propto \frac{\partial^2 E_q}{\partial V_m^2}$.

Increasing the dynamical longitudinal coupling $\tilde{g}_\parallel$ [Eq. (4)] also suppresses the resonator (Johnson) noise infidelity $\delta\varepsilon_\xi$ [Eq. (52)] while decreasing the gate time t_π [Eq. (23)]. The smallness of $\delta\varepsilon_\xi$ implies a resonator Q factor of $Q \gtrsim 10^4\text{–}10^6$, see Fig. 7. Increasing the charging energy from 0.4 meV to currently available values ≈ 1 meV (see, e.g., Refs. [2,9,28,35,81,97]) will require a 4 times increase of the tunneling rate to keep C_q constant. Such high tunneling rates of ~ 160 μeV were demonstrated recently for QDs filled with three electrons [98].

At a full sweet spot one avoids dealing with the qubit's electric dipole moment, however, a static curvature interaction appears even without qubit gate modulation, that is the always-on dispersivelike (or quantum capacitance) interaction $\mathcal{H}_{\delta\omega}$ [Eq. (7)]. While this interaction could be interesting for entangling gates on its own, see Sec. I A, $\mathcal{H}_{\delta\omega}$ is an obstacle for the accumulated phase gates discussed in this paper and need to be suppressed, as no simple cancellation scheme exists for the case of interest $\delta\omega_s \gg \kappa$, see Appendix C 3.

In order to suppress the infidelity $\delta\varepsilon_{\kappa,\delta\omega}$ [Eqs. (39) and (44)], one requires a small ratio of $\frac{\delta\omega_s}{\tilde{g}_\parallel} \equiv \frac{\eta}{\hbar}\frac{\hbar\omega_r}{e\tilde{V}_m}$ (effect of κ is negligible for high Q-factor resonator), see Eq. (16), Figs. 5

and 6, and Table I. This implies a smaller coupling ratio $\frac{\eta}{\hbar}$ [Eq. (2)], smaller resonator frequency ω_r, and larger qubit gate modulation amplitude $\tilde{V}_m$, while this infidelity is independent of C_q. The smaller coupling ratio of $\frac{\eta}{\hbar}$, however, will generally make the entangling gate slower, which can be compensated only by larger modulation $\tilde{V}_m$.

The curvature interactions (dispersivelike and longitudinal) also induce qubit dephasings and AC-Stark frequency shifts via the resonator shot noise, implying the infidelities $\delta\varepsilon_{\phi,\text{shot}}$, $\delta\varepsilon_{\delta\omega,\text{shot}}$ [Eqs. (69) and (68)]. In addition, an infidelity $\delta\epsilon_{\tilde{g}_\parallel,1/f}$ [Eq. (83)] induced via charge noise fluctuation of the longitudinal coupling $\tilde{g}_\parallel$ is considered. All these infidelities are shown to be of the order of $10^{-4}\text{–}10^{-5}$ for a range of parameters, Table I.

The largest infidelity $\delta\varepsilon_{\phi,1/f}$, see Table I, is due to qubit gate $1/f$-charge noise which scales with the qubit charge dephasing rate and gate time as $\delta\varepsilon_{\phi,1/f} \propto (\bar{\Gamma}_\phi t_\pi)^2$. With the scalings of the charge noise infidelity with t_l and U_{charge}, see Eq. (80), the increase of U_{charge} by two times (to ≈ 1 meV) will require an increase of tunneling by ≈ 6 times, which could be experimentally challenging. While the charge noise infidelity is also quadratically suppressed by $\tilde{V}_m$, Table I, too high modulation amplitude will require including of higher-curvature corrections [62]. As mentioned at the end of Sec. III A, these corrections are not harmful: on one hand corrections to $\delta\omega_s$ and $\tilde{g}_\parallel$ could be significant [62], however the ratio $\frac{\delta\omega_s}{\tilde{g}_\parallel}$ will remain approximately the same; on the other hand, the generated higher-order nonlinear Hamiltonians [62],

in addition to the lowest-curvature one, Eqs. (3) and (7), brings only small correction of the order of $\lesssim 10^{-4}$.

In the estimation of the charge noise infidelity in Table I, we have used for the $1/f$-noise spectral density constant a value $S_{t_l} \simeq 10^{-5}$ $(\mu\text{eV})^2$, extracted from the experiment, see Appendix E 5. Here the qubit defining gate voltages [as $V_{1,2,3}$ and V_{t_l}, V_{t_r} in Fig. 1(a)] have a typical spectral density constant $S_{V_{\text{gate}}} \lesssim 1$ $(\mu\text{eV})^2$ for Si heterostructures [99,100]. From a simple biquadratic model of a DQD (see, e.g., Refs. [96,101]) one can relate $S_{V_{\text{gate}}}$ to the spectral density constants of interest S_{t_l}:

$$S_{t_l} = \left(\frac{t_l}{U_{\text{charge}}}\right)^2 S_{V_{\text{gate}}}. \tag{91}$$

Thus, S_{t_l} can be decreased either by decreasing the ratio t_l/U_{charge} or by decreasing $S_{V_{\text{gate}}}$. Recent experiment with holes in a SiGe/Ge/SiGe heterostructure shows a 2–4 times improvement for $S_{V_{\text{gate}}}$ with respect to a Si quantum well 2DEG system [102]. This would make the realization of our proposal for *remote geometric phase gate entanglement of encoded spin qubits via longitudinal couplings to a SC resonator* possible in the near future, with a proposed target infidelity of 10^{-3}.

Longitudinal coupling of a TQD or DQD spin qubit to a SC resonator is a viable route to medium distance range ($l \sim 1$ mm) quantum gates across/off chip. It offers a way to couple always-on exchange-only TQD qubits while staying at their charge dephasing sweet spot. All the above analysis is applicable to DQD singlet-triplet qubits at the symmetric operating point (see Ref. [62]). The modulation scheme allows selectivity via a potentially large on/off coupling ratio (by setting off the gate modulation of relevant qubits $\tilde{V}_r^{(j)} \to 0$). In addition, by setting relevant dots' tunnelings to zero, $t_{l,r}^{(j)} \to 0$, one can switch off the curvature couplings and the tunneling gate charge noise, since $C_q \equiv \frac{\partial^2 E_q}{\partial \varepsilon_G^2} \propto t_{l,r}^2$, and $S_{t_l} \propto t_{l,r}^2$, respectively.

The longitudinal coupling rates of tens to hundred MHz can be larger than the best transverse couplings for a similar TQD system, where the latter needs a large electric dipole moment, and therefore are subject to charge noise dephasing. In addition, here the qubits can be of low frequency (e.g., highly detuned from the resonator). Although entangling via geometric phase, as studied in this paper, requires some overhead in cycles and correction strategy, it may be useful over a more simple circuit-QED like coupling scheme due to potentially much lower values of the qubit gates' charge noise.

In previous publications [62,63] we have shown how both curvature couplings $\tilde{g}_\parallel$, $\delta\omega_s$ can be used for a potentially quantum-limited QND measurement of an encoded spin qubit, while at the full qubit sweet spot. In a forthcoming work we will consider n-qubit entanglement preparation via joint qubits measurement (as discussed preliminary here [63]) that is based on an extension of previous "entanglement-by-measurement" proposals [103–105].

APPENDIX A: GEOMETRIC PHASES

1. Driving a resonator: Single resonator phase

The dynamical longitudinal Hamiltonian [Eq. (3)] is providing a spin-dependent force: $\hat{F} = -\partial\mathcal{H}_\parallel/\partial\hat{x}$, where $\hat{x} \equiv \Delta x_0(\hat{a} + \hat{a}^\dagger)$ is the "position" operator, see Eqs. (B2) and (B3) below.

To get an intuition, we first consider a constant force F_0 applied to the resonator: $\mathcal{H} = \hbar\omega_r\hat{a}^\dagger\hat{a} - \Delta x_0(\hat{a} + \hat{a}^\dagger)F_0$. Diagonalizing $\mathcal{H}$ by the transformation $\hat{b} = \hat{a} - \frac{\Delta x_0 F_0}{\hbar\omega_r}$ gives the Hamiltonian $\mathcal{H} \to \tilde{\mathcal{H}} = \hbar\omega_r\hat{b}^\dagger\hat{b}$. The new vacuum state $\hat{b}|0'\rangle = 0$ is a coherent state: $\hat{a}|0'\rangle = \frac{\Delta x_0 F_0}{\hbar\omega_r}|0'\rangle = \alpha_0|\alpha_0\rangle$, displaced from the ground state of an unbiased resonator by $\alpha_0 \equiv \frac{\Delta x_0 F_0}{\hbar\omega_r}$. This is represented via a displacement operator $D(\alpha)$: $|\alpha_0\rangle \equiv D(\alpha_0)|0\rangle \equiv \exp(\alpha_0\hat{a}^\dagger - \alpha_0^*\hat{a})|0\rangle$.

For a force modulated in time, $F(t) = F_0\cos(\omega_m t + \varphi_m)$, the above Hamiltonian can be rewritten [73,106] in a rotating frame (with ω_r) and in a rotating wave approximation (RWA) as

$$\tilde{\mathcal{H}}_m(t) = \hbar\Omega(\hat{a}e^{i(\delta t + \varphi_m)} + \hat{a}^\dagger e^{-i(\delta t + \varphi_m)}), \tag{A1}$$

where we defined $\hbar\Omega \equiv -\frac{\Delta x_0 F_0}{2}$, and $\delta = \omega_m - \omega_r$ is the detuning of the modulation frequency from the resonance. The evolution due to $\tilde{\mathcal{H}}_m(t)$ for small time step dt is an infinitesimal displacement

$$e^{-i\frac{\tilde{\mathcal{H}}_m(t)dt}{\hbar}} = D[d\alpha(t)] \equiv \exp[d\alpha(t)\hat{a}^\dagger - d\alpha^*(t)\hat{a}], \tag{A2}$$

with $d\alpha(t) = -i\,\Omega e^{-i(\delta t + \varphi_m)}dt$. Integrating for finite times one gets the (ideal) evolution of a resonator under a driving periodic force:

$$\alpha^{\text{id}}(t) = \alpha(0) - \left(\frac{\Omega}{\delta}\right)e^{-i\varphi_m}(1 - e^{-it\delta}). \tag{A3}$$

In the phase space of $\{\text{Re}\alpha(t), \text{Im}\alpha(t)\}$ this describes a clockwise rotating circle path starting at the origin [for $\alpha(0) = 0$], with radius $R = \frac{\Omega}{\delta}$ and center $O_m = \frac{\Omega}{\delta}(-\cos\varphi_m, \sin\varphi_m)$:

$$\text{Re}\alpha(t) = \left(\frac{\Omega}{\delta}\right)[-\cos\varphi_m + \cos(\delta t + \varphi_m)], \tag{A4}$$

$$\text{Im}\alpha(t) = \left(\frac{\Omega}{\delta}\right)[\sin\varphi_m - \sin(\delta t + \varphi_m)]. \tag{A5}$$

For further reference, in Fig. 10 we show a full circle (for a gate time $t_g = \frac{2\pi}{\delta}$) with an initial phase φ_m and a second circle with $\varphi_m' = \varphi_m + \pi$.

Using the standard relation for displacement operators

$$D(\alpha)D(\beta) = D(\alpha + \beta)e^{i\,\text{Im}(\alpha\beta^*)} \tag{A6}$$

one obtains the total displacement for a finite time in the form [73,106]

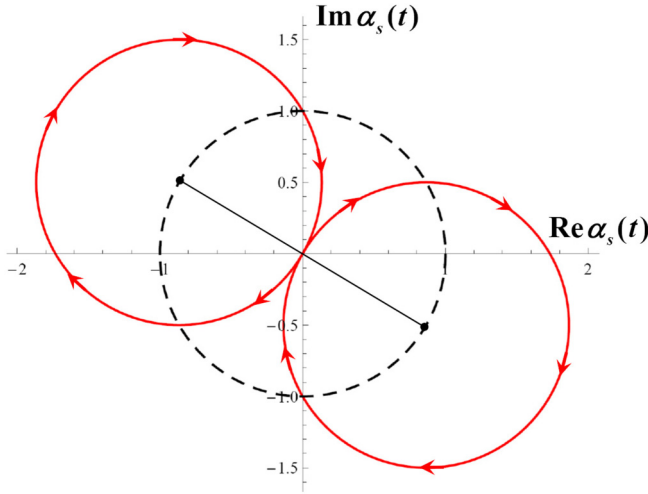$$D_{\text{tot}} = \lim_{n\to\infty} D[d\alpha(t_n)]\cdots D[d\alpha(0)] = D[\alpha(t)]\,e^{i\Phi(t)} \tag{A7}$$

FIG. 10. The ideal circular oscillator trajectories for two different initial phases: φ_m and $\varphi'_m = \varphi_m + \pi$ (red, solid circles). The radius of the circles is $\frac{\Omega}{\delta}$ and their centers lie on a circle with the same radius put at the origin (black, dashed circle). Interchanging the phase φ_m at each odd circle allows cancellation of small imperfections of the ideal evolution (see Fig. 4 and Appendix B).

substituting for an ideal accumulated (geometric) phase $\Phi^{\mathrm{id}}(t)$:

$$\Phi^{\mathrm{id}}(t) = \mathrm{Im}\left[\int_0^t \alpha^*(t')d\alpha(t')\right] = \left(\frac{\Omega}{\delta}\right)^2 [\sin \delta t - \delta t]. \quad (A8)$$

For a gate time $t_g = 2\pi/\delta$, when $\alpha(t)$ makes a full circle in the phase space $\{\mathrm{Re}\alpha, \mathrm{Im}\alpha\}$, Fig. 10, the accumulated phase is $\Phi_g = 2\pi(\Omega/\delta)^2$ which is twice the encircled area of radius Ω/δ and is independent of the initial phase φ_m.

2. Accumulated phases for resonator with n qubits

One considers the Hamiltonian of a resonator with n modulated qubits, Eq. (3),

$$\mathcal{H}/\hbar = \omega_r \hat{a}^\dagger \hat{a} + \sum_{j=1}^n \left[\tilde{g}_\parallel^{(j)} \sigma_z^{(j)} + \tilde{g}_0^{(j)}\right] \cos(\omega_m t + \varphi_m)(\hat{a} + \hat{a}^\dagger)$$
$$(A9)$$

for a chosen n-qubit spin state $|s\rangle \equiv |i_1, i_2, \ldots, i_n\rangle$ with $|i_k\rangle = |\uparrow\rangle$ or $|\downarrow\rangle$ being the eigenstates of the kth qubit, $\sigma_z^{(k)}|i_k\rangle = i_k|i_k\rangle$. Since $|s\rangle$ are eigenstates of $\mathcal{H}_\parallel$, for each particular spin state the driving strength of the resonator Ω in Eq. (A1) is replaced by

$$\Omega_{\parallel,s} \equiv \langle s|\hat{\Omega}_\parallel|s\rangle \equiv \langle s|\frac{1}{2}\sum_{k=1}^n \left[\tilde{g}_0^{(k)} + \tilde{g}_\parallel^{(k)}\sigma_z^{(k)}\right]|s\rangle$$

$$= \frac{1}{2}\sum_{k=1}^n \left[\tilde{g}_0^{(k)} + \tilde{g}_\parallel^{(k)}i_k\right]. \quad (A10)$$

See also Eqs. (17)–(20) of the main text.

One can also derive the *accumulated phase matrix for n qubits*, since $\hat{\Omega}_\parallel$ and $\hat{\Omega}_\parallel^2$ have the same eigenstates $|s\rangle$. After little algebra and dropping the common phase, the

accumulated phase matrix for time t reads

$$\hat{\Phi}(t) = \frac{(\sin \delta t - \delta t)}{2\delta^2}$$
$$\times \left[\sum_{j<k}^n \tilde{g}_\parallel^{(j)}\tilde{g}_\parallel^{(k)} \sigma_z^{(j)} \otimes \sigma_z^{(k)} + \sum_{j=1}^n \tilde{g}_0^{(j)} \sum_{k=1}^n \tilde{g}_\parallel^{(k)} \sigma_z^{(k)}\right].$$
$$(A11)$$

For further applications one considers a gate time with N cycles $t_g = \frac{2\pi N}{\delta}$. Up to single-qubit operations, the accumulated phase for n qubits and for N cycles becomes

$$\hat{\Phi}_N = -\frac{\pi N}{\delta^2} \sum_{j<k}^n \tilde{g}_\parallel^{(j)}\tilde{g}_\parallel^{(k)} \sigma_z^{(j)} \otimes \sigma_z^{(k)}. \quad (A12)$$

3. Controlled π-phase gate for two qubits

For two qubits one requires the relation

$$\frac{\pi N \tilde{g}_\parallel^{(1)}\tilde{g}_\parallel^{(2)}}{\delta^2} = \frac{\pi}{4}, \quad (A13)$$

which sets the required frequency difference $\delta = 2\sqrt{N\tilde{g}_\parallel^{(1)}\tilde{g}_\parallel^{(2)}}$ to obtain the phase matrix $\hat{\Phi}_N = -\frac{\pi}{4}\sigma_z^{(1)} \otimes \sigma_z^{(2)}$. One can show that this is equivalent to a controlled π-phase gate (up to single-qubit operations)

$$|\uparrow\uparrow\rangle \rightarrow |\uparrow\uparrow\rangle,$$
$$|\uparrow\downarrow\rangle \rightarrow e^{i\frac{\pi}{2}}|\uparrow\downarrow\rangle,$$
$$|\downarrow\uparrow\rangle \rightarrow e^{i\frac{\pi}{2}}|\downarrow\uparrow\rangle,$$
$$|\downarrow\downarrow\rangle \rightarrow |\downarrow\downarrow\rangle = e^{-i\pi}\left(e^{i\frac{\pi}{2}}|\downarrow_1\rangle\right)\left(e^{i\frac{\pi}{2}}|\downarrow_2\rangle\right). \quad (A14)$$

APPENDIX B: EQUATIONS OF MOTION FOR THE PARTIAL DENSITY MATRICES $\hat{\rho}ss(t)$, $\hat{\rho}ss'(t)$, AND RESPECTIVE QUANTUM AVERAGES, SUCH AS $\alpha_s(t)$, ETC.

One starts from the Caldeira-Leggett master equation that was derived [82,107] for superconducting Josephson circuits in the context of searching for the macroscopic quantum coherence. While the first derivation was only for the high temperature limit, the result was later extended to zero temperatures as well [83]. The time evolution of the n qubits plus a SC resonator density matrix reads ($\tilde{\mathcal{H}}_{\mathrm{tot}}$ is in the rotating frame with ω_d)

$$\frac{d\rho}{dt} = -i[\tilde{\mathcal{H}}_{\mathrm{tot}}, \rho] - i\frac{\kappa}{2\hbar}[\hat{x}, \{\hat{p}, \rho\}_+] - \frac{K_d}{\hbar^2}[\hat{x}, [\hat{x}, \rho]], \quad (B1)$$

where $\{\hat{p}, \rho\}_+ \equiv \hat{p}\rho + \rho\hat{p}$ is an anticommutator,

$$\hat{x} \equiv \Delta x_0(\hat{a} + \hat{a}^\dagger), \quad \hat{p} \equiv -i\Delta p_0(\hat{a} - \hat{a}^\dagger) \quad (B2)$$

are the position and momentum operators, and the zero-point fluctuations are given by

$$\Delta x_0 \equiv \sqrt{\frac{\hbar}{2\omega_r L_r}}, \quad \Delta p_0 \equiv \sqrt{\frac{\hbar\omega_r L_r}{2}} \quad (B3)$$

($\Delta x_0 \Delta p_0 = \frac{\hbar}{2}$). Note, that as inductance plays the role of *a mass*, Δx_0 has dimension of charge [84]. Using Eq. (B2) one can show that Eq. (B1) coincides with the analogous equation

of the quantum optics [86] in the RWA. Namely, the damping and diffusion term can be reduced in the RWA to the familiar quantum optics decoherence terms expressed via $\hat{a}$, $\hat{a}^\dagger$:

$$-i\frac{\kappa}{2\hbar}[\hat{x}, \{\hat{p}, \rho\}_+] - \frac{K_d}{\hbar^2}[\hat{x}, [\hat{x}, \rho]]$$

$$\simeq \frac{\kappa}{2}(n_{\text{th}} + 1)(2\hat{a}\rho\hat{a}^\dagger - \hat{a}^\dagger\hat{a}\rho - \rho\hat{a}^\dagger\hat{a})$$

$$+ \frac{\kappa}{2}n_{\text{th}}(2\hat{a}^\dagger\rho\hat{a} - \hat{a}\hat{a}^\dagger\rho - \rho\hat{a}\hat{a}^\dagger), \quad \text{(B4)}$$

where $n_{\text{th}} \equiv \frac{1}{2}(\coth\frac{\hbar\omega_r}{2T_r} - 1)$. In what follows we will use both the Caldeira-Leggett and the quantum optics forms depending on the case of study.

1. Evolution for the partial density matrices $\hat{\rho}_{ss}(t)$, $\hat{\rho}_{ss'}(t)$

By expanding the qubit-resonator density matrix in the complete set of qubit operators $|s\rangle\langle s'|$ [87]:

$$\rho = \sum_{s,s'} \hat{\rho}_{s,s'}|s\rangle\langle s'| \quad \text{(B5)}$$

one is to obtain equations for the partial density matrices $\hat{\rho}_{s,s'}$ by substituting into Eq. (B1) and finding the respective (anti)commutators.

Starting with the unitary evolution $\propto [\tilde{\mathcal{H}}_{\text{tot}}, \rho]$, the Hamiltonian $\tilde{\mathcal{H}}_{\text{tot}}$ [Eq. (1)] contains the linear form $\hat{A}(\hat{a}, \hat{a}^\dagger) \equiv \hat{a}e^{i(\tilde{\delta}t+\varphi_d)} + \hat{a}^\dagger e^{-i(\tilde{\delta}t+\varphi_d)}$ and the higher operators

$$\hat{n} \equiv \hat{a}^\dagger\hat{a}, \quad \text{(B6)}$$

$$\hat{X}_\varphi\,\hat{\Omega}_\parallel \equiv [\hat{a}e^{i(\tilde{\delta}t+\varphi)} + \hat{a}^\dagger e^{-i(\tilde{\delta}t+\varphi)}]\hat{\Omega}_\parallel, \quad \text{(B7)}$$

$$\delta\hat{\omega}\,\hat{a}^\dagger\hat{a}. \quad \text{(B8)}$$

Here and below, the frequency differences are in general rotating frame with $\omega_{r'}$ and we assume $\omega_d = \omega_m$, Eq. (6),

$$\tilde{\omega}_r = \omega_r - \omega_{r'}, \quad \tilde{\delta} = \omega_m - \omega_{r'}. \quad \text{(B9)}$$

The n-qubit operators and their eigenvalues are denoted as

$$\hat{\Omega}_\parallel \equiv \frac{1}{2}\sum_j[\tilde{g}_0^{(j)} + \tilde{g}_\parallel^{(j)}\sigma_z^{(j)}], \quad \hat{\Omega}_\parallel|s\rangle = \Omega_{\parallel,s}|s\rangle, \quad \text{(B10)}$$

$$\delta\hat{\omega} \equiv \sum_j \delta\omega^{(j)}\sigma_z^{(j)}, \quad \delta\hat{\omega}|s\rangle = \delta\omega_s|s\rangle. \quad \text{(B11)}$$

The essential commutators are calculated as

$$[\hat{A}(\hat{a}, \hat{a}^\dagger), \hat{\rho}_{s,s'}|s\rangle\langle s'|] = [\hat{A}(\hat{a}, \hat{a}^\dagger), \hat{\rho}_{s,s'}]|s\rangle\langle s'|, \quad \text{(B12)}$$

$$[\delta\hat{\omega}\,\hat{a}^\dagger\hat{a}, \hat{\rho}_{s,s'}|s\rangle\langle s'|] = (\hat{n}\,\hat{\rho}_{s,s'}\,\delta\omega_s - \hat{\rho}_{s,s'}\,\hat{n}\,\delta\omega_{s'})|s\rangle\langle s'|, \quad \text{(B13)}$$

$$[\hat{X}_{\varphi_m}\hat{\Omega}_\parallel, \hat{\rho}_{s,s'}|s\rangle\langle s'|]$$
$$= (\hat{a}\,\hat{\rho}_{s,s'}\,\Omega_{\parallel,s} - \hat{\rho}_{s,s'}\,\hat{a}\,\Omega_{\parallel,s'})|s\rangle\langle s'|e^{i(\tilde{\delta}t+\varphi_m)}$$
$$+ (\tilde{\delta} \to -\tilde{\delta}, \varphi_m \to -\varphi_m, \hat{a} \to \hat{a}^\dagger). \quad \text{(B14)}$$

By introducing the shortcomings

$$B_{\pm,ss'} \equiv \Omega_{\parallel,s} \pm \Omega_{\parallel,s'}, \quad A_{\pm,ss'} \equiv \frac{\delta\omega_s \pm \delta\omega_{s'}}{2} \quad \text{(B15)}$$

one obtains the following equation of motion for $\hat{\rho}_{ss'}(t)$ in a rotating frame with $\omega_{r'}$:

$$\frac{d\hat{\rho}_{ss'}}{dt} = -i\,\tilde{\omega}_r[\hat{n}, \hat{\rho}_{s,s'}]$$

$$- \frac{i}{2}B_{+,ss'}[\hat{X}_{\varphi_m}, \hat{\rho}_{s,s'}] - \frac{i}{2}B_{-,ss'}\{\hat{X}_{\varphi_m}, \hat{\rho}_{s,s'}\}_+$$

$$- iA_{+,ss'}[\hat{n}, \hat{\rho}_{s,s'}] + iA_{-,ss'}\{\hat{n}, \hat{\rho}_{s,s'}\}_+$$

$$- i\varepsilon_d[\hat{X}_{\varphi_d}, \hat{\rho}_{s,s'}] + \{\text{qubits evolution}\}$$

$$- i\frac{\kappa}{2\hbar}[\hat{x}, \{\hat{p}, \hat{\rho}_{ss'}\}_+] - \frac{K_d}{\hbar^2}[\hat{x}, [\hat{x}, \hat{\rho}_{ss'}]]. \quad \text{(B16)}$$

For $s = s'$ one recovers the evolution of the diagonal partial density matrix $\hat{\rho}_{ss}(t)$, Eq. (30) of the main text.

2. Uncorrelated T_1, T_2 processes

The term {qubits evolution} contains the collection of qubits Hamiltonians $\frac{\mathcal{H}_q}{\hbar} = \sum_{j=1}^n \frac{\omega_q^{(j)}}{2}\sigma_z^{(j)}$ and qubits relaxation and dephasing. Using the notation for the n-qubits spin states,

$$|s\rangle \equiv |i_1 \cdots i_j \cdots i_n\rangle, \quad |s'\rangle \equiv |i'_1 \cdots i'_j \cdots i'_n\rangle \quad (i_j, i'_j = \pm 1) \quad \text{(B17)}$$

one obtains for the s, s' term in the expansion of Eq. (B5):

$$\langle s|\frac{(-i)}{\hbar}[\mathcal{H}_q, \rho]|s'\rangle = \hat{\rho}_{s,s'}\sum_j(-i)\frac{\omega_q^{(j)}}{2}(i_j - i'_j), \quad \text{(B18)}$$

$$\langle s|\sum_j \gamma_1^{(j)}\mathcal{D}[\sigma_-^{(j)}]\rho|s'\rangle, \quad \text{(B19)}$$

$$\langle s|\sum_j \frac{\gamma_\phi^{(j)}}{2}\mathcal{D}[\sigma_z^{(j)}]\rho|s'\rangle = -\hat{\rho}_{s,s'}\sum_{j\subset\{i_j\neq i'_j\}}\gamma_\phi^{(j)}. \quad \text{(B20)}$$

Equation (B19) is the contribution generated by the qubits relaxation (T_1 process), which we will not show explicitly here. Nevertheless, it is worth mentioning that the dephasing of the s, s' subspace generated by the relaxations can be calculated via the following mnemonic rule: "For each population that leaves the state s or the state s' with rate $\gamma_1^{(j)} \equiv 1/T_1^{(j)}$ one obtains the dephasing contribution $-\frac{\gamma_1^{(j)}}{2}\rho_{q,ss'}$" summed up over all such cases:

$$\frac{d\rho_{q,ss'}}{dt} \propto -\sum_{j\subset\{\text{subset}\}}\frac{\gamma_1^{(j)}}{2}\rho_{q,ss'}. \quad \text{(B21)}$$

The above relaxation and dephasing contributions are given here for further reference. In a full sweet spot for each of the qubits involved, both relaxation $\gamma_1^{(j)}$ and charge dephasing $\gamma_\phi^{(j)}$ arising via the transverse and longitudinal dipole moments *vanish in this regime*.

3. Degression on the equations of motion for averages and variances: Gaussian resonator states

For each partial density matrix $\hat{\rho}_{s,s'}$ one can derive equations for the averages and variances of the position and

momentum operators [88]. One defines the averages and the variances (here $\sigma \equiv \{s, s'\}$ is a compound index):

$$\bar{x}_\sigma \equiv \langle \hat{x} \rangle_\sigma = \text{Tr}[\hat{x} \hat{\rho}_\sigma], \quad \bar{p}_\sigma \equiv \langle \hat{p} \rangle_\sigma = \text{Tr}[\hat{p} \hat{\rho}_\sigma], \quad \text{(B22)}$$

$$D_x^{(\sigma)} \equiv \langle \hat{x}^2 \rangle_\sigma - \langle \hat{x} \rangle_\sigma^2, \quad \text{(B23)}$$

$$D_p^{(\sigma)} \equiv \langle \hat{p}^2 \rangle_\sigma - \langle \hat{p} \rangle_\sigma^2, \quad \text{(B24)}$$

$$D_{xp}^{(\sigma)} \equiv \frac{\langle \hat{x} \hat{p} + \hat{p} \hat{x} \rangle_\sigma}{2} - \langle \hat{x} \rangle_\sigma \langle \hat{p} \rangle_\sigma. \quad \text{(B25)}$$

Below we consider only the diagonal density matrices and replace $\{s, s'\} \to s$ (the nondiagonal case can be calculated similarly). In a general rotating frame with the frequency $\omega_{r'}$ one gets for the evolution equations for the averages and variances, the latter are made dimensionless via the zero-point fluctuations Δx_0, Δp_0: $d_x^{(s)} \equiv D_x^{(s)}/(\Delta x_0)^2$, $d_p^{(s)} \equiv D_p^{(s)}/(\Delta p_0)^2$, $d_{xp}^{(s)} \equiv D_{xp}^{(s)}/(\Delta x_0 \Delta p_0)$:

$$\frac{\dot{\bar{x}}_s}{\Delta x_0} = \frac{\bar{p}_s}{\Delta p_0}(\tilde{\omega}_r - \delta\omega_s) - 2\Omega_{\parallel,s} \sin(\tilde{\delta} t + \varphi_m), \quad \text{(B26)}$$

$$\frac{\dot{\bar{p}}_s}{\Delta p_0} = -\frac{\bar{x}_s}{\Delta x_0}(\tilde{\omega}_r - \delta\omega_s) - 2\Omega_{\parallel,s} \cos(\tilde{\delta} t + \varphi_m)$$

$$-2\varepsilon_d e^{-i(\tilde{\delta} t + \varphi_d)}) - \kappa \frac{\bar{p}_s}{\Delta p_0}, \quad \text{(B27)}$$

$$\dot{d}^{(s)}_x = (\tilde{\omega}_r - \delta\omega_s) 2d_{xp}^{(s)}, \quad \text{(B28)}$$

$$\dot{d}^{(s)}_p = -(\tilde{\omega}_r - \delta\omega_s) 2d_{xp}^{(s)} - 2\kappa \, d_p^{(s)} + 2\frac{K_d}{(\Delta p_0)^2}, \quad \text{(B29)}$$

$$\dot{d}^{(s)}_{xp} = (\tilde{\omega}_r - \delta\omega_s)\{d_p^{(s)} - d_x^{(s)}\} - \kappa \, d_{xp}^{(s)}. \quad \text{(B30)}$$

Equations (B26)–(B30) are correct *for any density matrix* and the derivation is straightforward from Eq. (B16): one is just using the commutation relations (e.g., $[\hat{x}, \hat{p}] = i\hbar$, etc.) and the cyclic property of the trace.

For a Gaussian density matrix the higher moments are expressed via the five moments, Eqs. (B22)–(B25), and the evolution of the state is completely described by them. It is important to mention that Eq. (B16) as well as Eq. (B1) preserves the Gaussianity of the state. Moreover, under continuous quantum measurement of a resonator a non-Gaussian state rapidly goes to a Gaussian state (see, e.g., Ref. [88]).

It is worth mentioning that Eqs. (B26) and (B27) are exactly the classical Hamilton equations of a damped driven oscillator. By combining them, we reproduce the more familiar equation of motion for the field variable $\alpha_s \equiv \langle \hat{a} \rangle_s = \frac{1}{2}(\frac{\bar{x}_s}{\Delta x_0} + i\frac{\bar{p}_s}{\Delta p_0})$:

$$\dot{\alpha}_s = -i(\tilde{\omega}_r - \delta\omega_s)\alpha_s - i\Omega_{\parallel,s} e^{-i(\tilde{\delta} t + \varphi_m)}$$

$$-i\varepsilon_d e^{-i(\tilde{\delta} t + \varphi_d)} - \frac{\kappa}{2}(\alpha_s - \alpha_s^*), \quad \text{(B31)}$$

where the difference from the quantum optics equation is the last (contrarotating) term that can be neglected in a RWA. For a coherent state $|\alpha\rangle$ (defined via $\hat{a}|\alpha\rangle = \alpha|\alpha\rangle$) its density matrix has minimal variances $d_x = d_p = 1$, $d_{xp} = 0$. This property is preserved by Eqs. (B28)–(B30) at zero resonator temperature $T_r = 0$. The variances are not affected by the resonator driving ($\sim \varepsilon_d$) and qubit modulation $\sim \Omega_{\parallel,s}$.

Also one mentions that the diffusion term $\sim K_d [\hat{x}, [\hat{x}, \hat{\rho}_{ss'}]]$ enters only in the equations for the variances. This last property will be used below to calculate the resonator noise induced n-qubit phase gate error (see Appendix D).

4. Positive $P^{(+)}$ representation and the derivation of the partial dephasing rates $\Gamma_{s,s'}$ for an n-qubit system coupled to a resonator at $T_r = 0$

For the derivation of the dephasing rates we will assume zero resonator temperature $T_r = 0$ as a good approximation (since $\hbar\omega_r \gg k_B T_r$ for a 5–10 GHz resonator and typical SC resonator temperatures T_r of 20–50 mK).

The partial density matrices [87] $\hat{\rho}_{s,s'}$ of the expansion Eq. (B5) can be represented using the positive $P^{(+)}$ representation [108]

$$\hat{\rho}_{ss'}(t) = \int d^2\alpha \, d^2\beta \, \frac{|\alpha\rangle\langle\beta^*|}{\langle\beta^*|\alpha\rangle} P_{ss'}(\alpha, \beta, t), \quad \text{(B32)}$$

where $|\alpha\rangle$ is a coherent state.

From the definition of coherent states one gets the relations

$$\hat{a}|\alpha\rangle = \alpha|\alpha\rangle, \quad \text{(B33)}$$

$$\hat{a}^\dagger|\alpha\rangle = \left(\frac{\partial}{\partial\alpha} + \frac{\alpha^*}{2}\right)|\alpha\rangle. \quad \text{(B34)}$$

One then derives useful correspondences between various terms of the equation of motion, Eq. (B16), and the corresponding $P^{(+)}$-representation kernels:

$$\frac{d\hat{\rho}_{ss'}}{dt} \to \frac{dP_{ss'}(\alpha, \beta, t)}{dt}, \quad \text{(B35)}$$

$$[\hat{a}^\dagger \hat{a}, \hat{\rho}_{ss'}] \to \left(\beta\frac{\partial}{\partial\beta} - \alpha\frac{\partial}{\partial\alpha}\right) P_{ss'}(\alpha, \beta), \quad \text{(B36)}$$

$$\{\hat{a}^\dagger \hat{a}, \hat{\rho}_{ss'}\}_+ \to \left[2\alpha\beta - \frac{\partial}{\partial\alpha}(\alpha \cdot) - \frac{\partial}{\partial\beta}(\beta \cdot)\right] P_{ss'}(\alpha, \beta), \quad \text{(B37)}$$

$$[(\hat{a}^\dagger + \hat{a}), \hat{\rho}_{ss'}] \to \left(\frac{\partial}{\partial\beta} - \frac{\partial}{\partial\alpha}\right) P_{ss'}(\alpha, \beta), \quad \text{(B38)}$$

$$[\hat{X}_\varphi, \hat{\rho}_{ss'}] \to \left(e^{i\varphi}\frac{\partial}{\partial\beta} - e^{-i\varphi}\frac{\partial}{\partial\alpha}\right) P_{ss'}(\alpha, \beta), \quad \text{(B39)}$$

$$\{\hat{X}_\varphi, \hat{\rho}_{ss'}\}_+$$

$$\to \left(2\alpha e^{i\varphi} + 2\beta e^{-i\varphi} - e^{i\varphi}\frac{\partial}{\partial\beta} - e^{-i\varphi}\frac{\partial}{\partial\alpha}\right) P_{ss'}(\alpha, \beta), \quad \text{(B40)}$$

$$\mathcal{D}[\hat{a}]\hat{\rho}_{ss'} \to \frac{1}{2}\left[\frac{\partial}{\partial\alpha}(\alpha \cdot) + \frac{\partial}{\partial\beta}(\beta \cdot)\right] P_{ss'}(\alpha, \beta). \quad \text{(B41)}$$

Substituting Eqs. (B35)–(B41) into Eq. (B16) one derives equation for the positive kernel $P_{ss'}(\alpha, \beta)$:

$$\frac{dP_{ss'}(\alpha,\beta)}{dt} = \frac{i\,\partial}{\partial\alpha}\left[\left((\tilde{\omega}_r + \delta\omega_s)\alpha + \tilde{\varepsilon}_d + \Omega_{\parallel,s}\,e^{-i(\tilde{\delta}t+\varphi_m)} - i\frac{\kappa\alpha}{2}\right)P_{ss'}\right] - \frac{i\,\partial}{\partial\beta}\left[\left((\tilde{\omega}_r + \delta\omega_{s'})\beta + \tilde{\varepsilon}_d^* + \Omega_{\parallel,s'}\,e^{i(\tilde{\delta}t+\varphi_m)} + i\frac{\kappa\beta}{2}\right)P_{ss'}\right]$$

$$- i\,B_{-,ss'}\left(\alpha\,e^{i(\tilde{\delta}t+\varphi_m)} + \beta\,e^{-i(\tilde{\delta}t+\varphi_m)}\right)P_{ss'} - i\,A_{-,ss'}\,2\alpha\beta\,P_{ss'}; \tag{B42}$$

here $\tilde{\varepsilon}_d \equiv \varepsilon_d\,e^{-i(\tilde{\delta}t+\varphi_d)}$ and $A_{-,ss'}$, $B_{-,ss'}$ are from Eq. (B15).

For the diagonal kernel $P_{ss}(\alpha,\beta)$ one then obtains

$$\frac{dP_{ss}(\alpha,\beta)}{dt} = \frac{i\,\partial}{\partial\alpha}\left[\left((\tilde{\omega}_r + \delta\omega_s)\alpha + \tilde{\varepsilon}_d + \Omega_{\parallel,s}\,e^{-i(\tilde{\delta}t+\varphi_m)} - i\frac{\kappa\alpha}{2}\right)P_{ss}\right] - \frac{i\,\partial}{\partial\beta}\left[\left((\tilde{\omega}_r + \delta\omega_s)\beta + \tilde{\varepsilon}_d^* + \Omega_{\parallel,s}\,e^{i(\tilde{\delta}t+\varphi_m)} + i\frac{\kappa\beta}{2}\right)P_{ss}\right]. \tag{B43}$$

5. Coherent state ansatz for $P_{ss'}(\alpha,\beta)$ and solutions of the equations of motion

For $T_r = 0$ we consider coherent (pure Gaussian) states and Eqs. (B42) and (B43) can be solved via coherent state ansatz [109]

$$P_{ss'}(\alpha,\beta) = \rho_{ss'}^q(t)\delta^{(2)}[\alpha - \alpha_s(t)]\,\delta^{(2)}[\beta - \alpha_{s'}^*(t)]. \tag{B44}$$

In this case, by substituting into Eq. (B32) one obtains

$$\hat{\rho}_{s,s'} = \int d^2\alpha\,d^2\beta\,\frac{|\alpha\rangle\langle\beta^*|}{\langle\beta^*|\alpha\rangle}\,\rho_{ss'}^q(t)$$

$$\times \delta^{(2)}[\alpha - \alpha_s(t)]\,\delta^{(2)}[\beta - \alpha_{s'}^*(t)]$$

$$= \rho_{ss'}^q(t)\frac{|\alpha_s(t)\rangle\langle\alpha_{s'}(t)|}{\langle\alpha_{s'}(t)|\alpha_s(t)\rangle}, \tag{B45}$$

and the total qubits-resonator density matrix becomes

$$\rho = \sum_{s,s'}\hat{\rho}_{s,s'}|s\rangle\langle s'| = \sum_{s,s'}\rho_{ss'}^q(t)\frac{|\alpha_s(t)\rangle\langle\alpha_{s'}(t)|}{\langle\alpha_{s'}(t)|\alpha_s(t)\rangle}|s\rangle\langle s'|. \tag{B46}$$

It is straightforward to obtain from this representation the reduced density matrix of the n qubits or of the resonator by tracing out the other degrees of freedom:

$$\rho_{\text{qb}} = \text{Tr}_{\text{res}}[\rho] = \sum_{s,s'}\rho_{ss'}^q(t)\,|s\rangle\langle s'|, \tag{B47}$$

$$\rho_{\text{res}} = \text{Tr}_{\text{qb}}[\rho] = \sum_s\rho_{ss}^q(t)\,|\alpha_s(t)\rangle\langle\alpha_s(t)|, \tag{B48}$$

where for the trace over the resonator we have used $\text{Tr}_{\text{res}}[\cdots] = \frac{1}{\pi}\int d^2\alpha_1\langle\alpha_1|\cdots|\alpha_1\rangle$. It is interesting to note that the reduced resonator density matrix ρ_{res} is a mixed state with weights being the diagonal qubits density matrix elements $\rho_{ss}^q(t)$. Note, however, that $|\alpha_s(t)\rangle$ states are not orthogonal in general: $\langle\alpha_{s'}(t)|\alpha_s(t)\rangle \neq 0$.

From Eq. (B43) for $\dot{P}_{ss}(\alpha,\beta)$ one obtains for the quantum average of the field $\alpha_s(t) \equiv \langle\alpha_s(t)|\hat{a}|\alpha_s(t)\rangle$, the equations in RWA (in a rotating frame with $\omega_{r'}$):

$$\dot{\alpha}_s = -i\left(\tilde{\omega}_r + \delta\omega_s - i\frac{\kappa}{2}\right)\alpha_s - i\varepsilon_d e^{-i(\tilde{\delta}t+\varphi_d)} - i\Omega_{\parallel,s}e^{-i(\tilde{\delta}t+\varphi_m)}, \tag{B49}$$

where $\tilde{\omega}_r \equiv \omega_r - \omega_{r'}$, $\tilde{\delta} \equiv \omega_m - \omega_{r'}$. As expected, Eq. (B49) that is derived for coherent states ($T_r = 0$), coincides with the general Eq. (B31), the latter being true for general Gaussian or non-Gaussian states at any $T_r \neq 0$. For the sake of further reference we write here the general solution of Eq. (B49),

$$\alpha_s(t) = \left(\alpha_s(0) - \frac{\Omega_{\parallel,s}\,e^{-i\varphi_m} + \varepsilon_d\,e^{-i\varphi_d}}{\tilde{\delta} - o_s}\right)e^{-io_s t}$$

$$+ \left(\frac{\Omega_{\parallel,s}\,e^{-i\varphi_m} + \varepsilon_d\,e^{-i\varphi_d}}{\tilde{\delta} - o_s}\right)e^{-i\tilde{\delta}t}, \tag{B50}$$

where $o_s \equiv \tilde{\omega}_r - \delta\omega_s - i\frac{\kappa}{2}$.

With this solution the average photon number in the resonator can be calculated for times $t \lesssim \frac{2\pi}{\delta}$ [assuming $\alpha_s(0) = 0$]:

$$\langle\hat{n}\rangle = |\alpha_s(t)|^2 \simeq 2\left(\frac{\Omega_{\parallel,s}^\varepsilon}{\delta}\right)^2(1 - \cos\delta t) \leqslant 4\left(\frac{\Omega_{\parallel,s}^\varepsilon}{\delta}\right)^2, \tag{B51}$$

where we have used that in the parameter regime of interest, see Table I, $\delta \sim \tilde{g}_\parallel \gg \delta\omega_s \gg \kappa$. For a two-qubit controlled π-phase gate one gets $\langle\hat{n}\rangle \leqslant \frac{1}{2}$.

From Eq. (B42) for $\dot{P}_{ss'}(\alpha,\beta)$, and using the solution of Eq. (B49) for $\alpha_s(t)$, one obtains an equation for the reduced density matrix of the n qubits:

$$\frac{d\rho_{ss'}^q(t)}{dt} = -i[\omega_{q,ss'} - i\gamma_{2,ss'}]\,\rho_{ss'}^q - 2iA_{-,ss'}\alpha_s(t)\,\alpha_{s'}^*(t)\,\rho_{ss'}^q$$

$$- iB_{-,ss'}(\alpha_s(t)\,e^{i(\tilde{\delta}t+\varphi_m)} + \alpha_{s'}^*(t)\,e^{-i(\tilde{\delta}t+\varphi_m)})\,\rho_{ss'}^q. \tag{B52}$$

In the derivation of the equation of motion we have used a relation for the Dirac delta function:

$$x\frac{\partial\delta(x - x_0)}{\partial x} = x_0\frac{\partial\delta(x - x_0)}{\partial x} - \delta(x - x_0). \tag{B53}$$

In Eq. (B52) the first term includes the s, s'-transition frequency, Eq. (B18),

$$\omega_{q,ss'} = \sum_j\frac{\omega_q^{(j)}}{2}(i_j - i_j'), \tag{B54}$$

and the linear s, s' dephasing is arising as a particular sum of all qubits internal dephasings, Eqs. (B20) and (B21):

$$\gamma_{2,ss'} = \sum_{j\subset\{i_j\neq i_j'\}}\gamma_\phi^{(j)} + \sum_{j\subset\{\text{subset}\}}\frac{\gamma_1^{(j)}}{2}. \tag{B55}$$

6. *n*-qubit dephasing rates and frequency shifts mediated by the resonator photon shot noise

The second and third term of Eq. (B52) will provide the qubits dephasing due to resonator leakage (photon shot noise) *mediated by the curvature (quantum capacitance) interactions with the resonator*. Indeed, by integrating Eq. (B52) one obtains the solution

$$\rho_{ss'}^{q}(t) = \rho_{ss'}^{q}(0) \, e^{-i[\omega_{q,ss'} - i\gamma_{2,ss'}]t} \, e^{-2iA_{-,ss'} \int_0^t dt' \alpha_s(t') \alpha_{s'}^*(t')}$$
$$\times \, e^{-iB_{-,ss'} \int_0^t dt' (\alpha_s(t') e^{i(\tilde{\delta}t' + \varphi_m)} + \alpha_{s'}^*(t') e^{-i(\tilde{\delta}t' + \varphi_m)})}. \quad (B56)$$

For the accumulated phase gates of this paper we consider the equal modulation and driving frequencies $\omega_m = \omega_d$ in order to fulfill the cancellation of the spin-independent curvature couplings $\tilde{g}_0^{(j)}$, see Eq. (6). For a rotating frame with ω_r, $\tilde{\delta} \equiv \omega_m - \omega_r \equiv \delta$ and $\tilde{\omega}_r = 0$. Using then the solution of Eq. (B49) for $t \gg 1/\kappa$,

$$\alpha_s^{t \gg} = \frac{\Omega_{\parallel,s} e^{-i\varphi_m} + \varepsilon_d e^{-i\varphi_d}}{\delta - \delta\omega_s - i\frac{\kappa}{2}} e^{-i\delta t} \equiv \alpha_s^{st} e^{-i\delta t}, \quad (B57)$$

one obtains the qubit nondiagonal density matrix evolution in the long-time limit of Eq. (B56):

$$\rho_{ss'}^{q}(t) = \rho_{ss'}^{q}(0) \, e^{-i[\omega_{q,ss'} + \delta\omega_{ss'}^{shot}]t} e^{-[\gamma_{2,ss'} + \Gamma_{\phi,ss'}^{shot}]t}, \quad (B58)$$

where the resonator induced *shot noise* qubits dephasings and qubits frequency shifts (via curvature coupling) are given by

$$\Gamma_{\phi,ss'}^{shot} \equiv -2A_{-,ss'} \text{Im}[\alpha_s^{st} \alpha_{s'}^{st*}] - B_{-,ss'} \text{Im}[\alpha_s^{st} e^{i\varphi_m} + \alpha_{s'}^{st*} e^{-i\varphi_m}]$$
$$(B59)$$

and

$$\delta\omega_{ss'}^{shot} \equiv -2A_{-,ss'} \text{Re}[\alpha_s^{st} \alpha_{s'}^{st*}] - B_{-,ss'} \text{Re}[\alpha_s^{st} e^{i\varphi_m} + \alpha_{s'}^{st*} e^{-i\varphi_m}],$$
$$(B60)$$

respectively. By choosing in the above equations $\varphi_m = 0$ and $\varphi_d = \varphi_m + \pi$, one arrives at the long-time dephasing rates and frequency shifts of Eqs. (57)–(62) of the main text.

In the short-time limit, where $t \lesssim t_g = \frac{2\pi}{\delta} \ll \frac{1}{\delta\omega_s} \ll \frac{1}{\kappa}$, one explicitly integrates Eq. (B56) to obtain for the first time integral in the exponent:

$$-i \int_0^t dt' \alpha_s(t') \alpha_{s'}^*(t') \simeq -2\left(t - \frac{\sin \delta t}{\delta}\right) f_s f_{s'}$$
$$\times \left\{ \frac{\kappa}{2}(\delta\omega_s - \delta\omega_{s'}) + i\left[(\delta - \delta\omega_s)(\delta - \delta\omega_{s'}) + \frac{\kappa^2}{4}\right] \right\},$$
$$(B61)$$

where we denote $f_s \equiv \frac{\Omega_{\parallel,s}^{\varepsilon}}{(\delta - \delta\omega_s)^2 + \frac{\kappa^2}{4}}$. For the second time integral in the exponent in Eq. (B56) one obtains ($\varphi_m = 0$)

$$-i \int_0^t dt' (\alpha_s(t') e^{i\delta t'} + \alpha_{s'}^*(t') e^{-i\delta t'}) \simeq \left\{\left(t - \frac{\sin\delta t}{\delta}\right)\right.$$
$$\times \left[-\frac{\kappa}{2}(f_s - f_{s'}) - i[f_s(\delta - \delta\omega_s) + f_{s'}(\delta - \delta\omega_{s'})]\right]$$
$$+ \frac{\cos\delta t - 1}{\delta}$$
$$\left. \times \left[[f_s(\delta - \delta\omega_s) - f_{s'}(\delta - \delta\omega_{s'})] - i\frac{\kappa}{2}(f_s + f_{s'})\right]\right\}.$$
$$(B62)$$

The linear in time expressions in Eqs. (B61) and (B62) that survive for $t = t_g = \frac{2\pi N}{\delta}$ contribute to the effective dephasing rates $\tilde{\Gamma}_{\phi,ss'}^{shot}$ of Eq. (65), and AC-Stark shifts $\delta\tilde{\omega}_{ss'}^{shot}$ of Eq. (67) of the main text.

APPENDIX C: GATE INFIDELITY DUE TO RESONATOR DAMPING, ALWAYS-ON CURVATURE DISPERSIVELIKE COUPLING, AND DUE TO RESONATOR NOISE

1. Combined gate infidelity

For *n* qubits plus resonator one starts with an initial product state $|\psi_i\rangle \equiv \sum_s a_s|s\rangle |0\rangle$ [we assume vacuum resonator initial state $|\alpha_s(0)\rangle = |0\rangle$ for simplicity]. For an ideal evolution, performing complete N cycles at a gate time $t_g = \frac{2\pi N}{\delta}$, Fig. 10, one ends up in a product state:

$$\left|\psi_f^{id}\right\rangle = \sum_s a_s e^{i\Phi_s^{id}(t)}|s\rangle \, |\alpha_s^{id}(t)\rangle \, |_{t = \frac{2\pi N}{\delta}} \quad (C1)$$

since $\alpha_s^{id}(\frac{2\pi N}{\delta}) = 0$ and $\Phi_s^{id}(\frac{2\pi N}{\delta}) = 2\pi N \left(\frac{\Omega_{\parallel,s}^{\varepsilon}}{\delta}\right)^2$ is the ideal phase given by Eq. (20).

For a nonideal evolution, at the end of the gate cycle the resonator trajectory in the phase space obtains nonzero contributions from the resonator noise $\xi_f(t)$, the resonator damping κ, and from the spin-dependent frequency shift $\delta\omega_s$, Eq. (32), denoted as

$$\delta\alpha_s(t) = \delta\alpha_s^{\xi}(t) + \delta\alpha_s^{k,\delta\omega}(t), \quad (C2)$$

$$\delta\Phi_s(t; [\alpha_s(t)]) = \delta\Phi_s^{\xi}(t) + \delta\Phi_s^{k,\delta\omega}(t), \quad (C3)$$

the latter being path-dependent functionals of $\alpha_s(t)$. These contributions at gate time t_g lead to $|\alpha_s(t_g)\rangle \neq |0\rangle$, and thus leave some qubit-resonator entanglement leading to qubits' gate infidelity. Also, there appear nonlocal in time errors via the accumulated phases.

The fidelity of the actual final state with respect to the ideal final state is then expressed for a particular trajectory $\alpha_s(t)$,

$$\left|\langle\Psi_f|\Psi_f^{id}\rangle\right|^2$$
$$= \sum_s |a_s|^4 \, e^{-|\delta\alpha_s(t)|^2} + \sum_{s<s'} 2|a_s|^2|a_{s'}|^2 \, e^{-\frac{1}{2}(|\delta\alpha_s|^2 + |\delta\alpha_{s'}|^2)}$$
$$\times \cos(\delta\Phi_s - \delta\Phi_{s'}). \quad (C4)$$

Averaging over all initial *n*-qubit states leads to the replacements $|a_s|^4 \rightarrow \overline{|a_s|^4} \equiv f_1$, $2|a_s|^2|a_{s'}|^2 \rightarrow \overline{2|a_s|^2|a_{s'}|^2} \equiv f_{12}$, with $f_1 = f_{12}$ given by Eq. (C13), Appendix C 2.

Averaging over the noise is using the concavity of the exponent $\langle e^A\rangle \geqslant e^{\langle A\rangle}$, the relation (for small fluctuations) $\langle e^A \cos B\rangle_{\xi} \gtrsim \langle e^A e^{-\frac{B^2}{2}}\rangle_{\xi} > e^{\langle A\rangle_{\xi}} e^{-\langle B^2\rangle_{\xi}/2}$, and the zero noise averages $\langle\delta\alpha_s^{\xi}\rangle = 0$, $\langle\delta\Phi_s^{\xi}\rangle = 0$. Thus, for the combined average fidelity one obtains

$$F_{\xi,\kappa,\delta\omega} \equiv \langle|\langle\Psi_f|\Psi_f^{id}\rangle|^2\rangle_{\xi} \gtrsim f_1 \sum_s e^{-\left(\langle|\delta\alpha_s^{\xi}|^2\rangle_{\xi} + |\delta\alpha_s^{k,\delta\omega}|^2\right)}$$
$$+ f_{12} \sum_{s<s'} e^{-\frac{1}{2}\left(\langle|\delta\alpha_s^{\xi}|^2\rangle_{\xi} + |\delta\alpha_s^{k,\delta\omega}|^2 + \langle|\delta\alpha_{s'}^{\xi}|^2\rangle_{\xi} + |\delta\alpha_{s'}^{k,\delta\omega}|^2\right)}$$
$$\times e^{-\frac{\langle\left(\delta\Phi_s^{\xi} - \delta\Phi_{s'}^{\xi}\right)^2\rangle_{\xi}}{2}} e^{-\frac{\left(\delta\Phi_s^{k,\delta\omega} - \delta\Phi_{s'}^{k,\delta\omega}\right)^2}{2}}. \quad (C5)$$

For small fluctuations $\langle|\delta\alpha_s^\xi|^2\rangle_\xi$, $|\delta\alpha_s^{k,\delta\omega}|^2 \ll 1$ and $\langle|\delta\Phi_s^\xi|^2\rangle_\xi$, $|\delta\Phi_s^{k,\delta\omega}|^2 \ll 1$ the infidelity $\delta\epsilon \equiv 1 - F$ splits into two independent contributions:

$$\delta\epsilon_{\xi,\kappa,\delta\omega} = 1 - F_{\xi,\kappa,\delta\omega} \cong \delta\epsilon_{\kappa,\delta\omega} + \delta\epsilon_\xi, \qquad \text{(C6)}$$

$$\delta\epsilon_{\kappa,\delta\omega} = \frac{1}{2^n}\sum_s |\delta\alpha_s^{k,\delta\omega}|^2 + \frac{f_{12}^{(n)}}{2}\sum_{s<s'}\left(\delta\Phi_s^{k,\delta\omega} - \delta\Phi_{s'}^{k,\delta\omega}\right)^2,$$
$$\text{(C7)}$$

$$\delta\epsilon_\xi = \frac{1}{2^n}\sum_s \langle|\delta\alpha_s^\xi|^2\rangle_\xi + \frac{f_{12}^{(n)}}{2}\sum_{s<s'}\langle\left(\delta\Phi_s^\xi - \delta\Phi_{s'}^\xi\right)^2\rangle_\xi.$$
$$\text{(C8)}$$

Here Eq. (C7) for $\delta\epsilon_{\kappa,\delta\omega}$ and Eq. (C8) for $\delta\epsilon_\xi$ reproduce Eqs. (39) and (45) of the main text, respectively. In Eq. (C7) we have used that $f_1^{(n)} + f_{12}^{(n)}\frac{2^n-1}{2} = \frac{1}{2^n}$, which follows from Eq. (C12).

Similarly, one can consider the deviations of the resonator trajectory due to charge (ξ_q) noise fluctuations of the qubit tunnelings $\delta t_{l,r}(t)$. The corresponding infidelity is calculated in Sec. III D, similar to the Johnson noise, Eq. (C8), see Appendix D 2.

2. Averaging over the *n*-qubit initial state

With the initial state

$$|\Psi_i\rangle = \sum_s a_s|s\rangle \qquad \text{(C9)}$$

one needs to find the averages

$$f_s \equiv \overline{|a_s|^4}, \quad f_{s,s'} \equiv \overline{2|a_s|^2|a_s'|^2}, \qquad \text{(C10)}$$

where $\overline{(\cdots)}$ denotes averaging on the initial *n*-qubit state. Since the averages are invariant under any unitary transformation of the basis states $|s\rangle$, one can argue that the averages are s, s' independent and we denote $f_1^{(n)} = f_s^{(n)}$, $f_{s,s'}^{(n)} = f_{12}^{(n)}$ for any s, s'. Moreover, we will conjecture the *uniformity condition*

$$f_1^{(n)} = f_{12}^{(n)} \qquad \text{(C11)}$$

(for the one-qubit and two-qubit case see derivations below). Starting with the normalization condition $\sum_s |a_s|^2 = 1$ one obtains

$$1 = \overline{\left(\sum_s |a_s|^2\right)^2} = \sum_{s=1}^m \overline{|a_s|^4} + \sum_{s<s'}^m \overline{2|a_s|^2|a_s'|^2}$$
$$= mf_1^{(n)} + \frac{m^2-m}{2}f_{12}^{(n)}, \qquad \text{(C12)}$$

where $m \equiv 2^n$ is the *n*-qubit space dimension. Assuming the uniformity condition one obtains

$$f_1^{(n)} = f_s^{(n)} = f_{12}^{(n)} = f_{s,s'}^{(n)} = \frac{1}{2^n + \frac{2^{2n}-2^n}{2}}. \qquad \text{(C13)}$$

a. One-qubit and two-qubit cases

Equation (C13) can be confirmed for the one-qubit and two-qubit cases by explicit averaging over the corresponding Bloch sphere.

Indeed, for the one-qubit (pure state) density matrix one is using S^2 Bloch sphere representation (in 3D) with the amplitudes of $|\Psi_i\rangle = \sum_s a_s|s\rangle = a_1|\uparrow\rangle + a_2|\downarrow\rangle$, obtaining

$$x_0 = \cos\phi_0 = |a_1|^2 - |a_2|^2, \qquad \text{(C14)}$$

$$x_1 = \sin\phi_0\cos\phi_1 = 2\text{Re}(a_1 a_2^*), \qquad \text{(C15)}$$

$$x_2 = \sin\phi_0\sin\phi_1 = 2\text{Im}(a_1 a_2^*),$$
$$\phi_0 \in [0,\pi], \quad \phi_1 \in [0,2\pi), \qquad \text{(C16)}$$

with the S^2 area element $dS_2 = d\phi_0 d\phi_1 \sin\phi_0$, and the total area of $S_2 = 4\pi$. Noting that $|a_1|^4 = \frac{1+x_0^2+2x_0}{4}$, $|a_2|^4 = \frac{1+x_0^2-2x_0}{4}$, and $2|a_1|^2|a_2|^2 = \frac{x_1^2+x_2^2}{2}$, one obtains the averages

$$\overline{|a_1|^4} = \overline{|a_2|^4} = \frac{1+\overline{x_0^2}}{4} = \frac{1}{3}, \qquad \text{(C17)}$$

$$\overline{2|a_1|^2|a_2|^2} = \frac{\overline{x_1^2+x_2^2}}{2} = \frac{1}{3}, \qquad \text{(C18)}$$

where the averaging over the S^2 sphere is represented by

$$\overline{(\cdots)} = \frac{1}{S_2}\int dS_2 (\cdots). \qquad \text{(C19)}$$

The result of Eqs. (C17) and (C18) is in agreement with Eq. (C13) for $n = 1$. (More comprehensive one-qubit averages can be found in Ref. [110]).

For the two-qubit (pure state) $|\Psi_i\rangle = a_1|\uparrow\uparrow\rangle + a_2|\uparrow\downarrow\rangle + a_3|\downarrow\uparrow\rangle + a_4|\downarrow\downarrow\rangle$ one is using the S^4-Bloch sphere coordinates (in 5D), related to the density matrix elements (see, e.g., Ref. [111])

$$x_0 = \cos\phi_0 = |a_1|^2 + |a_2|^2 - |a_3|^2 - |a_4|^2, \quad \text{(C20)}$$

$$x_1 = \sin\phi_0\cos\phi_1 = 2\text{Re}(a_1^* a_3 + a_2^* a_4), \qquad \text{(C21)}$$

$$x_2 = \sin\phi_0\sin\phi_1\cos\phi_2 = 2\text{Im}(a_1^* a_3 + a_2^* a_4), \quad \text{(C22)}$$

$$x_3 = \sin\phi_0\sin\phi_1\sin\phi_2\cos\phi_3 = 2\text{Re}(a_1 a_4 - a_2 a_3),$$
$$\text{(C23)}$$

$$x_4 = \sin\phi_0\sin\phi_1\sin\phi_2\sin\phi_3 = 2\text{Im}(a_1 a_4 - a_2 a_3),$$
$$\phi_0, \phi_1, \phi_2, \in [0,\pi], \ \phi_3 \in [0,2\pi). \qquad \text{(C24)}$$

The area element is $dS_4 = d\phi_0 d\phi_1 d\phi_2 d\phi_3 \sin^3\phi_0 \sin^2\phi_1 \sin\phi_2$ and the total area of the S^4-Bloch sphere is $S_4 = \frac{8\pi^2}{3}$. Using the 5D Bloch sphere representation, it is straightforward to show that

$$f_s \equiv \overline{|a_s|^4} = f_{s,s'} \equiv \overline{2|a_s|^2|a_s'|^2} = \frac{1}{10}, \quad \forall s, s' = 1, 2, 3, 4,$$
$$\text{(C25)}$$

in agreement with Eq. (C13) for $n = 2$.

b. The *n*-qubit case

In the general *n*-qubit case an explicit averaging may be cumbersome. Instead, one can use symmetry arguments. Indeed, the *n*-qubit density matrix $\rho = \sum_{s,s'} a_s a_{s'}^*|s\rangle\langle s'|$ can be expanded in the $2^{2n} - 1$ basis operators (Kronecker products of Pauli matrices: here $\sigma_0 \equiv I_2$, $\sigma_{1,2,3} \equiv \sigma_{x,y,z}$), $\hat{f}_l = \sigma_{\mu_1} \otimes$

$\cdots \otimes \sigma_{\mu_n}$, $\mu_i = 0, 1, 2, 3$, $\forall i$:

$$\rho = \frac{1}{2^n}\left(1 + \sum_{l=1}^{2^{2n}-1} w_l \hat{f}_l\right). \tag{C26}$$

This expansion can be performed by writing the operators $|s\rangle\langle s'|$ as Kronecker products

$$|s\rangle\langle s'| \equiv |i_1,\ldots,i_n\rangle\langle i_1',\ldots,i_n'| = |i_1\rangle\langle i_1'| \otimes \cdots \otimes |i_n\rangle\langle i_n'|, \tag{C27}$$

and mentioning that (k enumerates the qubits)

$$|i_k\rangle\langle i_k'| = \tfrac{1}{2}\left(\sigma_0^{(k)} \pm \sigma_3^{(k)}\right) \quad \text{for } i_k = i_k', \tag{C28}$$

$$|i_k\rangle\langle i_k'| = \tfrac{1}{2}\left(\sigma_1^{(k)} \pm i\,\sigma_2^{(k)}\right) \quad \text{for } i_k \neq i_k'. \tag{C29}$$

Using symmetry arguments along the line of Ref. [112], one can show that averaging over the n-qubit initial state for the expansion coefficients w_k leads to

$$\overline{w_l} = 0, \quad \overline{w_l^2} = \frac{1}{1+2^n}. \tag{C30}$$

On the other hand, w_l^2 can be re-expanded as linear combinations of $|a_s|^4$ and $2|a_s|^2|a_{s'}|^2$, $s, s' \in \{1,\ldots,2^n\}$. Solving these equations one can re-establish the uniformity condition, Eq. (C13), for the n-qubit case.

3. The infidelity $\delta\epsilon_{\kappa,\delta\omega}$ in a simple strategy

In this section we perform exact calculations of the infidelity $\delta\epsilon_{\kappa,\delta\omega}$ in a simple strategy when the modulation amplitude $\Omega_{\parallel,s}$ changes sign on each subsequent cycle, see Fig. 4. This can be achieved by changing the phase of the qubits gate modulations, $\varphi_m \to \varphi_m + \pi$, and simultaneously changing the phase of the resonator driving, $\varphi_d \to \varphi_d + \pi$, while keeping the relation $\varphi_d = \varphi_m + \pi$, see Eq. (6). In Sec. III A of the main text we have shown that this simple strategy works well when the energy curvature resonator shift $\delta\omega_s$, Eq. (32), is small or can be neglected with respect to resonator damping κ. In general, one deals with the opposite case of $\delta\omega_s \gg \kappa$.

For the n-qubit state $|s\rangle$ one uses the general solution for the $\alpha_s(t)$, Eq. (B50), with $\omega_d = \omega_m$ and $\varphi_d = \varphi_m + \pi$ in a rotating frame with ω_r (see Appendix A) to obtain

$$\alpha_s(t) = \alpha_s(0)\, e^{-i(\delta\omega_s - i\frac{\kappa}{2})t} - \frac{\Omega_{\parallel,s}^{\varepsilon}\, e^{-i\varphi_m}}{[\delta - \delta\omega_s] + i\frac{\kappa}{2}}$$
$$\times \left[e^{-i(\delta\omega_s - i\frac{\kappa}{2})t} - e^{-i\delta t}\right]$$
$$\equiv A_s(t) + B_s(t), \tag{C31}$$

where $\delta = \omega_m - \omega_r$ and $\Omega_{\parallel,s}^{\varepsilon}$ is defined in Eq. (43). We note that by changing the modulation phase $\varphi_m \to \varphi_m + \pi$ after

each cycle the sign of $\Omega_{\parallel,s}^{\varepsilon}$ flips, allowing for essential cancellation of the effects of damping κ and energy curvature detuning $\delta\omega_s$, see Fig. 4.

Starting with $\alpha_s(0) = 0$, the deviation from zero after one cycle is

$$\alpha_s\left(\frac{2\pi}{\delta}\right) = \frac{-i\Omega_{\parallel,s}^{\varepsilon}}{b_s^*}\left[e^{b_s^* \frac{2\pi}{\delta}} - 1\right], \tag{C32}$$

where we denoted $b_s \equiv -i[\delta - \delta\omega_s] - \frac{\kappa}{2}$. For the deviation of $\alpha_s(t)$ accumulated after the Nth cycle ($N = 1, 2, 3, \ldots$) one then obtains, using recurrences (the deviation at the end of each cycle is an initial condition for the next cycle)

$$\delta\tilde{\alpha}_s\left(N\frac{2\pi}{\delta}\right) = \alpha_s\left(\frac{2\pi}{\delta}\right)\frac{e^{b_s^* N \frac{2\pi}{\delta}} - (-1)^N}{e^{b_s^* \frac{2\pi}{\delta}} + 1}. \tag{C33}$$

Here $\tilde{\alpha}_s(t)$ denotes a time evolution with flipping sign of the modulation strength $\Omega_{\parallel,s}^{\varepsilon}$. The quantity of interest that enters the gate error $\delta\varepsilon_{\kappa,\delta\omega}$ is then given by

$$\left|\delta\alpha_s^{\kappa,\delta\omega}\right|^2 \equiv \left|\delta\tilde{\alpha}_s\left(N\frac{2\pi}{\delta}\right)\right|^2$$
$$= \frac{(\Omega_{\parallel,s}^{\varepsilon})^2}{|b_s|^2}\frac{\left[\cosh\left(\frac{\pi\kappa}{\delta}\right) - \cos\left(\frac{2\pi\delta\omega_s}{\delta}\right)\right]}{\left[\cosh\left(\frac{\pi\kappa}{\delta}\right) + \cos\left(\frac{2\pi\delta\omega_s}{\delta}\right)\right]}e^{-\frac{N\pi\kappa}{\delta}}$$
$$\times \left[\cosh\left(\frac{N\pi\kappa}{\delta}\right) - (-1)^N \cos\left(\frac{N 2\pi\delta\omega_s}{\delta}\right)\right]. \tag{C34}$$

For the accumulated phases one uses the equation $\dot{\alpha}_s = -i(\delta\omega_s - i\frac{\kappa}{2})\alpha_s(t) - i\Omega_{\parallel,s}^{\varepsilon} e^{-i\varphi_m} e^{-i\delta t}$ and its solution, Eq. (C31). Thus, for the accumulated phase integral one obtains three contributions for the time of the n_1 cycle:

$$I_{\Phi,s} = \int_{t_1}^{t_2} dt'\, \alpha_s^*(t')\dot{\alpha}_s(t') \tag{C35}$$
$$= \int_{t_1}^{t_2} dt' \left\{-i\left(\delta\omega_s - i\frac{\kappa}{2}\right)|A_s(t') + B_s(t')|^2\right.$$
$$- iA_s^*(t')\,\Omega_{\parallel,s}^{\varepsilon}\, e^{-i\varphi_m}\, e^{-i\delta t'}$$
$$\left. - iB_s^*(t')\,\Omega_{\parallel,s}^{\varepsilon}\, e^{-i\varphi_m}\, e^{-i\delta t'}\right\} \tag{C36}$$
$$\equiv I_{\Phi,s}^{(1)} + I_{\Phi,s}^{(2)} + I_{\Phi,s}^{(3)}, \tag{C37}$$

where $t_1 = (n_1 - 1)\frac{2\pi}{\delta}$ and $t_2 = n_1\frac{2\pi}{\delta}$, and $\Delta t \equiv t_2 - t_1 = \frac{2\pi}{\delta}$. For the sake of further use we write down the result of the integration:

$$I_{\Phi,s}^{(1)} = -i\left(\delta\omega_s - i\frac{\kappa}{2}\right)\int_{t_1}^{t_2} dt'\, |A_s(t') + B_s(t')|^2$$

$$= -i\left(\delta\omega_s - i\frac{\kappa}{2}\right)\left\{|\alpha_s(0)|^2\frac{2\pi}{\delta} + \frac{(\Omega_{\parallel,s}^{\varepsilon})^2}{|b_s|^2}\left[\Delta t + \frac{1}{b_s}e^{b_s t_1}\left(1 - e^{b_s \Delta t}\right) + \frac{1}{b_s^*}e^{b_s^* t_1}\left(1 - e^{b_s^* \Delta t}\right) + \frac{1}{b_s + b_s^*}e^{(b_s + b_s^*)t_1}\left(e^{(b_s + b_s^*)\Delta t} - 1\right)\right]\right.$$

$$\left. + \frac{i\alpha_s(0)\Omega_{\parallel,s}^{\varepsilon}}{b_s}\left[\frac{1}{b_s + b_s^*}e^{(b_s + b_s^*)t_1}\left(e^{(b_s + b_s^*)\Delta t} - 1\right) - \frac{1}{b_s^*}e^{b_s^* t_1}\left(e^{b_s^* \Delta t} - 1\right)\right] + \text{c.c.}\right\}, \tag{C38}$$

$$I_{\Phi,s}^{(2)} = -i\Omega_{\parallel,s}^{\varepsilon} \, e^{-i\varphi_m} \int_{t_1}^{t_2} dt' \, A_s^*(t') \, e^{-i\delta t'} = \frac{-i\alpha_s(0)^* \Omega_{\parallel,s}^{\varepsilon}}{b_s} \, e^{b_s t_1}(e^{b_s \Delta t} - 1), \tag{C39}$$

$$I_{\Phi,s}^{(3)} = -i\Omega_{\parallel,s}^{\varepsilon} \, e^{-i\varphi_m} \int_{t_1}^{t_2} dt' \, B_s^*(t') \, e^{-i\delta t'} = \frac{(\Omega_{\parallel,s}^{\varepsilon})^2}{b_s} \left[\frac{1}{b_s} e^{b_s t_1}(e^{b_s \Delta t} - 1) - \Delta t \right]. \tag{C40}$$

The accumulated phase error $\delta\Phi_s^{\kappa \delta\omega}$ is then given by

$$\delta\Phi_s^{\kappa, \delta\omega} = \mathrm{Im} I_{\Phi,s} - \mathrm{Im} I_{\Phi,s} \Big|_{\kappa=0, \delta\omega_s=0}. \tag{C41}$$

APPENDIX D: MULTIQUBIT PHASE GATE INFIDELITY DUE TO RESONATOR (JOHNSON) NOISE

1. Diffusion term in the Caldeira-Leggett master equation as generated via a random force Hamiltonian

Here we show that the random force Hamiltonian $\mathcal{H}_f = -\xi_f(t)\hat{x}$, Eq. (36), is an unraveling of the diffusion term in the ensemble-averaged Caldeira-Leggett Eq. (27). By definition, the (single-sided) spectral density S_f is defined by the correlator

$$\langle \xi_f(t)\xi_f(t') \rangle_\xi = \frac{S_f}{2}\delta(t - t'), \tag{D1}$$

where $\langle \cdots \rangle_\xi$ denotes averaging over realizations of the noise process. It will be useful to work in the position representation, so that the generic density matrix element is $\rho(x, x') \equiv \rho_{xx'}$, with the position being a continuous index. By adding the random force Hamiltonian in the Stratonovich form of the equations of motion (as for any physical interaction, see, e.g., Refs. [87,113]) one obtains

$$\frac{d\rho_{xx'}}{dt} = -\frac{i}{\hbar}[\mathcal{H}_{\mathrm{tot}}, \rho]_{xx'} - \frac{i}{\hbar}[\mathcal{H}_f, \rho]_{xx'}$$
$$\equiv G_{\mathrm{Strat}}(\rho_{xx'}) + F(\rho_{xx'})\xi_f(t), \tag{D2}$$

where $G(\rho_{xx'})$ and $F(\rho_{xx'})\xi_f(t)$ are the regular and the noise part, respectively. The noise part is calculated from the commutator $[\hat{x}, \rho]_{xx'} = (x - x')\rho_{xx'}$:

$$F(\rho_{xx'}) = \frac{i}{\hbar}(x - x')\rho_{xx'}. \tag{D3}$$

The transition to the Itô form of the equation of motion follows the prescription of Refs. [114,115] for a system of differential equations, however with the replacing of a discrete index "i" (that enumerates the number of equations) with the continuous index (x, x'), and by replacing the partial derivatives $\frac{\partial F_i}{\partial \rho_k}$ with a *functional derivative* (let $x < x'$):

$$\frac{\delta F[\rho(x, x')]}{\delta \rho(x_1, x_2)} = \frac{i}{\hbar}(x - x')\,\delta(x - x_1)\,\delta(x' - x_2), \tag{D4}$$

with $\delta(x)$ being the Dirac delta function. Thus, the regular part in the Itô form is given by (see also Ref. [88])

$$G_{\mathrm{Ito}}(\rho_{xx'}) = G_{\mathrm{Strat}}(\rho_{xx'}) + \frac{S_f}{4}\int_{-\infty}^{\infty}\int_{-\infty}^{x_2} dx_1 dx_2$$

$$\times \frac{\delta F[\rho(x, x')]}{\delta \rho(x_1, x_2)} F[\rho(x_1, x_2)] \tag{D5}$$

$$= G_{\mathrm{Strat}}(\rho_{xx'}) - \frac{S_f}{4\hbar^2}(x - x')^2 \rho_{xx'} \tag{D6}$$

and the equation of motion for the density matrix in Itô form is given by

$$d\rho_{xx'} = -\frac{i}{\hbar}[\mathcal{H}_{\mathrm{tot}}, \rho]_{xx'} - \frac{S_f}{4\hbar^2}(x - x')^2 \rho_{xx'} \, dt$$
$$+ \frac{i}{\hbar}(x - x')\rho_{xx'} \, \xi_f(t) \, dt. \tag{D7}$$

Averaging over the noise in Eq. (D7) (by simply dropping the noise term) one can identify the second term in Eq. (D7) with the diffusion term in Eq. (27) by choosing the noise spectral density as

$$S_f = 4K_d \equiv 2\hbar\omega_r L_r \, \kappa \, \coth\frac{\hbar\omega_r}{2k_B T} \tag{D8}$$

and by noting that the double commutator in position representation is given by

$$[\hat{x}, [\hat{x}, \rho]]_{xx'} = (x - x')^2 \rho_{xx'}. \tag{D9}$$

By using the random force Hamiltonian one calculates its contribution to the equations of motion for the average position and momentum via Eq. (D7). (Below we have dropped the index "s" enumerating different n-qubit states.)

$$d\bar{x} = \mathrm{Tr}[\hat{x} \, d\rho] = \int dx \, x \, d\rho_{xx} = \int dx \, x\left(-\frac{i}{\hbar}\right)[\mathcal{H}_{\mathrm{tot}}, \rho]_{xx} \, dt$$

$$= -\frac{i}{\hbar}\mathrm{Tr}(\hat{x}\,[\mathcal{H}_{\mathrm{tot}}, \rho])dt, \tag{D10}$$

$$d\bar{p} = -\frac{i}{\hbar}\mathrm{Tr}[\hat{p} \, d\rho] = \mathrm{Tr}(\hat{p}\,[\mathcal{H}_{\mathrm{tot}}, \rho])dt + \xi_f(t) \, dt, \tag{D11}$$

where we have used the momentum operator in position representation:

$$(\hat{p})_{x\tilde{x}} = [-i\hbar\delta(x - \tilde{x})]\frac{\partial}{\partial \tilde{x}}. \tag{D12}$$

Using Eqs. (D10) and (D11) one obtains an additional noise term in the equation of motion of the field variable $\alpha_s \equiv \langle \hat{a} \rangle_s = \frac{1}{2}(\frac{\bar{x}_s}{\Delta x_0} + i\frac{\bar{p}_s}{\Delta p_0})$. Notice, that for the averages (first moments), Itô and Stratonovich forms of the equations coincide, and by going to the rotating frame with $\omega_{r'}$ one obtains

$$\dot{\alpha}_s = -i(\tilde{\omega}_r - \delta\omega_s)\alpha_s - i\Omega_{\parallel,s}e^{-i(\tilde{\delta}t + \varphi_m)} - i\varepsilon_d e^{-i(\tilde{\delta}t + \varphi_d)}$$
$$- \frac{\kappa}{2}(\alpha_s - \alpha_s^*) + i\frac{\xi_f(t)}{2\Delta p_0}e^{i\omega_{r'}t}, \tag{D13}$$

to be compared with Eq. (35). The noisy evolution of $\alpha_s(t)$ due to the last stochastic term is shown schematically in Fig. 4. [It cannot be neglected in a rotating wave approximation since the white noise $\xi_f(t)$ contains a frequency component that eliminates the fast rotating factor.]

2. The variances $\langle|\delta\alpha_s|^2\rangle_\xi$ and $\langle\delta\Phi_s\,\delta\Phi_{s'}\rangle_\xi$

Calculation of infidelity caused by the resonator (Johnson) noise requires the knowledge of the variances $\langle|\delta\alpha_s|^2\rangle_\xi$ and $\langle\delta\Phi_s\,\delta\Phi_{s'}\rangle_\xi$, see Eq. (45) or (C8). The resonator trajectory in the phase space $\alpha_s(t)$ obtains a fluctuating term $\delta\alpha_s(t)$, see Fig. 4 and Eq. (D13), with a zero average over the realizations of the noise process $\langle\delta\alpha_s(t)\rangle_\xi = 0$. Similarly, the average of the accumulated phase fluctuation is zero over the realizations $\langle\delta\Phi_s(t)\rangle_\xi = 0$, see below. The fluctuation at time t is obtained by integration of the last term in Eq. (D13) thus obtaining Eq. (46) of the main text (we have used that the vacuum fluctuations satisfy $\Delta x_0\,\Delta p_0 = \hbar/2$). From Eq. (D13) and in rotation frame with ω_r the variance of $\alpha_s(t)$ is

$$\langle|\delta\alpha_s(t)|^2\rangle_\xi$$
$$= \left(\frac{\Delta x_0}{\hbar}\right)^2 \int_0^t \int_0^t dt'dt'' e^{i\omega_r(t'-t'')}\langle\xi_f(t')\xi_f(t'')\rangle_\xi \tag{D14}$$

that is spin independent. By introducing the shortcoming for the noise $r(t) \equiv -\xi_f(t)\Delta x_0/\hbar$ one writes the white noise average:

$$\langle r(t')\,r(t'')\rangle_\xi = \frac{S_f(\Delta x_0)^2}{2\hbar^2}\,\delta(t'-t'') \equiv C_0\,\delta(t'-t''), \tag{D15}$$

$$C_0 \equiv \frac{\kappa}{2}\coth\left(\frac{\hbar\omega_r}{2k_BT}\right), \tag{D16}$$

also using the relations (B2) and (D8).

The accumulated phase variance $\langle\delta\Phi_s(t)^2\rangle_\xi = \langle[\mathrm{Im}\,\delta I_{\Phi,s}]^2\rangle_\xi$ is obtained via the fluctuations of the accumulated phase integral [scf. Eq. (A8)], assuming small variations $\delta\alpha_s(t)$. Expanding $I_{\Phi,s}(t)$ to first order one obtains

$$\delta I_{\Phi,s}(t) \simeq \int_0^t dt'\left[\delta\alpha_s^*(t')\frac{d\alpha_s^{\mathrm{id}}(t')}{dt'} + \alpha_s^{\mathrm{id}\,*}(t')\frac{d\delta\alpha_s(t')}{dt'}\right] \tag{D17}$$

$$\equiv \delta A_{1,s} + \delta A_{2,s}, \tag{D18}$$

$$A_{1s} \equiv \int_0^t dt'\,\delta\alpha_s^*(t')\frac{d\alpha_s^{\mathrm{id}}(t')}{dt'},$$
$$A_{2s} \equiv \int_0^t dt'\,\alpha_s^{\mathrm{id}\,*}(t')\frac{d\delta\alpha_s(t')}{dt'}, \tag{D19}$$

where the ideal resonator evolution is given by Eq. (18) or (A3), see Fig. 10, i.e., here we do not take into account higher corrections due to the resonator damping κ and the always-on curvature dispersivelike resonator frequency shifts $\delta\omega$ given by Eq. (7). Indeed, the error of such approximation is of second order in the small resonator trajectory deviations, e.g., $\sim\delta\alpha_s^\xi\,\delta\alpha_s^{\kappa,\delta\omega}$. Thus, the s dependence of the accumulated phase variation will come only through the *modulation driving strength* $\Omega_{\parallel,s}$, see Eq. (17) or (B10).

For the resonator driving conditions of Eq. (6), one is replacing the modulation strength by $\Omega_{\parallel,s}^\varepsilon$, Eq. (43), and the phase of the modulation is chosen as $\varphi_m = 0$. The ideal evolution (neglecting the κ and $\delta\omega_s$ terms) is recast to $\dot\alpha_s^{\mathrm{id}} = -i\Omega_{\parallel,s}^\varepsilon e^{-i\delta t}$.

The fluctuation of the accumulated phase is then

$$\delta\Phi_s = \mathrm{Im}(\delta I_{\Phi_s}) \equiv \mathrm{Im}(A_{1s}) + \mathrm{Im}(A_{2s}), \tag{D20}$$

$$\mathrm{Im}(A_{1s}) = -\Omega_{\parallel,s}^\varepsilon \int_0^t dt' \int_0^{t'} dt''r(t'')\sin(\delta t'+\omega_r t''), \tag{D21}$$

$$\mathrm{Im}(A_{2s}) = \frac{\Omega_{\parallel,s}^\varepsilon}{\delta}\int_0^t dt'r(t')[\cos(\omega_r t') - \cos(\omega_m t')]. \tag{D22}$$

The variance of the accumulated phase $\langle\delta\Phi_s\,\delta\Phi_{s'}\rangle_\xi$ is obtained via explicit time integration with Eqs. (D21) and (D22), using Eq. (D15) for the noise average:

$$\langle\mathrm{Im}(A_{1s})\,\mathrm{Im}(A_{1s'})\rangle_\xi \simeq \left(\Omega_{\parallel,s}^\varepsilon\Omega_{\parallel,s'}^\varepsilon\right)C_0 \tag{D23}$$

$$\times\left[\frac{t}{\delta^2} - \frac{\sin(\delta t)}{\delta^3}\right], \tag{D24}$$

$$\langle\mathrm{Im}(A_{1s})\mathrm{Im}(A_{2s'})\rangle_\xi \simeq -\left(\Omega_{\parallel,s}^\varepsilon\frac{\Omega_{\parallel,s'}^\varepsilon}{\delta}\right)C_0\left\{\frac{t}{2\delta}[1+\cos(\delta t)]\right\},$$

$$\langle\mathrm{Im}(A_{2s})\,\mathrm{Im}(A_{2s'})\rangle_\xi \simeq \left(\frac{\Omega_{\parallel,s}^\varepsilon\Omega_{\parallel,s'}^\varepsilon}{\delta^2}\right)C_0\left[t - \frac{4\sin(\delta t)}{\delta}\right], \tag{D25}$$

where only leading contributions are shown, with corrections of the order of $\mathcal{O}(\frac{\delta}{\omega_r})$. One can see that these averages, Eqs. (D23)–(D25), oscillate in time, as expected for variances of a modulating resonator. For a complete number of cycles, $\delta t = 2\pi N$, $N = 2, 4, \ldots$ some of these are zeroed or minimized, and the average of interest is obtained:

$$\langle[\delta\Phi_s(t) - \delta\Phi_{s'}(t)]^2\rangle_\xi = 4C_0\frac{\left[\Omega_{\parallel,s}^\varepsilon - \Omega_{\parallel,s'}^\varepsilon\right]^2}{\delta^2}\frac{2\pi N}{\delta}, \tag{D26}$$

as is Eq. (49) of the main text. The variance of the accumulated phase fluctuations is linear in time units of $t = \frac{2\pi N}{\delta}$.

APPENDIX E: INFIDELITY OF n-QUBIT PHASE GATE DUE TO QUBITS' CHARGE NOISE

For an initial product state of n-qubits plus resonator the ideal final state after one cycle $t = \frac{2\pi}{\delta}$ is defined by the accumulated (geometric) phases and the frequency ω_s of the $|s\rangle$ state: $|\psi_f^{\mathrm{id}}\rangle = \sum_s a_s e^{i\Phi_s(t)}e^{-i\omega_s t}|s\rangle|0\rangle$, where

$$\omega_s = \sum_j\langle s|\frac{\omega_q^{(j)}}{2}\sigma_z^{(j)}|s\rangle \tag{E1}$$

is the frequency of the $|s\rangle$ state. Since the qubit energy defining parameters (voltage gates) fluctuate, an additional fluctuating phase is accumulated. Thus, for the (j)th qubit with a fluctuation, $\omega_q^{(j)} + \delta\omega_q^{(j)}(t)$ one obtains the phase factor

$$e^{-i\omega_q^{(j)}t}\,e^{-i\Delta\phi^{(j)}(t)}, \quad \Delta\phi^{(j)}(t) \equiv \int_0^t dt'\,\delta\omega_q^{(j)}(t') \tag{E2}$$

(we consider only longitudinal noise, see, e.g., Ref. [24]). The accumulated phase noise of the $|s\rangle$ state is then expressed via

individual qubit noises

$$\Delta\phi_s(t) = \sum_j \langle s | \frac{\Delta\phi^{(j)}(t)}{2} \sigma_z^{(j)} | s \rangle, \tag{E3}$$

and the actual final state acquires noisy phases $|\psi_f\rangle = \sum_s a_s e^{i\Phi_s(t)} e^{-i\omega_s t} e^{-i\Delta\phi_s(t)} |s\rangle |0\rangle$. The fidelity of a single realization of the noise process is obtained as

$$F = \left| \langle \psi_f^{\mathrm{id}} | \psi_f \rangle \right|^2 = \sum_s |a_s|^4$$

$$+ \sum_{s<s'} 2 |a_s|^2 |a_{s'}|^2 e^{-i[\Delta\phi_s(t)-\Delta\phi_{s'}(t)]} \cos\delta\tilde{\tilde{\omega}}_{ss'} t, \tag{E4}$$

where the deterministic qubit evolutions is due to possibly induced AC-Stark shifts, see Eq. (67), and Appendix B 6, Eq. (B62). One then averages over the initial n-qubit state and over the noise realizations to get

$$\overline{\langle F \rangle}_{\xi_q} = 2^n f_1^{(n)} + f_{12}^{(n)} \sum_{s<s'} \langle e^{-i[\Delta\phi_s(t)-\Delta\phi_{s'}(t)]} \rangle_{\xi_q} \cos\delta\tilde{\tilde{\omega}}_{ss'} t. \tag{E5}$$

Here $f_1 \equiv \overline{|a_s|^4} = f_{12} \equiv \overline{2|a_s|^2|a_{s'}|^2}$ are the averages over the initial qubit states, given by Eq. (C13).

One calculates the dephasing factor assuming that the random variable $X_{ss'} \equiv [\Delta\phi_s(t) - \Delta\phi_{s'}(t)]$ has zero mean and is Gaussian distributed and obtains

$$\langle e^{-i[\Delta\phi_s(t)-\Delta\phi_{s'}(t)]} \rangle_{\xi_q} = e^{-\frac{1}{2}\langle [\Delta\phi_s(t)-\Delta\phi_{s'}(t)]^2 \rangle_{\xi_q}}. \tag{E6}$$

Assuming small variances and using Eq. (C12) one obtains the n-qubit infidelity due to charge noise in a general form:

$$\delta\varepsilon_\phi^{\mathrm{n\,Qb}} \equiv 1 - \overline{\langle F \rangle}_{\xi_q} = f_{12}^{(n)} \sum_{s<s'} \frac{1}{2} \langle [\Delta\phi_s(t) - \Delta\phi_{s'}(t)]^2 \rangle_{\xi_q}. \tag{E7}$$

1. Correlated white noises

If the noises impinged on the qubits are white noise correlated (with correlation matrix A^{jk})

$$\langle \delta\omega_q^{(j)}(t') \delta\omega_q^{(j)}(t'') \rangle = A^{jk} \delta(t'-t''), \tag{E8}$$

the correlation of interest in Eq. (E7) can be represented as

$$\frac{1}{2} \langle [\Delta\phi_s(t) - \Delta\phi_{s'}(t)]^2 \rangle_{\xi_q} = \Gamma_{\phi,ss'} \, t. \tag{E9}$$

To see this, one rewrites the random variable $\Delta\phi_s(t) - \Delta\phi_{s'}(t)$ as

$$\Delta\phi_s(t) - \Delta\phi_{s'}(t) = \int_0^t dt' \sum_j \frac{\delta\omega_q^{(j)}(t')}{2} (i_j - i'_j), \tag{E10}$$

$$|s\rangle \equiv |i_1, \ldots, i_n\rangle, \quad |s'\rangle \equiv |i'_1, \ldots, i'_n\rangle, \tag{E11}$$

$$\langle s | \sigma_z^{(j)} | s \rangle = i_j, \quad \langle s' | \sigma_z^{(j)} | s' \rangle = i'_j, \tag{E12}$$

and obtain the average via the δ correlation, Eq. (E8):

$$\frac{1}{2} \langle [\Delta\phi_s(t) - \Delta\phi_{s'}(t)]^2 \rangle = \sum_{j,k} (i_j - i'_j)(i_k - i'_k) \frac{A^{jk}}{8} t. \tag{E13}$$

Thus, one obtains the n-qubit dephasing rates for correlated white noise:

$$\Gamma_{\phi,ss'}^{\mathrm{n\,Qb}} = \sum_{j,k} (i_j - i'_j)(i_k - i'_k) \frac{A^{jk}}{8}. \tag{E14}$$

The dephasing rates cannot be represented as a sum of individual qubit rates (for uncorrelated white noises see next section). This is, e.g., the case of collective qubits dephasing due to resonator shot noise, considered in Appendix B 6.

The infidelity [Eq. (E7)] is recast to

$$\delta\varepsilon_{\phi,\mathrm{shot}}^{\mathrm{n\,Qb}} = f_{12}^{(n)} \sum_{s<s'} \tilde{\Gamma}_{\phi,ss'}^{\mathrm{shot}} \, t. \tag{E15}$$

From Eq. (E5) one gets additional infidelity at small t due to the AC-Stark shifts:

$$\delta\varepsilon_{\delta\omega,\mathrm{shot}}^{\mathrm{n\,Qb}} = \frac{f_{12}^{(n)}}{2} \sum_{s<s'} \left(\delta\tilde{\tilde{\omega}}_{ss'}^{\mathrm{shot}} t \right)^2. \tag{E16}$$

The dephasing rates $\tilde{\Gamma}_{\phi,ss'}^{\mathrm{shot}}$ and frequency shifts $\delta\tilde{\tilde{\omega}}_{ss'}^{\mathrm{shot}}$ for whole time periods $t = t_g = \frac{2\pi N}{\delta}$ are given by Eqs. (65) and (67), respectively, see also Appendix B 6.

2. Uncorrelated white noises

For uncorrelated white noise impinged on the qubits frequencies one gets the relation

$$\langle \delta\omega_q^{(j)}(t') \delta\omega_q^{(j)}(t'') \rangle_{\xi_q} = A_j \delta^{jk} \delta(t'-t''), \tag{E17}$$

where the constants A_j can be represented via the spectral densities $S_{x^{(j)}}$ of the gate voltages of the (j)th qubit:

$$A_j = \sum_x \frac{S_{x^{(j)}}}{2\hbar^2} \left(\frac{\partial E_q^{(j)}}{\partial x^{(j)}} \right)^2. \tag{E18}$$

Here we have used that the frequency fluctuations are expressed via the qubit's gate voltage fluctuations $\delta\omega_q^{(j)}(t') = \frac{1}{\hbar} \sum_x \frac{\partial E_q^{(j)}}{\partial x^{(j)}} \delta x^{(j)}$, with $x^{(j)} = \{\varepsilon_v^{(j)}, \varepsilon_m^{(j)}, t_l^{(j)}, t_r^{(j)}\}$ being the qubit's defining gate voltage differences and interdot tunneling amplitudes (for a TQD qubit). We assumed for simplicity that these variables are mutually uncorrelated, while each is white noise correlated

$$\langle \delta x^{(j)}(t') \delta x^{(j)}(t'') \rangle_{\xi_q} = \frac{S_{x^{(j)}}}{2} \delta(t'-t''), \tag{E19}$$

where $S_{x^{(j)}}$ are the (single-sided) white noise spectral densities for each of the variables of the (j)th qubit.

The resulting n-qubit dephasing rates are then given by

$$\Gamma_{\phi,ss'} = \sum_j \frac{A_j}{4} (1 - i_j i'_j), \tag{E20}$$

which allows us to express the n-qubit dephasing rates via the single-qubit one. The n-qubit infidelity $\delta\varepsilon_\phi^{\mathrm{n\,Qb}}$ is expressed by the same Eq. (E15).

The single-qubit dephasing rate is then a sum of contributions,

$$\Gamma_\phi^{\mathrm{white}} = \frac{A_1}{2} = \sum_{x=\varepsilon_v, \varepsilon_m, t_l, t_r} \frac{S_x}{4\hbar^2} \left(\frac{\partial E_q}{\partial x} \right)^2, \tag{E21}$$

and is minimized, as $\frac{\partial E_q}{\partial \varepsilon_v} = \frac{\partial E_q}{\partial \varepsilon_m} = 0$ at a full sweet spot.

For two-qubit states, $|1\rangle = |\downarrow\downarrow\rangle$, $|2\rangle = |\downarrow\uparrow\rangle|3\rangle = |\uparrow\downarrow\rangle$, $|4\rangle = |\uparrow\uparrow\rangle$, one renders via Eq. (E20) the two-qubit rates expressed via the single-qubit one:

$$\Gamma_{\phi,12} = \frac{A_2}{2} = \Gamma_\phi^{(2)}, \quad \Gamma_{\phi,13} = \frac{A_1}{2} = \Gamma_\phi^{(1)}, \quad \text{(E22)}$$

$$\Gamma_{\phi,14} = \frac{A_1}{2} + \frac{A_2}{2} = \Gamma_\phi^{(1)} + \Gamma_\phi^{(2)}, \quad \text{etc.} \quad \text{(E23)}$$

which is also illustrated in Fig. 9. The two-qubit infidelity in this case is expressed via the sum $\sum_{s<s'} \Gamma_{ss'} t = 4[\Gamma_\phi^{(1)} + \Gamma_\phi^{(2)}]t$. For equal qubit dephasings, $\Gamma_\phi^{(1)} = \Gamma_\phi^{(2)} = \Gamma_\phi^{\text{white}}$, one obtains

$$\delta\varepsilon_\phi^{2\text{Qb}} = \frac{8}{10} \Gamma_\phi^{\text{white}} t, \quad \text{(E24)}$$

where $t = t_g = \frac{2\pi N}{\delta}$ is the gate time. The result of Eq. (E24) was first presented at the QCPR in August 2016, and also at the 2017 APS March meeting.

3. Phase gate infidelity in the case of uncorrelated $1/f$-charge noise

One is assuming that the accumulated random phases of individual qubits are uncorrelated:

$$\langle \Delta\phi^{(j)}(t)\, \Delta\phi^{(k)}(t)\rangle_{\xi_q} \propto \delta^{jk} \quad \text{(E25)}$$

[that is more general than Eq. (E17)]. Using the representation of the n-qubit states, $|s\rangle = |i_1, \ldots, i_n\rangle$, Eq. (E11), one obtains from Eq. (E25)

$$\langle [\Delta\phi_s(t) - \Delta\phi_{s'}(t)]2\rangle_{\xi_q} = \frac{1}{2} \sum_{j=1}^n \langle (\Delta\phi^{(j)}(t))^2\rangle_{\xi_q} (1 - i_j\, i_j'), \quad \text{(E26)}$$

which allows us to express the n-qubit dephasing rates via the single-qubit one.

For noise fluctuations subject to $1/f$-noise spectrum the dephasing factor in Eq. (E6) has a Gaussian time dependence

$$e^{-\frac{1}{2}\langle[\Delta\phi_{s'}(t)-\Delta\phi_{s'}(t)]^2\rangle_{\xi_q}} = e^{-(\tilde{\Gamma}_{ss'}\, t)^2}. \quad \text{(E27)}$$

(Here $\tilde{\Gamma}$ denotes an $1/f$-noise dephasing rate.) In the case of uncorrelated charge noise to each of the qubits, applying Eq. (E26), one obtains the relation

$$(\tilde{\Gamma}_{ss'}\, t)^2 = \frac{1}{4} \sum_{j=1}^n \langle (\Delta\phi^{(j)}(t))^2\rangle (1 - i_j\, i_j')$$

$$= \frac{1}{2} \sum_{j=1}^n (\tilde{\Gamma}^{(j)}\, t)^2 (1 - i_j\, i_j'), \quad \text{(E28)}$$

where $\tilde{\Gamma}^{(j)}$ is the single-qubit $1/f$-noise dephasing rate (for the jth qubit). The n-qubit infidelity is then obtained:

$$\delta\varepsilon_{\phi,1/f}^{\text{n Qb}} = f_{12}^{(n)} \sum_{s<s'} (\tilde{\Gamma}_{ss'}\, t)^2. \quad \text{(E29)}$$

For the two-qubit case, analogous to Eq. (E23), one gets the relations

$$\tilde{\Gamma}_{12} = \tilde{\Gamma}_\phi^{(2)}, \quad \tilde{\Gamma}_{13} = \tilde{\Gamma}_\phi^{(1)}, \quad \text{(E30)}$$

$$\tilde{\Gamma}_{14} = \sqrt{\left(\tilde{\Gamma}_\phi^{(1)}\right)^2 + \left(\tilde{\Gamma}_\phi^{(2)}\right)^2}, \quad \text{etc.} \quad \text{(E31)}$$

Assuming equal qubits' dephasing, $\tilde{\Gamma}_\phi^{(1)} = \tilde{\Gamma}_\phi^{(2)} \equiv \tilde{\Gamma}_\phi$, one obtains the two-qubit infidelity

$$\delta\varepsilon_{\phi,1/f}^{2\text{Qb}} = \frac{8}{10} (\tilde{\Gamma}_\phi\, t)^2. \quad \text{(E32)}$$

4. $1/f$ dephasing: Scaling of parameters

For the discussion here we use the expression for the single-qubit dephasing $\tilde{\Gamma}_\phi$ calculated in Refs. [24,25] (see also Refs. [116,117]):

$$\tilde{\Gamma}_\phi = \frac{1}{\hbar}[I + II + III + IV]^{1/2}, \quad \text{(E33)}$$

$$I \equiv \frac{1}{2} \sum_k \left(\frac{\partial E_q}{\partial \varepsilon_k}\right)^2 S_{\varepsilon_k} \log r_c, \quad \text{(E34)}$$

$$II \equiv \frac{1}{4} \sum_k \left(\frac{\partial^2 E_q}{\partial \varepsilon_k^2}\right)^2 S_{\varepsilon_k}^2 \log^2 r_c, \quad \text{(E35)}$$

$$III \equiv \frac{1}{2} \sum_{k\neq l} \left(\frac{\partial^2 E_q}{\partial \varepsilon_k \partial \varepsilon_l}\right)^2 S_{\varepsilon_k} S_{\varepsilon_l} \log^2 r_c, \quad \text{(E36)}$$

$$IV \equiv \frac{1}{8} \sum_{k\neq l} \left(\frac{\partial^2 E_q}{\partial \varepsilon_k^2}\right) \left(\frac{\partial^2 E_q}{\partial \varepsilon_l^2}\right) S_{\varepsilon_k} S_{\varepsilon_l}, \quad \text{(E37)}$$

where $\varepsilon_k = \varepsilon_v, \varepsilon_m$ are the TQD qubit energy detunings $\varepsilon_v \equiv e(V_1 - V_3)$ and $\varepsilon_m \equiv e[(V_1 + V_3)/2 - V_2]$, and $\varepsilon_k = t_l, t_r$ are the left and right tunneling amplitudes. The ratio $r_c \equiv \frac{\omega_{\text{UV}}}{\omega_{\text{IR}}}$ includes the ultraviolet and infrared frequency cutoffs needed to deal with $1/f$-noise spectral density. The spectral density of the $1/f$ noise is defined as $S(\omega) = \frac{S_{\varepsilon_k}}{|\omega|}$, where the spectral density constants S_{ε_k} are subject to experimental determination [28,29]. For illustration purposes we will assume $S_{\varepsilon_v} \approx S_{\varepsilon_m}$ and $S_{\varepsilon_v}, S_{\varepsilon_m} \gg S_{t_l}, S_{t_r}$ (see below). For $r_c = 10^6$ one can safely neglect the term IV. Below we argue that II and III contributes only small corrections of the order of 10^{-3} to the leading term I.

At the full sweet spot the term I is minimized since $\frac{\partial E_q}{\partial \varepsilon_v}, \frac{\partial E_q}{\partial \varepsilon_m} = 0$. Despite that $\log r_c \ll \log^2 r_c$ and the smallness of the spectral density constants $S_{t_l}, S_{t_r} \ll S_{\varepsilon_v} S_{\varepsilon_m}$ (see below) it turns out that for typical parameters $I \gg II \sim III$. To see this it is useful to write down the corresponding first derivatives and second derivatives (energy curvatures) for the TQD qubit at the full sweet spot [62]. By using the expressions for a TQD qubit energy [62] $E_q(\varepsilon_v, \varepsilon_m, t_l, t_r)$ one obtains at the full sweet spot:

$$E_q = \frac{8t_l^2}{a_l} \sqrt{1 - r + r^2}, \quad r \equiv \frac{t_r^2 a_l}{t_l^2 a_r}, \quad \text{(E38)}$$

$$\frac{\partial E_q}{\partial t_l} = \frac{16t_l}{a_l} \frac{1 - r/2}{\sqrt{1 - r + r^2}}, \quad \text{(E39)}$$

$$\frac{\partial^2 E_q}{\partial \varepsilon_v^2} = \frac{\partial^2 E_q}{\partial \varepsilon_m^2} = \frac{64t_l^2}{a_l^3} \frac{\left\{1 - \frac{r}{2}\left(1 + \frac{a_l^2}{a_r^2}\right) + r^2 \frac{a_l^2}{a_r^2}\right\}}{\sqrt{1 - r + r^2}}, \quad \text{(E40)}$$

$$\frac{\partial^2 E_q}{\partial \varepsilon_v \partial \varepsilon_m} = \frac{64t_l^2}{a_l^3} \frac{\left\{-1 + \frac{r}{2}\left(1 - \frac{a_l^2}{a_r^2}\right) + r^2 \frac{a_l^2}{a_r^2}\right\}}{\sqrt{1 - r + r^2}}, \quad \text{(E41)}$$

$$\frac{\partial^2 E_q}{\partial t_l^2} = \frac{8}{a_l} \frac{(2 - 3r + 6r^2 - r^3)}{(1 - r + r^2)^{3/2}}, \qquad \text{(E42)}$$

$$\frac{\partial^2 E_q}{\partial t_l \partial t_r} = -\frac{24}{a_l} \frac{t_l}{t_r} \frac{r^2}{(1 - r + r^2)^{3/2}}. \qquad \text{(E43)}$$

Here and in the following, $a_l \equiv \tilde{U}_1 + \tilde{U}_2'$ and $a_r \equiv \tilde{U}_2 + \tilde{U}_3$ are the combinations of the charging energy costs $\tilde{U}_i$ to fill the ith dot with 2 electrons starting from the $(1, 1, 1)$ configuration [62]. In this TQD model some of the curvatures are zero always, e.g., $\frac{\partial^2 E_q}{\partial \varepsilon_v \partial t_r} = \frac{\partial^2 E_q}{\partial \varepsilon_m \partial t_r} = 0$, while $\frac{\partial^2 E_q}{\partial \varepsilon_v \partial \varepsilon_m} = 0$ in the symmetric case $a_l = a_r$ and $r \equiv \frac{t_l^2 a_l}{t_r^2 a_r} = 1$. By taking the ratios of the surviving terms at the full sweet spot one obtains the important scalings:

$$\frac{II'}{I} = \frac{\frac{1}{2}\left(\frac{\partial^2 E_q}{\partial \varepsilon_v^2}\right)^2 S_{\varepsilon_v}^2 \log r_c}{\left(\frac{\partial E_q}{\partial t_l}\right)^2 S_{t_l}} = \frac{\log r_c}{2} \frac{S_{\varepsilon_v}^2 t_l^2}{S_{t_l} a_l^4} \approx 10^{-3}, \qquad \text{(E44)}$$

$$\frac{II''}{I} = \frac{\frac{1}{2}\left(\frac{\partial^2 E_q}{\partial t_l^2}\right)^2 S_{t_l}^2 \log r_c}{\left(\frac{\partial E_q}{\partial t_l}\right)^2 S_{t_l}} = 8 \log r_c \frac{S_{t_l}}{t_l^2} \approx 10^{-3}, \qquad \text{(E45)}$$

$$\frac{III}{I} = \frac{\left(\frac{\partial^2 E_q}{\partial t_l \partial t_r}\right)^2 S_{t_l} S_{t_r} \log r_c}{\left(\frac{\partial E_q}{\partial t_l}\right)^2 S_{t_l}} = 9 \log r_c \frac{S_{t_r}}{t_r^2} \approx 10^{-3}. \qquad \text{(E46)}$$

In these estimations we have used tunnelings $t_{l,r} = 40~\mu$eV, a dot charging energy, $U_{\text{ch}} \approx \tilde{U}_i \approx 0.4$ meV, $S_{\varepsilon_v} = S_{\varepsilon_m} = (1~\mu$eV$)^2$, and $S_{t_l} = S_{t_r} = 10^{-2} S_{\varepsilon_v}$. By increasing tunneling [98,118] to $t_{l,r} = 160~\mu$eV and $U_{\text{ch}} = 0.8$ meV, which is beneficial for larger quantum capacitance (see below), the smallness of these ratios remains a fact. Thus, to a very good

approximation one can write for the $1/f$-dephasing rate

$$\tilde{\Gamma}_\phi \simeq \frac{1}{\hbar}\sqrt{I} \qquad \text{(E47)}$$

$$= \frac{1}{\hbar}\left\{\frac{\log r_c}{2}\left[\left(\frac{\partial E_q}{\partial t_l}\right)^2 S_{t_l} + \left(\frac{\partial E_q}{\partial t_r}\right)^2 S_{t_r}\right]\right\}^{1/2} \qquad \text{(E48)}$$

$$\simeq \frac{16}{\hbar}\left\{\frac{\log r_c \, S_{t_l}}{2(1 - r + r^2)}\right.$$

$$\left. \times \left[\left(\frac{t_l}{a_l}\right)^2\left(1 - \frac{r}{2}\right)^2 + \left(\frac{t_r}{a_r}\right)^2\left(r - \frac{1}{2}\right)^2\right]\right\}^{1/2}. \qquad \text{(E49)}$$

In the symmetric case, $a_l = a_r$ and $r \equiv \frac{t_l^2 a_l}{t_r^2 a_r} = 1$, one obtains for the single-qubit $1/f$-dephasing rate, Eq. (79) of the main text. Using Eqs. (E32) and (79) one obtains the two-qubit infidelity for $1/f$ noise expressed through all relevant parameters, see Eq. (80) of the main text.

5. Spectral density constant of tunnelings from the experiment

The spectral density constant S_{t_l} can be extracted from the experiment [28]. To this end one uses typical tunneling $t_l = 10$–$20~\mu$eV, dot charging energy $U_{\text{ch}} = 0.6$–2.4 meV, and ratio $r_c \equiv \frac{\omega_{\text{UV}}}{\omega_{\text{IR}}} = 10^6$. These parameters fit Eqs. (E38) and (79) with the experimental values for qubit splitting $E_q \simeq 160$ MHz, and measured dephasing time (Rabi oscillations) of the current experiment [28] (DQD singlet-triplet qubit at the symmetric operating point), which assumes $S_{t_l} \simeq 10^{-4}$–$10^{-5}~(\mu$eV$)^2$.

[1] J. R. Petta, A. C. Johnson, J. M. Taylor, E. A. Laird, A. Yacoby, M. D. Lukin, C. M. Marcus, M. P. Hanson, and A. C. Gossard, Science **309**, 2180 (2005).

[2] B. M. Maune, M. G. Borselli, B. Huang, T. D. Ladd, P. W. Deelman, K. S. Holabird, A. A. Kiselev, I. Alvarado-Rodriguez, R. S. Ross, A. E. Schmitz, M. Sokolich, C. A. Watson, M. F. Gyure, and A. T. Hunter, Nature (London) **481**, 344 (2012).

[3] J. Medford, J. Beil, J. M. Taylor, E. I. Rashba, H. Lu, A. C. Gossard, and C. M. Marcus, Phys. Rev. Lett. **111**, 050501 (2013).

[4] M. Veldhorst, C. H. Yang, J. Hwang, W. Huang, J. Dehollain, J. Muhonen, S. Simmons, A. Laucht, F. Hudson, K. Itoh, A. Morello, and A. Dzurak, Nature (London) **526**, 410 (2015).

[5] E. E. Kawakami, T. Jullien, P. Scarlino, D. R. Ward, D. E. Savage, M. G. Lagally, V. V. Dobrovitski, M. Friesen, S. N. Coppersmith, M. A. Eriksson, and L. M. K. Vandersypen, Proc. Natl. Acad. Sci. USA **113**, 11738 (2016).

[6] D. R. Ward, D. Kim, D. E. Savage, M. G. Lagally, R. H. Foote, M. Friesen, S. N. Coppersmith, and M. A. Eriksson, Quant. Inf. **2**, 16032 (2016).

[7] J. J. Pla, K. Y. Tan, J. P. Dehollain, W. H. Lim, J. J. L. Morton, D. N. Jamieson, A. S. Dzurak, and A. Morello, Nature (London) **489**, 541 (2012).

[8] J. T. Muhonen, J. P. Dehollain, A. Laucht, F. E. Hudson, R. Kalra, T. Sekiguchi, K. M. Itoh, D. N. Jamieson, J. C. McCallum, A. S. Dzurak, and A. Morello, Nat. Nanotech. **9**, 986 (2014).

[9] X. Mi, J. V. Cady, D. M. Zajac, P. W. Deelman, and J. R. Petta, Science **355**, 156 (2017).

[10] X. Mi, M. Benito, S. Putz, D. M. Zajac, J. M. Taylor, G. Burkard, and J. R. Petta, Nature (London) **555**, 599 (2018).

[11] A. J. Landig, J. V. Koski, P. Scarlino, U. C. Mendes, A. Blais, C. Reichl, W. Wegscheider, A. Wallraff, K. Ensslin, and T. Ihn, Nature (London) **560**, 179 (2018).

[12] K. C. Nowack, F. H. L. Koppens, Y. V. Nazarov, and L. M. K. Vandersypen, Science **318**, 1430 (2007).

[13] C. H. Yang, A. Rossi, R. Ruskov, N. S. Lai, F. A. Mohiyaddin, S. Lee, C. Tahan, G. Klimeck, A. Morello, and A. S. Dzurak, Nat. Commun. **4**, 2069 (2013).

[14] M. Veldhorst, R. Ruskov, C. H. Yang, J. C. C. Hwang, F. E. Hudson, M. E. Flatté, C. Tahan, K. M. Itoh, A. Morello, and A. S. Dzurak, Phys. Rev. B **92**, 201401(R) (2015).

[15] D. P. DiVincenzo, D. Bacon, J. Kempe, G. Burkard, and K. B. Whaley, Nature (London) **408**, 339 (2000).

[16] B. H. Fong and S. M. Wandzura, Quantum Inf. Comput. **11**, 1003 (2011).

[17] L. Gaudreau, S. A. Studenikin, A. S. Sachrajda, P. Zawadzki, A. Kam, J. Lapointe, M. Korkusinski, and P. Hawrylak, Phys. Rev. Lett. **97**, 036807 (2006).

[18] L. Gaudreau, A. Kam, G. Granger, S. A. Studenikin, P. Zawadzki, and A. S. Sachrajda, Appl. Phys. Lett. **95**, 193101 (2009).

[19] E. A. Laird, J. M. Taylor, D. P. DiVincenzo, C. M. Marcus, M. P. Hanson, and A. C. Gossard, Phys. Rev. B **82**, 075403 (2010).

[20] L. Gaudreau, G. Granger, A. Kam, G. C. Aers, S. A. Studenikin, P. Zawadzki, M. Pioro-Ladrière, Z. R. Wasilewski, and A. S. Sachrajda, Nat. Phys. **8**, 54 (2011).

[21] J. Medford, J. Beil, J. M. Taylor, S. D. Bartlett, A. C. Doherty, E. I. Rashba, D. P. DiVincenzo, H. Lu, A. C. Gossard, and C. M. Marcus, Nat. Nanotechnol. **8**, 654 (2013).

[22] K. Eng, T. D. Ladd, A. Smith, M. G. Borselli, A. A. Kiselev, B. H. Fong, K. S. Holabird, T. Hazard, B. Huang, P. W. Deelman, I. Milosavljevic, A. E. Schmitz, R. S. Ross, M. F. Gyure, and A. T. Hunter, Sci. Adv. **1**, e1500214 (2015).

[23] J. M. Taylor, V. Srinivasa, and J. Medford, Phys. Rev. Lett. **111**, 050502 (2013).

[24] M. Russ and G. Burkard, Phys. Rev. B **92**, 205412 (2015).

[25] M. Russ, F. Ginzel, and G. Burkard, Phys. Rev. B **94**, 165411 (2016).

[26] Y.-P. Shim and C. Tahan, Phys. Rev. B **93**, 121410(R) (2016).

[27] R. Ruskov, M. Veldhorst, A. S. Dzurak, and C. Tahan, Phys. Rev. B **98**, 245424 (2018).

[28] M. D. Reed, B. M. Maune, R. W. Andrews, M. G. Borselli, K. Eng, M. P. Jura, A. A. Kiselev, T. D. Ladd, S. T. Merkel, I. Milosavljevic, E. J. Pritchett, M. T. Rakher, R. S. Ross, A. E. Schmitz, A. Smith, J. A. Wright, M. F. Gyure, and A. T. Hunter, Phys. Rev. Lett. **116**, 110402 (2016).

[29] F. Martins, F. K. Malinowski, P. D. Nissen, E. Barnes, S. Fallahi, G. C. Gardner, M. J. Manfra, C. M. Marcus, and F. Kuemmeth, Phys. Rev. Lett. **116**, 116801 (2016).

[30] M. Pioro-Ladrière, T. Obata, Y. Tokura, Y.-S. Shin, T. Kubo, K. Yoshida, T. Taniyama, and S. Tarucha, Nat. Phys. **4**, 776 (2008).

[31] E. E. Kawakami, P. Scarlino, D. R. Ward, F. R. Braakman, D. E. Savage, M. G. Lagally, M. Friesen, S. N. Coppersmith, M. A. Eriksson, and L. M. K. Vandersypen, Nat. Nanotechnol. **9**, 666 (2014).

[32] O. E. Dial, M. D. Shulman, S. P. Harvey, H. Bluhm, V. Umansky, and A. Yacoby, Phys. Rev. Lett. **110**, 146804 (2013).

[33] A. C. Doherty and M. P. Wardrop, Phys. Rev. Lett. **111**, 050503 (2013).

[34] G. Burkard and A. Imamoglu, Phys. Rev. B **74**, 041307(R) (2006).

[35] T. Frey, P. J. Leek, M. Beck, A. Blais, T. Ihn, K. Ensslin, and A. Wallraff, Phys. Rev. Lett. **108**, 046807 (2012).

[36] K. D. Petersson, L. W. McFaul, M. D. Schroer, M. Jung, J. M. Taylor, A. A. Houck, and J. R. Petta, Nature (London) **490**, 380 (2012).

[37] G. Tosi, F. A. Mohiyaddin, H. Huebl, and A. Morello, AIP Adv. **4**, 087122 (2014).

[38] J. J. Viennot, M. C. Dartiailh, A. Cottet, and T. Kontos, Science **349**, 408 (2015).

[39] F. Borjans, X. Croot, S. Putz, X. Mi, S. M. Quinn, A. Pan, J. Kerckhoff, E. J. Pritchett, C. A. Jackson, L. F. Edge, R. S. Ross, T. D. Ladd, M. G. Borselli, M. F. Gyure, and J. R. Petta, Appl. Phys. Lett. **116**, 234001 (2020).

[40] P. Harvey-Collard, G. Zheng, J. Dijkema, N. Samkharadze, A. Sammak, G. Scappucci, and L. M. K. Vandersypen, Phys. Rev. Appl. **14**, 034025 (2020).

[41] A. Blais, R.-S. Huang, A. Wallraff, S. M. Girvin, and R. J. Schoelkopf, Phys. Rev. A **69**, 062320 (2004).

[42] J. Majer, J. M. Chow, J. M. Gambetta, J. Koch, B. R. Johnson, J. A. Schreier, L. Frunzio, D. I. Schuster, A. A. Houck, A. Wallraff, A. Blais, M. H. Devoret, S. M. Girvin, and R. J. Schoelkopf, Nature (London) **449**, 443 (2007).

[43] L. DiCarlo, M. D. Reed, L. Sun, B. R. Johnson, J. M. Chow, J. M. Gambetta, L. Frunzio, S. M. Girvin, M. H. Devoret, and R. J. Schoelkopf, Nature (London) **467**, 574 (2010).

[44] R. Vijay, C. Macklin, D. H. Slichter, S. J. Weber, K. W. Murch, R. Naik, A. N. Korotkov, and I. Siddiqi, Nature (London) **490**, 77 (2012).

[45] D. Ristè, M. Dukalski, C. A. Watson, G. de Lange, M. J. Tiggelman, Y. M. Blanter, K. W. Lehnert, R. N. Schouten, and L. DiCarlo, Nature (London) **502**, 350 (2013).

[46] N. Roch, M. E. Schwartz, F. Motzoi, C. Macklin, R. Vijay, A. W. Eddins, A. N. Korotkov, K. B. Whaley, M. Sarovar, and I. Siddiqi, Phys. Rev. Lett. **112**, 170501 (2014).

[47] V. Srinivasa, J. M. Taylor, and C. Tahan, Phys. Rev. B **94**, 205421 (2016).

[48] L. Childress, A. S. Sørensen, and M. D. Lukin, Phys. Rev. A **69**, 042302 (2004).

[49] P.-Q. Jin, M. Marthaler, A. Shnirman, and G. Schön, Phys. Rev. Lett. **108**, 190506 (2012).

[50] X. Hu, Y.-x. Liu, and F. Nori, Phys. Rev. B **86**, 035314(R) (2012).

[51] N. Samkharadze, G. Zheng, N. Kalhor, D. Brousse, A. Sammak, U. C. Mendes, A. Blais, G. Scappucci, and L. M. K. Vandersypen, Science **359**, 1123 (2018).

[52] A. W. Cross and J. M. Gambetta, Phys. Rev. A **91**, 032325 (2015).

[53] H. Paik, A. Mezzacapo, M. Sandberg, D. T. McClure, B. Abdo, A. D. Corcoles, O. Dial, D. F. Bogorin, B. L. T. Plourde, M. Steffen, A. W. Cross, J. M. Gambetta, and J. M. Chow, Phys. Rev. Lett. **117**, 250502 (2016).

[54] A. Blais, J. M. Gambetta, A. Wallraff, D. I. Schuster, S. M. Girvin, M. H. Devoret, and R. J. Schoelkopf, Phys. Rev. A **75**, 032329 (2007).

[55] A. Wallraff, D. I. Schuster, A. Blais, J. M. Gambetta, J. Schreier, L. Frunzio, M. H. Devoret, S. M. Girvin, and R. J. Schoelkopf, Phys. Rev. Lett. **99**, 050501 (2007).

[56] P. J. Leek, S. Filipp, P. Maurer, M. Baur, R. Bianchetti, J. M. Fink, M. Göppl, L. Steffen, and A. Wallraff, Phys. Rev. B **79**, 180511(R) (2009).

[57] J. Q. You, X. Hu, S. Ashhab, and F. Nori, Phys. Rev. B **75**, 140515(R) (2007).

[58] A. J. Kerman, Phys. Rev. Lett. **104**, 027002 (2010).

[59] M. Khezri, J. Dressel, and A. N. Korotkov, Phys. Rev. A **92**, 052306 (2015).

[60] D. Sank, Z. Chen, M. Khezri, J. Kelly, R. Barends, B. Campbell, Y. Chen, B. Chiaro, A. Dunsworth, A. Fowler, E. Jeffrey, E. Lucero, A. Megrant, J. Mutus, M. Neeley, C. Neill, P. J. J. O'Malley, C. Quintana, P. Roushan, A. Vainsencher, T.

White, J. Wenner, A. N. Korotkov, and J. M. Martinis, Phys. Rev. Lett. **117**, 190503 (2016).

[61] A. J. Kerman, New J. Phys. **15**, 123011 (2013).

[62] R. Ruskov and C. Tahan, Phys. Rev. B **99**, 245306 (2019).

[63] R. Ruskov and C. Tahan, arXiv:1704.05876.

[64] A static longitudinal coupling $\propto [g_{\parallel}^{st} \sigma_z + g_0^{st}](\hat{a} + \hat{a}^\dagger)$ would lead to an always-on entangling interaction: $\mathcal{H}_{2Qbs} = \frac{2g_{1,\parallel}^{st}g_{2,\parallel}^{st}}{\omega_r} \sigma_z^{(1)} \otimes \sigma_z^{(2)}$, derived via a Lang-Firsov transformation (see, e.g., Ref. [75]). This coupling is, however, parametrically small ($g_{i,\parallel}^{st} \ll \omega_r$).

[65] D. V. Averin, A. B. Zorin, and K. K. Likharev, Zh. Eksp. Teor. Fiz. **88**, 692 (1985) [Sov. Phys. JETP **61**, 407 (1985)].

[66] D. V. Averin and C. Bruder, Phys. Rev. Lett. **91**, 057003 (2003).

[67] M. A. Sillanpää, T. Lehtinen, A. Paila, Y. Makhlin, L. Roschier, and P. J. Hakonen, Phys. Rev. Lett. **95**, 206806 (2005).

[68] T. Duty, G. Johansson, K. Bladh, D. Gunnarsson, C. Wilson, and P. Delsing, Phys. Rev. Lett. **95**, 206807 (2005).

[69] N. Samkharadze, A. Bruno, P. Scarlino, G. Zheng, D. P. DiVincenzo, L. DiCarlo, and L. M. K. Vandersypen, Phys. Rev. Appl. **5**, 044004 (2016).

[70] D. Niepce, J. Burnett, and J. Bylander, Phys. Rev. Appl. **11**, 044014 (2019).

[71] K. Mølmer and A. Sørensen, Phys. Rev. Lett. **82**, 1835 (1999).

[72] G. J. Milburn, S. Schneider, and D. F. V. James, Fortschr. Phys. **48**, 801 (2000).

[73] D. Leibfried, B. DeMarco, V. Meyer, D. Lucas, M. Barrett, J. Britton, W. M. Itano, B. Jelenković, C. Langer, T. Rosenband, and D. J. Wineland, Nature (London) **422**, 412 (2003).

[74] P. C. Haljan, K.-A. Brickman, L. Deslauriers, P. J. Lee, and C. Monroe, Phys. Rev. Lett. **94**, 153602 (2005).

[75] P. M. Billangeon, J. S. Tsai, and Y. Nakamura, Phys. Rev. B **91**, 094517 (2015).

[76] N. Didier, J. Bourassa, and A. Blais, Phys. Rev. Lett. **115**, 203601 (2015).

[77] S. Richer and D. P. DiVincenzo, Phys. Rev. B **93**, 134501 (2016).

[78] B. Royer, A. L. Grimsmo, N. Didier, and A. Blais, Quantum **1**, 11 (2017).

[79] F. Beaudoin, D. Lachance-Quirion, W. A. Coish, and M. Pioro-Ladrière, Nanotechnology **27**, 464003 (2016).

[80] L. A. Orona, J. M. Nichol, S. P. Harvey, C. G. L. Bøttcher, S. Fallahi, G. C. Gardner, M. J. Manfra, and A. Yacoby, Phys. Rev. B **98**, 125404 (2018).

[81] A. Stockklauser, P. Scarlino, J. V. Koski, S. Gasparinetti, C. K. Andersen, C. Reichl, W. Wegscheider, T. Ihn, K. Ensslin, and A. Wallraff, Phys. Rev. X **7**, 011030 (2017).

[82] A. O. Caldeira and A. J. Leggett, Ann. Phys. N.Y. **149**, 374 (1983).

[83] A. O. Caldeira, H. A. Cerdeira, and R. Ramaswamy, Phys. Rev. A **40**, 3438 (1989).

[84] For the purposes of this paper one can use the RLC equation for the resonator: $Ld^2Q(t)/dt^2 + RdQ(t)/dt + Q(t)/C = 0$ and interpret inductance L as a mechanical mass and charge $Q(t)$ as position variable. This allows us, in the style of Devoret's Les Houches lectures [119], to interpret $Q(t)$ as a loop charge, see Ref. [62].

[85] We assume a Markovian environment, so that the typical timescale $\hbar/k_B T_r$ is much shorter than the system timescales.

[86] D. F. Walls and G. J. Milburn, *Quantum Optics* (Springer. Berlin, 2008).

[87] H. M. Wiseman and G. J. Milburn, *Quantum Measurement and Control* (Cambridge University Press, Cambridge, 2010).

[88] R. Ruskov, K. Schwab, and A. N. Korotkov, Phys. Rev. B **71**, 235407 (2005).

[89] D. Hayes, S. M. Clark, S. Debnath, D. Hucul, I. V. Inlek, K. W. Lee, Q. Quraishi, and C. Monroe, Phys. Rev. Lett. **109**, 020503 (2012).

[90] We note that more sophisticated coupling sign flips via the so-called Walsh functions [89] do not help either.

[91] A. A. Clerk and D. W. Utami, Phys. Rev. A **75**, 042302 (2007).

[92] This "matrix phase factor" is a member of a more general non-Abelian phase transformation of an arbitrary two-qubit state [111] that leaves the two-qubit density matrix intact .

[93] S. P. Harvey, C. G. L. Bøttcher, L. A. Orona, S. D. Bartlett, A. C. Doherty, and A. Yacoby, Phys. Rev. B **97**, 235409 (2018).

[94] R. Ruskov, Spin-cavity longitudinal coupling for two-qubit gates and measurement, Poster at the Silicon quantum electronics conference, Delft, The Netherlands, June 13–14, 2016, https://qutech.nl/newsroom/events/siliconworkshop2016/.

[95] C. Tahan, Talk at the Quantum Computing Program Review, Alexandria, VA, July 18–21, 2016, http://tahan.com/charlie/pages/talks/.

[96] X. Hao, R. Ruskov, M. Xiao, C. Tahan, and H. Jiang, Nat. Commun. **5**, 3860 (2014).

[97] X. Mi, J. V. Cady, D. M. Zajac, J. Stehlik, L. F. Edge, and J. R. Petta, Appl. Phys. Lett. **110**, 043502 (2017).

[98] A. West, B. Hensen, A. Jouan, T. Tanttu, C. Yang, A. Rossi, M. Gonzalez-Zalba, F. Hudson, A. Morello, D. Reilly, and A. Dzurak, Nat Nanotechnol. **14**, 437 (2019).

[99] B. M. Freeman, J. S. Schoenfield, and H.-W. Jiang, Appl. Phys. Lett. **108**, 253108 (2016).

[100] E. J. Connors, J. J. Nelson, H. Qiao, L. F. Edge, and J. M. Nichol, Phys. Rev. B **100**, 165305 (2019).

[101] D. Culcer, Ł. Cywiński, Q. Li, X. Hu, and S. Das Sarma, Phys. Rev. B **82**, 155312 (2010).

[102] M. Lodari, N. W. Hendrickx, W. I. L. Lawrie, T. K. Hsiao, L. M. K. Vandersypen, A. Sammak, M. Veldhorst, and G. Scappucci, arXiv:2007.06328.

[103] R. Ruskov and A. N. Korotkov, Phys. Rev. B **67**, 241305(R) (2003).

[104] R. Ruskov, A. N. Korotkov, and A. Mizel, Phys. Rev. B **73**, 085317 (2006).

[105] K. Lalumiere, J. M. Gambetta, and A. Blais, Phys. Rev. A **81**, 040301(R) (2010).

[106] C. F. Roos, New J. Phys. **10**, 013002 (2008).

[107] A. O. Caldeira and A. J. Leggett, Physica A **121**, 587 (1983).

[108] C. W. Gardiner and P. Zoller, *Quantum Noise* (Springer, Berlin, 2000).

[109] J. M. Gambetta, A. Blais, M. Boissonneault, A. A. Houck, D. I. Schuster, and S. M. Girvin, Phys. Rev. A **77**, 012112 (2008).

[110] K. Keane and A. N. Korotkov, Phys. Rev. A **86**, 012333 (2012).

[111] R. Mosseri and R. Dandoloff, J. Phys. A: Math. Gen. **34**, 10243 (2001).

[112] R. Cabrera and W. E. Baylis, Phys. Lett. A **368**, 25 (2007).

[113] H. M. Wiseman and G. J. Milburn, Phys. Rev. A **49**, 1350 (1994).

[114] B. Øksendal, *Stochastic Differential Equations* (Springer, Berlin, 1998).

[115] A. N. Korotkov, Phys. Rev. B **63**, 115403 (2001).

[116] Y. Makhlin and A. Shnirman, Phys. Rev. Lett. **92**, 178301 (2004).

[117] G. Ithier, E. Collin, P. Joyez, P. J. Meeson, D. Vion, D. Esteve, F. Chiarello, A. Shnirman, Y. Makhlin, J. Schriefl, and G. Schön, Phys. Rev. B **72**, 134519 (2005).

[118] B. Kratochwil, J. V. Koski, A. J. Landig, P. Scarlino, J. C. Abadillo-Uriel, C. Reichl, S. N. Coppersmith, W. Wegscheider, M. Friesen, A. Wallraff, T. Ihn, and K. Ensslin, arXiv:2006.05883.

[119] M. H. Devoret, in *Quantum Fluctuations*, edited by S. Reynaud, E. Giacobino, and J. Zinn-Justin, Lecture notes of July 1995 Les Houches LXIII (Elsevier, Amsterdam 1997), p. 351.